

Diaphragm Forming: Innovation and Application to Ocean Engineering

by

Gilles Langlois

Diplôme d'ingénieur

Ecole Nationale Supérieure de Techniques Avancées, June 1993

Option Architecture de Systèmes Navales

Submitted to the Department of Ocean Engineering
in Partial Fulfillment of the Requirements for the Degree of
MASTER OF SCIENCE IN OCEAN ENGINEERING

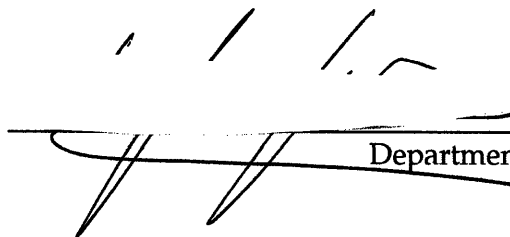
at the

MASSACHUSETTS INSTITUTE OF TECHNOLOGY

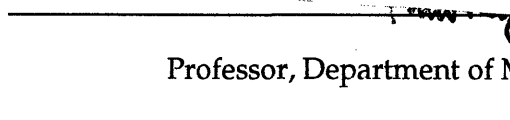
September 1994

© 1994 Massachusetts Institute of Technology

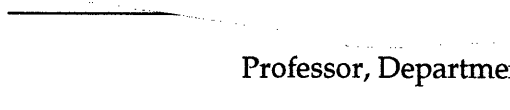
Signature of Author:


Department of Ocean Engineering
August, 1994

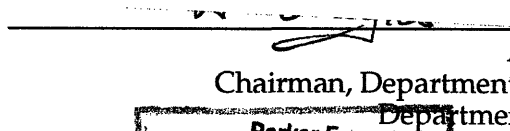
Certified by:

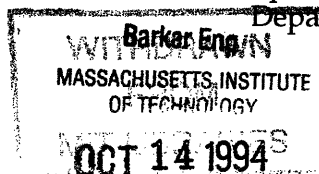

Timothy G. Gutowski
Professor, Department of Mechanical Engineering
Thesis Supervisor

Certified by:


A. Douglas Carmichael
Professor, Department of Ocean Engineering
Thesis Reader

Accepted by:


A. Douglas Carmichael,
Chairman, Departmental Graduate Committee
Department of Ocean Engineering



Diaphragm Forming: Innovation and Application to Ocean Engineering

by

Gilles Langlois

Submitted to the Department of Ocean Engineering
On August 6, 1994 in Partial Fulfillment of the
Requirements for the Degree of
Master of Science in Ocean Engineering

ABSTRACT

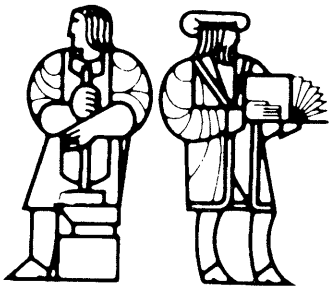
Composite materials have high mechanical specific properties such as strength or stiffness per weight or corrosion resistance which make them very attractive for Ocean Engineering Applications. But these excellent properties compared to those of metals are somewhat undermined because of the prohibitive cost of manufacturing composite parts. This is mainly due to the fact that composite parts are made by a labor intensive hand lay-up process. Automating the development of complex composite parts is potentially a cost effective technique. In terms of cost, one of the most promising of these techniques is the Diaphragm Forming Process. However some undesirable deformation modes such as laminate wrinkling can predominate under certain forming conditions.

The purpose of this study is to concentrate on this laminate wrinkling and see what should be done in order to understand and avoid this undesirable mode. This study will concentrate on increasing the stiffness of the diaphragm by reinforcement (patent pending). This study, also focuses on the applicability of diaphragm forming to Ocean Engineering applications.

A technique for reinforcing the diaphragm using woven wires has been developed. The work involves determining the feasibility of weaving reinforcement from different engineering materials such as Kevlar and steel, evaluating how bad is the indentation problem, where the reinforcements become embedded in the deforming composites, causing surface irregularities, and determining the relationships between the reinforcement orientation, the optimum spacing of the wires and the materials.

Thesis Supervisor: Timothy G. Gutowski
Professor, Department of Mechanical Engineering

Thesis Reader: Koichi Masubuchi
Professor, Department of Ocean Engineering



Acknowledgments

Sincere thanks go to Professor T. Gutowski for supervising my thesis and providing me the opportunity to work on this project, I also thank Professor K. Masubuchi for his comments and for allowing me to work with his laser microscope.

I would like also to thank Dr. Greg Dillon for his spirit, guidance and advice throughout this project.

Thanks also to Fred for helping me out in the work shop.

In addition, I would like to thank all the students of the lab, for their help and good humor, Sukyoung, Haorong, Ein-teck, and Maurilio.

Finally, I would like to thank the "Direction des Constructions Navales" for sponsoring my studies at MIT.



Contents

List of Figures

1 INTRODUCTION

1.1	Background.15
1.2	Diaphragm forming.19
1.3	Thesis Overview.21

2 FORMING LIMITS

2.1	Introduction.23
2.2	Deformation modes.24
2.2.1	Coordinate system.24
2.2.2	Constraints.25
2.2.3	Deformation modes25
2.3	Kinematic analysis30
2.3.1	Ideal fiber mapping30
2.3.2	In-plane Shear33
2.3.3	Inter-ply shear36
2.4	Rheological properties of the material37
2.5	Process analysis41
2.5.1	Mechanism of supporting the laminate.41
2.5.1.1	Friction transmission42
2.5.1.2	Support the laminate43
2.5.2	Forming sequence48
2.5.3	Tool heating.49
2.6	Forming limit diagram51
2.6.1	Mechanisms causing Laminate Wrinkling.51
2.6.2	Mechanism suppressing the wrinkles52

2.6.3	Forming limit diagram	52
-------	---------------------------------	----

3 DIAPHRAGM FORMING FOR OCEAN ENGINEERING APPLICATIONS

3.1	Introduction.53
3.2	Different applications related to diaphragm forming . .	.54
3.2.1	Assisting RTM.54
3.2.2	Glass reinforced thermoplastics.56
3.2.3	Forming whole hulls57
3.2.4	Forming advanced composite for marine applications60
3.3	Design and proof of concept61
3.3.1	Design of the part	61
3.3.2	Experimental approach.	65

4 INNOVATION IN DIAPHRAGM FORMING

4.1	Introduction.75
4.2	Exposition of the problem76
4.3	The woven Fabric78
4.4	The indentation problem	81
4.5	Experimental set-up	84
4.6	Optimization of the fabrics	87
4.6.1	Rods	89
4.6.2	Effect of the reinforcement size	91
4.6.3	Threads	92
4.7	Effect of reinforced diaphragm forming.	93
4.8	Design reinforcement for different shapes.	99

5 CONCLUSION	103
-------------------------------	------------

BIBLIOGRAPHY.105
------------------------------	-------------

Appendices

LIST OF FIGURES

Figure 1.1:	Operating depth potential of submersibles made in different materials	16
Figure 1.2:	lay-up of the prepreg in order to get the preform.	18
Figure 1.3:	Schematic of diaphragm forming process.	19
Figure 1.4:	Illustration of reinforced diaphragm forming.	20
Figure 2.1:	Illustration of the material coordinate system.	24
Figure 2.2:	Between-plane deformation modes of laminated plies.	26
Figure 2.3:	Out-of-plane deformation modes.	27
Figure 2.4:	In-plane deformation modes.	28
Figure 2.5:	Illustration of trellising behavior of 0/90 woven fabric.	29
Figure 2.6:	Illustration of first fiber placement in the ideal fiber mapping of a box with round edges.	31
Figure 2.7:	Placement of the neighboring fibers on a cube with round edges	31
Figure 2.8:	Illustration of a preform for an hemisphere	32
Figure 2.9:	Illustration of strain shear of fibers.	33
Figure 2.10:	Integration domains	34
Figure 2.11:	Comparison between actual shear and calculated shear for hemisphere and C-channel. [Li]	35
Figure 2.12:	Illustration of inter-ply slippage in the rich resin layer.	36
Figure 2.13:	Drape test set-up, three point bending apparatus.	38
Figure 2.14:	Illustration of the sensitivity of the applied load to the cross-head speed.	39

Figure 2.15: Apparent viscosity versus shear rate [Neoh].	40
Figure 2.16: Apparent viscosity versus temperature	40
Figure 2.17: Illustration of the laminate being clamped by the diaphragms	42
Figure 2.18: Laser microscope views of the fibers in different ply on the location of a wrinkle. (a) 0 deg ply (b) 90 deg ply (c) +45 deg ply (d) -45 deg ply (magnification X40).	45
Figure 2.19: Illustration of the wrinkle patterns of a [0/90/+45/-45]s Toray C-channel	46
Figure 2.20: Illustration of the wrinkle patterns of a [90/90/+45/-45]s Toray C-channel	46
Figure 2.21: Effect of the pressure on the diaphragms.	47
Figure 2.22: Illustration of the forming sequence for the case of the flange of a C-channel.	48
Figure 2.23: Illustration of the heating of the laminate.	49
Figure 2.24: Qualitative illustration of the non-isothermal heating on the stress inside the laminate.	50
Figure 2.25: Forming limit diagram for C-channels of different sizes	52
Figure 3.1: Trellising deformation of woven fabric draped over a sphere.	55
Figure 3.2: Illustration of FRTM process flow diagram.	56
Figure 3.3: Illustration of automatic spray-up	58
Figure 3.4: Inflated Tool Forming	60
Figure 3.5: Single skin hull typical stiffener top hat shape.	61
Figure 3.6: Transversely framed single skin hull	62
Figure 3.7: Stiffened plate with transverse and longitudinal	

	stiffeners.	63
Figure 3.8:	Longitudinally stiffened single skin hull.	63
Figure 3.9:	Illustration of a Top-hat shape intersection cross with sharp	64
Figure 3.10:	joining part for different stiffeners sizes.	65
Figure 3.11:	Top view and front view of the top-hat shape intersection part.	66
Figure 3.12:	Illustration of the set up of the forming machine.	67
Figure 3.13:	Illustration of the forming of (0/90)s	69
Figure 3.14:	Illustration of the wrinkling phenomena for (+/-45) plies.	70
Figure 3.15:	Illustration of the cut out of second set of experiments.	71
Figure 3.16:	Another design of cuts out	71
Figure 3.17:	Effect of the cut-outs on (+/-45) lay-up	72
Figure 3.18:	16 plies part formed at 180°C with cut-outs	73
Figure 4.1:	Illustration of a C-channel and its structural application as an element of an curved I-Beam.	77
Figure 4.2:	Illustration of the wrinkles patterns (a) on the Web (b) on the back flange	78
Figure 4.3:	Shaping assembly	79
Figure 4.4:	Reinforcement.	79
Figure 4.5:	Loom.	80
Figure 4.6:	Illustration of the indentation problem for a two foot long C-channel	81
Figure 4.7:	Part formed with reinforced diaphragm forming and cured in the autoclave.	82

Figure 4.8:	Laser microscope views of the cross section of part made (a) without reinforcement (b) with reinforcement.(magnification X40).	83
Figure 4.9:	Small forming machine.	85
Figure 4.10:	6 foot long forming machine used for forming 2 foot long and 4 foot long parts.	85
Figure 4.11:	Forming a part with reinforcement.	86
Figure 4.12:	Removal of the reinforcement.	87
Figure 4.13:	Illustration of a typical mild steel fabric	88
Figure 4.14:	Illustration of a polyethylene fabric.	89
Figure 4.15:	Illustration of the effect of reinforcement on the back flange of Toray C-channels. (a) case of thin rod reinforcement (b) case of thick rods reinforcement. . .	90
Figure 4.16:	Small reinforcement.	91
Figure 4.17:	Illustration of the marks left by the small reinforcement	92
Figure 4.18:	Forming limit diagram for 1 foot long Hercules C-channel with a [0/90/+45] lay-up.	92
Figure 4.19:	Forming limit diagram for 1 foot long Toray C-channels with a [0/90/+45] lay-up.	94
Figure 4.20:	Difference between a small Toray C-channel made with reinforcement and without reinforcement.	95
Figure 4.21:	Forming limit diagram for 2 foot long Toray C-channels	96
Figure 4.22:	Difference between a small Toray C-channel made with reinforcement and without reinforcement.	97
Figure 4.23:	Illustration of knit.	99
Figure 4.24:	Illustration of chopped rods embedded into a rubber matrix.	100

Figure 4.25: Illustration of curved rods embedded into a rubber matrix.	101
Figure 4.26: Illustration of stiff particles embedded into a rubber matrix.	101

Chapter 1

INTRODUCTION

1.1 Background

Since the 1950's, the use of Fiber Reinforced Plastic (FRP) for marine applications has grown substantially. Initially, FRP was used for small crafts only, but now structures having a mass of several hundred tons are being produced. The uses of composites in marine applications range from components like radar domes, masts, shafts and propellers to large ship hulls, ship superstructures and submersibles.

Composite materials are of interest because they provide high strength-to-weight and high stiffness-to-weight ratios. Because composite components are lighter they allow an increase in the payload fraction (ratio between the weight of the payload and the weight of the ship) and better stability due to lighter structures above the waterline. Other advantages of composites include good fire protection, low thermal conductivity, good corrosion resistance and design flexibility. It is now possible to manufacture FRP structures which outperform their metal counterparts in term of strength, weight, and cost. This is illustrated in Figure 1.1 which compares the potential

operating depth of submersibles made of different materials. (It should be cautioned that this graph is mainly based on strength-to-weight ratio, no concern was given to fracture toughness, resistance to stress corrosion cracking...)

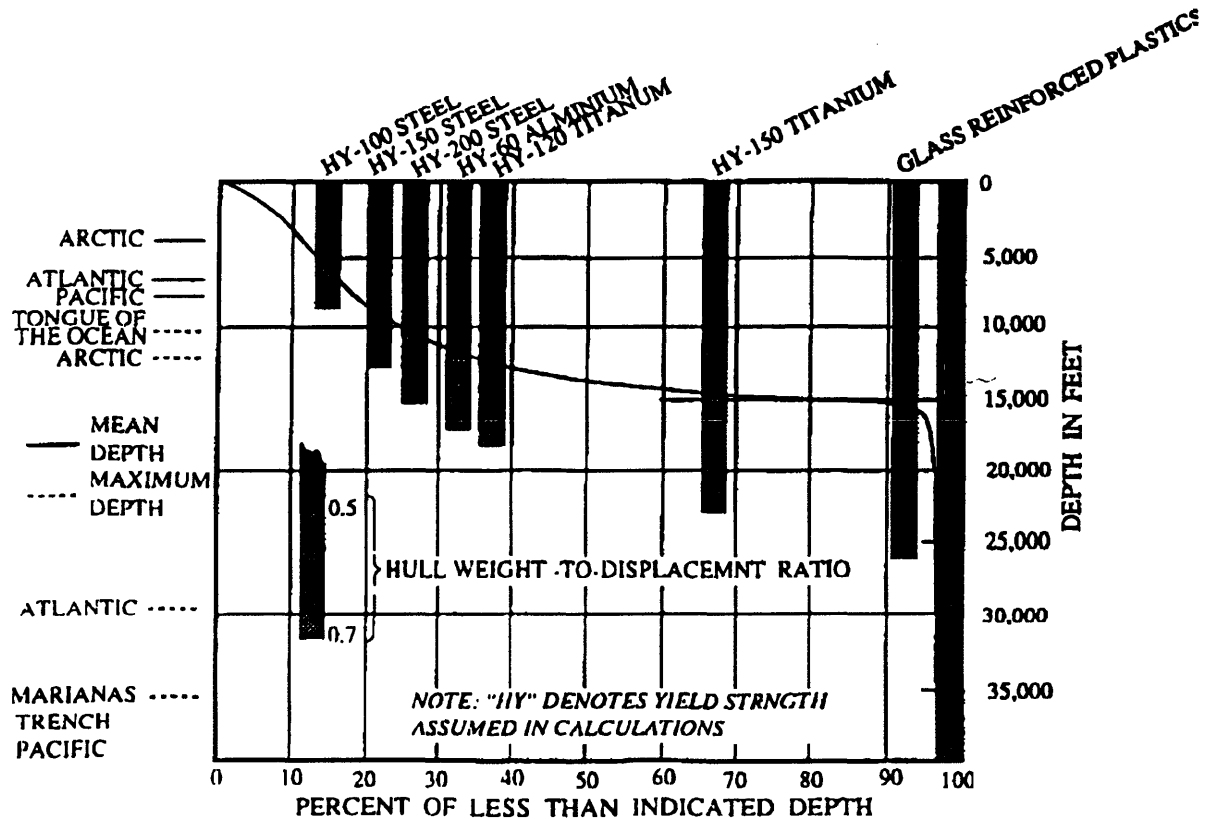


Figure 1.1: Operating depth potential of submersibles made in different materials [Masubuchi].

FRP is very competitive on the market of small ships and is confined to vessels below 50 m. The economical viability of welded steel being higher for vessels over 50 m. The construction of bigger FRP ships could become feasible in term of cost if:

- Material and construction costs are reduced relative to steel.

- Laminate stiffness is increased to use the potentially high specific strength effectively.
- The use of prefabricated laminates, or closed mold technique increases, because they can eliminate the large environmentally controlled laminating sheds.

Another problem pointed out by some Japanese shipyards is the recycling of these materials which may be a great subject of concern in case of wider uses of FRP. [Masubuchi]

A wide variety of composites are used in marine applications. Cost being a primary driver in the marine industry, most of its composite applications use glass fibers reinforced by polyester or vinyl ester resins which allows a good compromise between price and performance. But some specific applications such as racing boats, submarines, high speed boats, SWATH (Small Water plane Area Twin Hull), SES (Surface Effect Ship) require advanced composite materials, with longer and stiffer fibers, stronger resins and higher fiber contents, which enable larger weight savings, strength increases and performance advantages.

Although composite materials are used in very modern equipment such as aircrafts, satellites, and deep-submersibles, they are manufactured by extremely low technology processes. In fact most parts are manufactured by a hand lay-up process. In this process layers of prepreg material, which is a combination of fibers embedded in an uncured or thermoformable matrix, are placed ply by ply over a tool having the required shape. For complex shapes, this process requires many hours work by skillful operators, and

many parts are lost because of manual errors. This increases the cost of composite parts and prohibits wider use.

In order to improve the competitiveness of composite materials over its metal counterparts some new manufacturing processes, which can be automated, have been developed such as filament winding, pultrusion, resin transfer molding, drape forming, matched die forming, automatic tape and double diaphragm forming. Among these techniques, the diaphragm forming process seems to offer the most cost effective means of producing complex shapes. In this technique, woven fabric, unidirectional thermoset or thermoplastic prepregs, or random chopped fiber mat embedded in a thermoplastic matrix can be used as the based material. In the case of prepreg, strips of materials are laid up in orientations determined by directional stiffness requirements and then trimmed to the preform shape (see Figure 1.2). After the preform is placed between two diaphragms, the whole unit is formed over a tool by application of pressure or vacuum. (See Figure 1.3). After the forming is completed the part is removed from the forming machine and goes through an autoclave cure cycle. The same machine can accommodate a variety of tools.

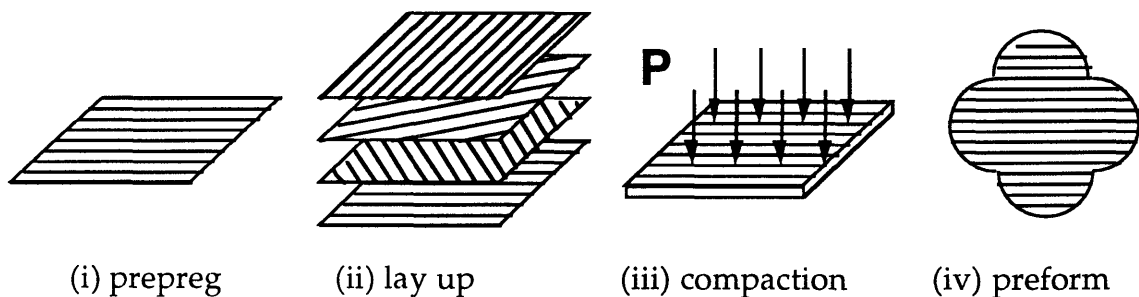


Figure 1.2: lay-up of the prepreg in order to get the preform

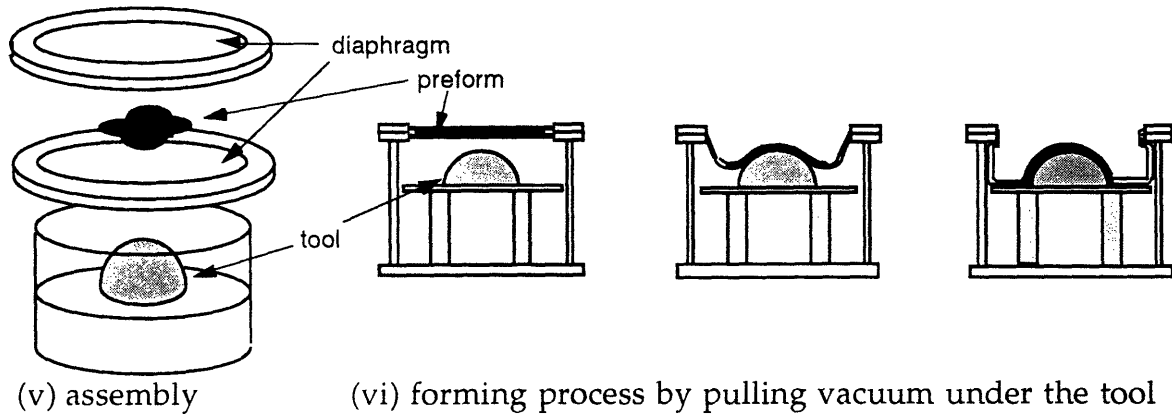


Figure 1.3: Schematic of diaphragm forming process.

1.2 Research Objectives

Before diaphragm forming can be used in industry the process needs to be studied in more detail in order to avoid undesirable deformation modes like in-plane buckling, fiber spreading, fiber bunching and laminate wrinkling.

One unique feature of this research is that it is aimed at studying continuous aligned fibers embedded into a thermoset matrix. Some experimental work aimed at studying the forming limits determine by the presence of wrinkles has already been carried out. Significant changes in the formability of the composite have been found by varying the composite properties, the part geometry, the diaphragm properties, the temperature, and the forming rate. This work has led to the concept of the Forming Limit

Diagram as a design tool for engineering applications. This research shows the limits of the process in terms of the part sizes that can be achieved and points the way to innovations that could extend the process.

The objective of this research is to assess a recent innovation on diaphragm forming which consists of increasing the stiffness of the diaphragm material by reinforcement as shown on Figure 1.4. This technique using woven wires has been developed, tested by the author and included in the forming limit analysis.

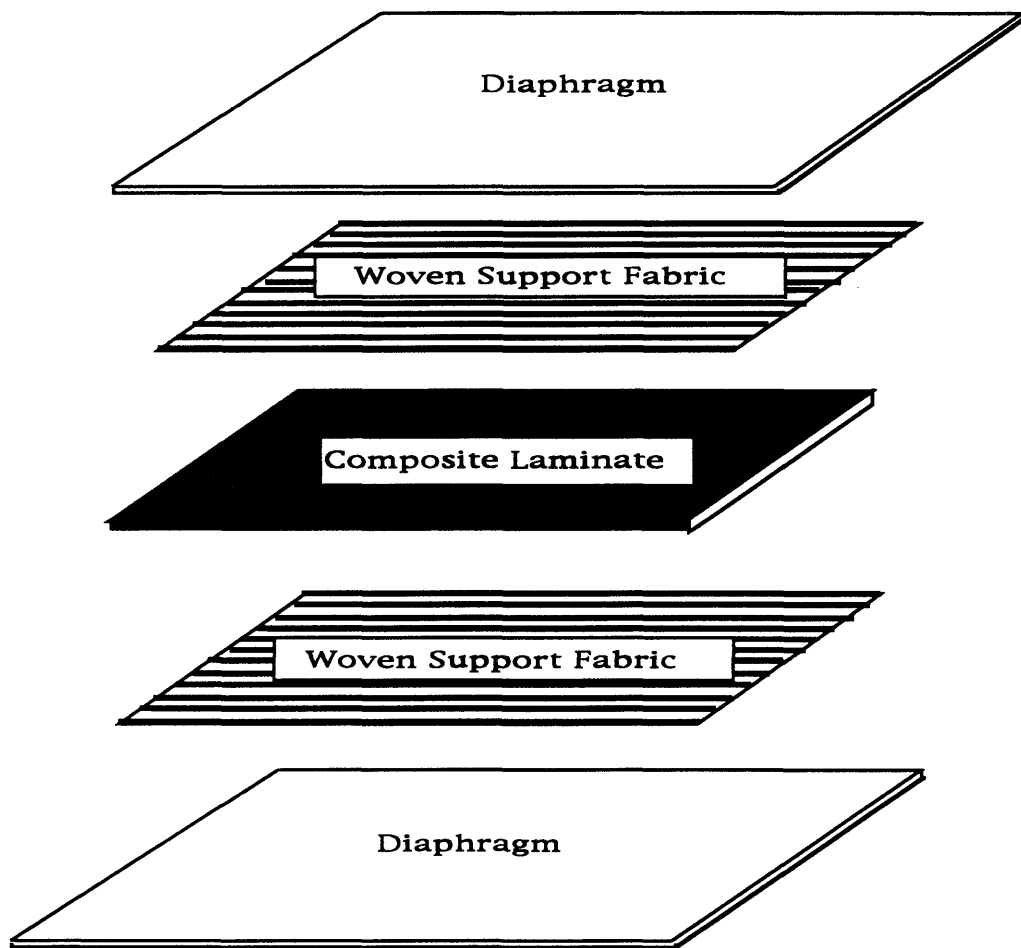


Figure 1.4: Illustration of reinforced diaphragm forming

Another aspect of this study is to expand the range of parts that can be made by diaphragm forming. A part which is the intersection of two top hat ship stiffeners is design and manufactured. This is a direct application of diaphragm forming to a component of interest in Ocean Engineering.

1.3 Thesis Overview

Chapter 2 describes the forming process for a flat laminate and illustrates its limits. This chapter introduces the different deformation modes, the concept of shear, a basic theory of laminate wrinkling and the concept of a Forming Limit Diagram.

Chapter 3 emphasizes the application of diaphragm forming to Ocean Engineering. This is done by pointing out some applications using glass fibers, and by the design of and experimentation on a cross shape part that can be used to join a longitudinal and transverse top-hat stiffeners used in the marine industry.

Chapter 4 gives an overview of the experimental work which has been carried out by the author and the main results of reinforced diaphragm forming included in the forming limit analysis.

Chapter 5 presents the main concluding remarks.



Chapter 2

FORMING LIMITS

2.1 Introduction

The problem of forming flat laminates of continuous fibers into different shapes, can be summarized as “inducing desirable deformation modes while suppressing the undesirable ones”. This chapter is aimed at explaining in more detail the mechanisms required to achieve this.

Numerous experiments ([Chey], [Monaghan and al.],...) show that the quality of a part is strongly influenced by the process, the material system and the part geometry. And if these parameters are not optimized the part is not acceptable and can undergo undesirable deformation modes, the most serious of which is laminate wrinkling.

First, we will examine the fundamental differences between the deformation modes, then, we will study the relationship between the part geometry and the occurrence of undesirable modes from a kinematic point of view. A few issues related to the behavior of the material and its rheology will be discussed and trends influencing the process will be highlighted. All of these parameters have an influence in the limits of diaphragm forming

which culminate into the concept of a forming limit diagram. Borrowed from sheet metal forming, this concept is aimed at predicting *a priori* if the part is achievable with diaphragm forming.

2.2 Deformation modes

2.2.1 Coordinate system

In order to account for the non-isotropy of composite laminates in our analysis we define the material coordinate system as shown in Figure 2.1.

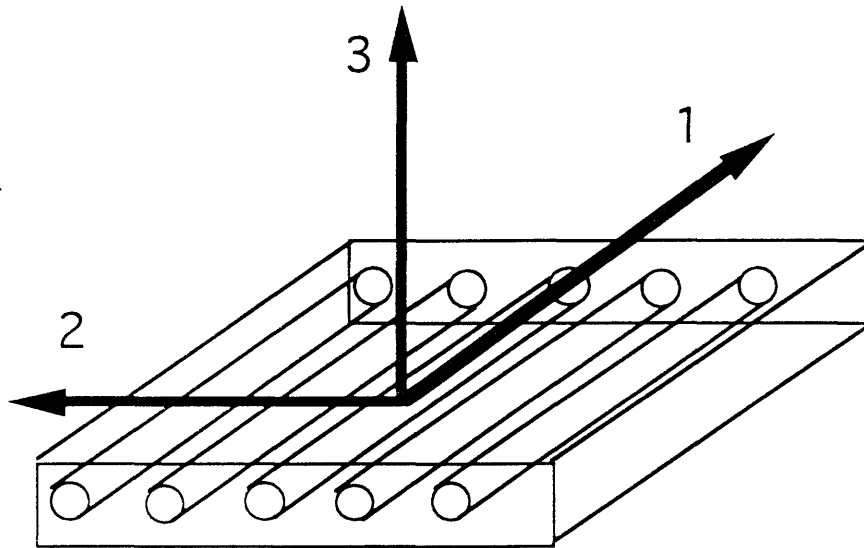


Figure 2.1: Illustration of the material coordinate system

Axis 1 lies along the fiber direction, axis 2 is transverse to the fibers within the plane of the laminate and axis 3 is perpendicular to the ply (through the thickness direction)

2.2.2 Constraints

Because of the nature of advanced composite prepreg, three basic assumptions, which will restrict the way the laminate can deform, must be stated.

- (a)- The fibers are considered inextensible i.e. they do not stretch, or contract during the forming process.
- (b)- The material (matrix and fibers) is incompressible, the deformation must be volume conserving.
- (c)- The fibers remain evenly spaced throughout the deformation.

These constraints define an ideal composite, which forms the basis of our kinematic analysis, and provides a standard to which formed parts can be compared.

These three basic assumptions lead to the following consequences:

- a- Desirable deformation modes are in-planes.
- b- The local deformation must propagate out to the edge of the ply. This is due to the lack of local plastic deformation which exists in isotropic materials. As a result, the maximum shear occurs at the edge of the ply.

2.2.3 Deformation modes

The different deformation modes that can be encountered during forming have been categorized as follows [Tam]:

1. Between-plane modes (Figure 2.2). The inter-ply slippage shown in Figures 2.2.a and 2.2.b is necessary to achieve simple bending, and double curved shapes respectively.

2. Out-of-plane modes (Figure 2.3). These modes are highly undesirable and the out-of-plane buckling (Figure 2.3.a) is also designated laminate wrinkling.

3. In-plane modes (Figure 2.4). The in-plane slippage described in Figure 2.4.a, is a desirable mode which allows the fibers to conform to double-curvatures. This slippage is usually very difficult to achieve. Transverse shear may occur in an ideal fiber mapping as long as thickness variation does not result. The other deformation modes (Figure 2.4.c,d,e) are undesirable.

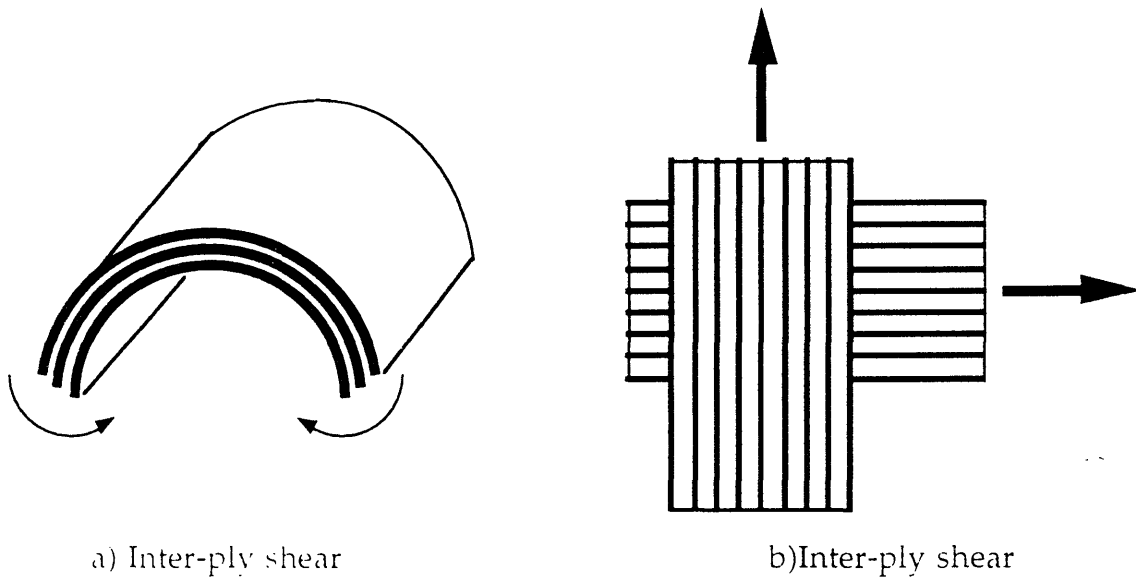
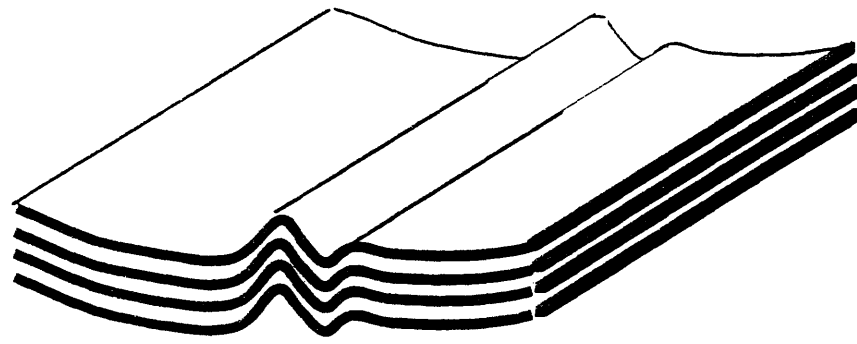
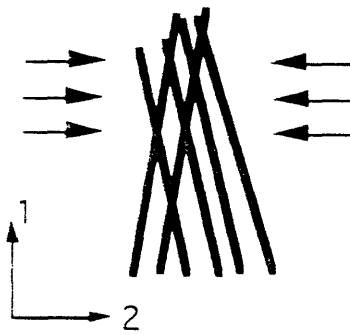


Figure 2.2: Between-plane deformation modes of laminated plies.

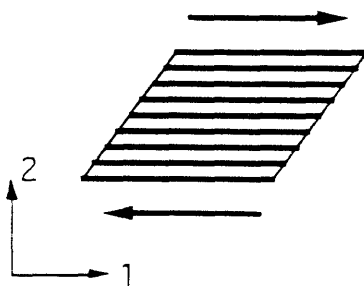


a) Out-of-plane buckling (Wrinkling)

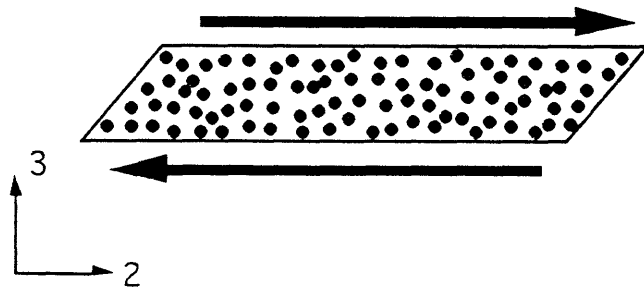


b) Fiber crossing

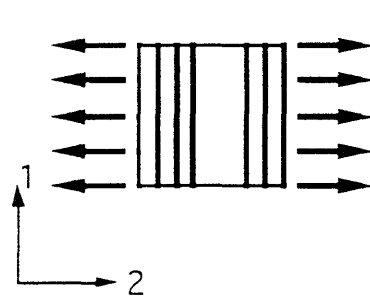
Figure 2.3: Out-of-plane deformation modes.



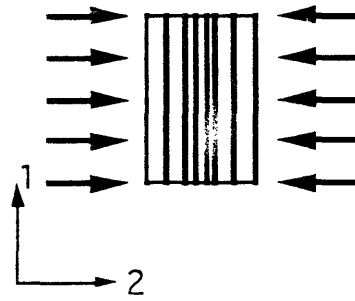
a) In-plane slippage



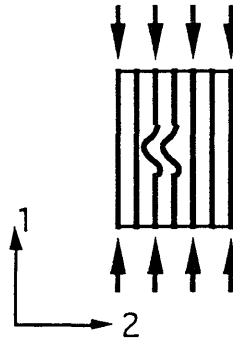
b) Transverse shear



c) Fiber splitting



d) Fiber bunching-up



e) In-plane buckling

Figure 2.4: In-plane deformation modes.

For fabrics, another deformation mode known as trellising (Figure 2.5) can occur and replace the in-plane slippage. This gives rise to some deviation from the ideal fiber mapping, because the fibers are not evenly spaced.

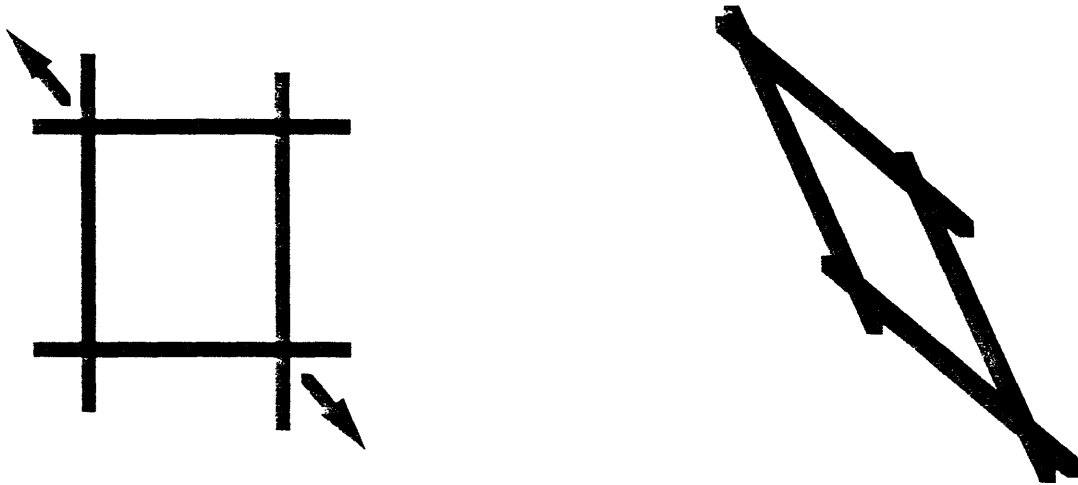


Figure 2.5: Illustration of trellising behavior of 0/90 woven fabric

The deformation of the laminate is a combination of these modes.

The intra-plane slippage (Figure 2.4.a) and the inter-ply slippage (Figure 2.2.a,b) must occur in order to alleviate the shear stresses that build up while the laminate is being deformed. When these modes cannot be achieved, undesirable modes such as laminate wrinkling may occur. The difficulty in achieving sufficient in-plane slippage or inter-ply slippage arises with double curved shapes. And most of the undesirable modes occur while forming these parts. We will term double curved surfaces as complex shapes. Therefore, it is important to link the geometry of the part to the deformation modes required. This can be done through a kinematic analysis of an ideal fiber mapping. The theoretical in-plane shear can be calculated using the Gauss-bonnet theorem, and the inter-ply shear can also be evaluated. We will briefly discuss how these theoretical results deviates from the experimental ones.

2.3 Kinematic analysis

The fibers are modeled as 3d curves and the laminates as 3d surfaces. The analysis applies the principles of differential geometry.

2.3.1 Ideal fiber mapping

Some important results from differential geometry are related to geodesic curves on a surface. A geodesic path on a surface does not have in-plane curvature and so it does not shear relative to its in-plane neighbor. Therefore, during the forming it is better if the fibers follow geodesic paths.

An ideal fiber mapping preserves even thickness throughout the part and therefore even fiber spacing. The method to obtain an ideal fiber mapping is to draw on the shape an initial fiber according to the lay-up orientation required, usually following a geodesic path (See Figure 2.6 for the case of a box with round edges). The mapping is continued by laying down the neighboring fibers and maintaining a constant spacing between the fibers as shown on Figure 2.7).

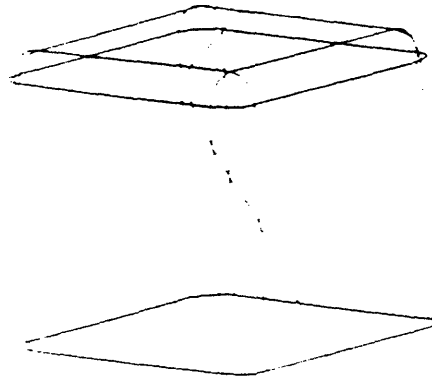


Figure 2.6: Illustration of first fiber placement in the ideal fiber mapping of a box with round edges.

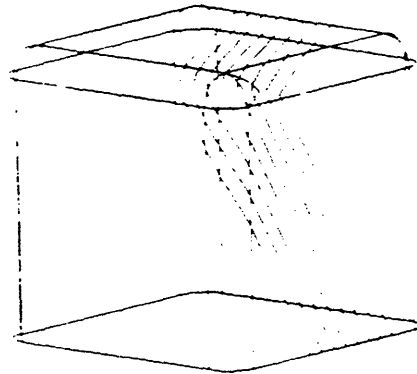


Figure 2.7: Placement of the neighboring fibers on a cube with round edges

Once the ideal mapping for a shape is determined it is possible to back calculate and determine the flat preform that is required to make the part with no waste. Figure 2.8 illustrates the shape of a preform for an ideal hemisphere.

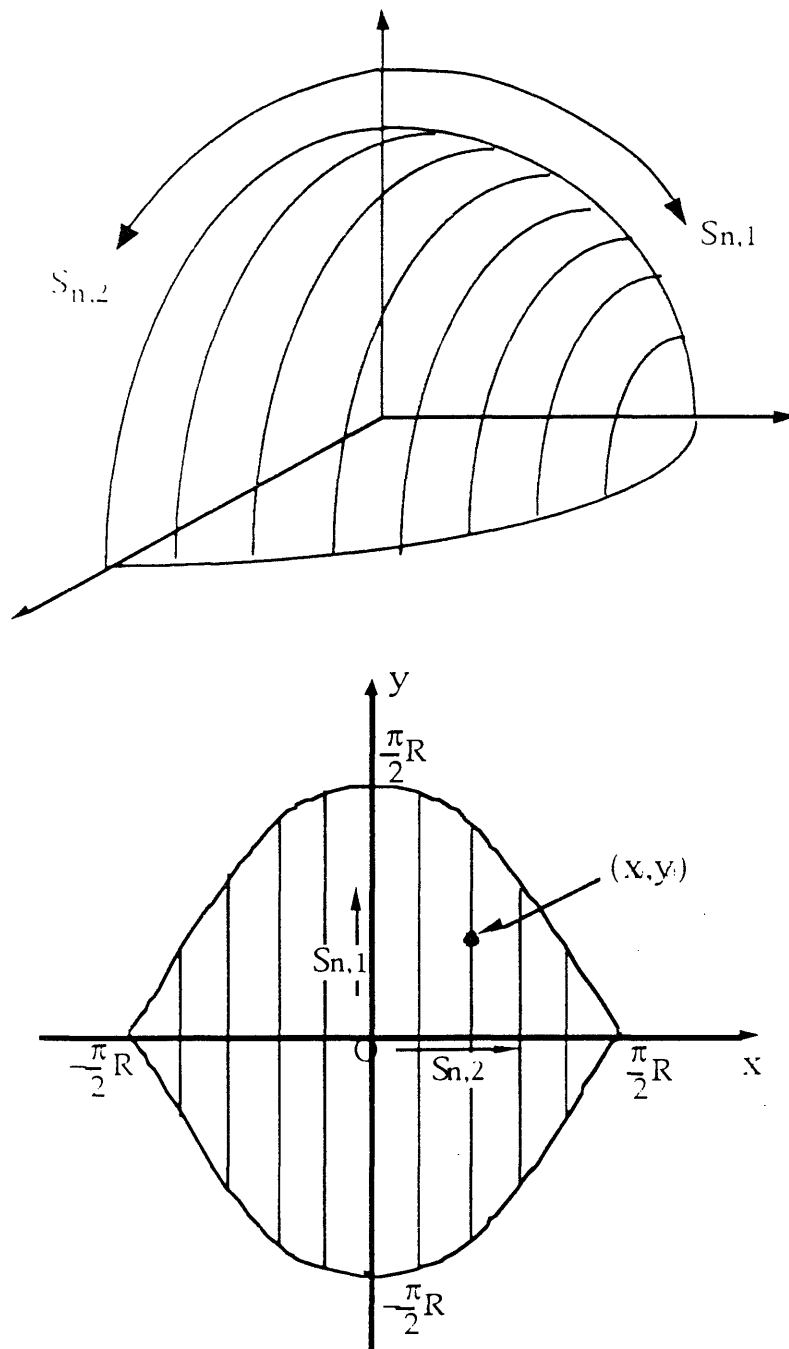


Figure 2.8: Illustration of a preform for an hemisphere

2.3.2 In-plane Shear

Figure 2.9 shows parallel fiber elements before and after forming. Assuming the distance between two fibers is constant, the point B moves a distance d relative to its neighbor. We can define the in-plane shear as follows:

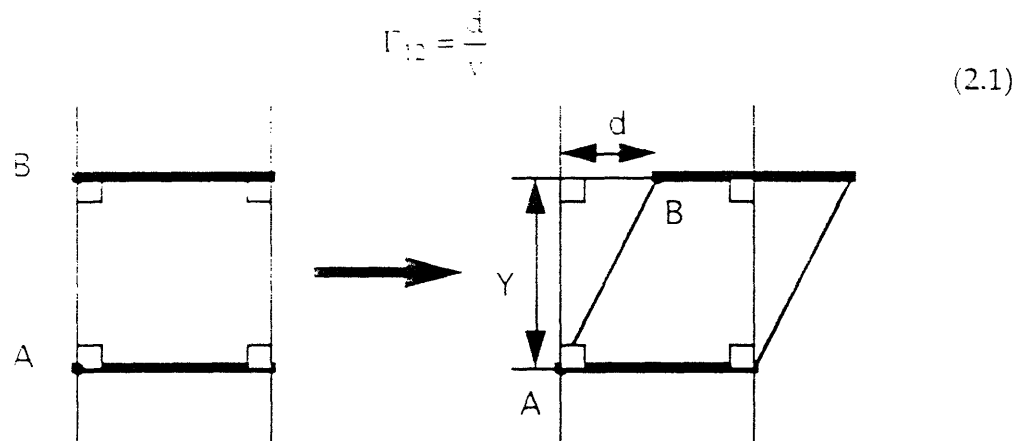


Figure 2.9: Illustration of strain shear of fibers.

We know that the in-plane shear is a desirable mode to obtain. We will explain how the in-plane shear can be evaluated from the ideal fiber placement. [Tam] We will only quickly overview the more important results.

From differential geometry it is possible to relate the in-plane shear to the geodesic curvature of a fiber by the following relationship [Tam]:

$$\Gamma_{12} = \int_0^L \kappa_g ds \quad (2.2)$$

where: Γ_{12} is the in-plane shear for a given fiber.

κ_g is the geodesic curvature as a function of distance along the fiber, s .

L is the length of the fiber.

And using the Gauss-Bonnet theorem, [Tam] has shown that the magnitude of the shear can be related to the curvature of the surface. The Gauss-Bonnet relation is expressed as follows:

$$\oint_C \kappa_g ds + \iint_R K dA = 2\pi - \sum_{i=1}^n \theta_i \quad (2.3)$$

where K is the Gaussian curvature of a surface, R is a region of the surface bounded by a closed curve C made of k smooth arcs having exterior angles θ_i , as shown in Figure 2.10.

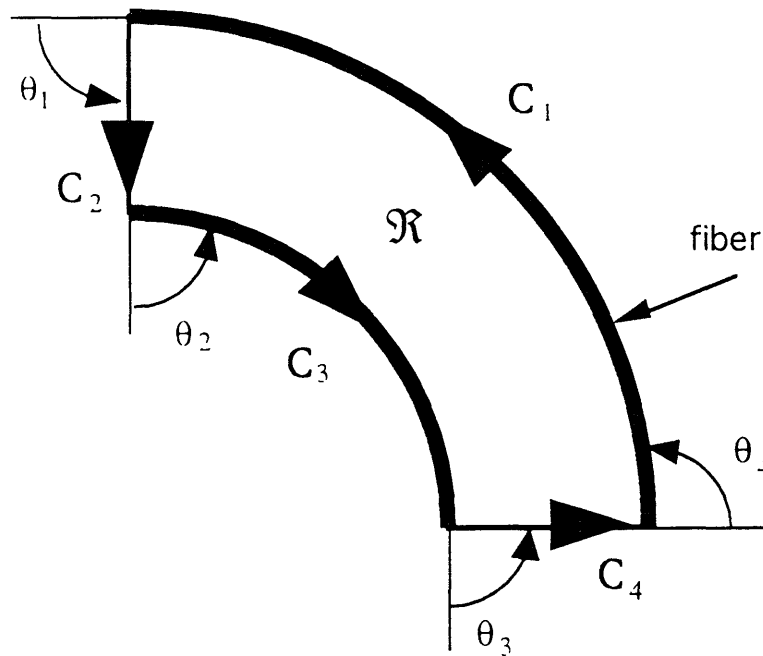


Figure 2.10: Integration domains

By choosing the path C to include two fibers and two orthogonal geodesics as shown on Figure 2.10. The shear can be expressed as [Tam]:

$$\Gamma_{12} = \int_{C_2} \kappa_2 ds = - \iint_R K dA = -K_T(R) \quad (2.4)$$

Therefore it becomes possible to calculate analytically the shear required for several simple geometries such as cones, hemispheres, and "C" channels. The ideal shear can then be compared with the actual shear, measured on a formed part as shown of figure 2.11.

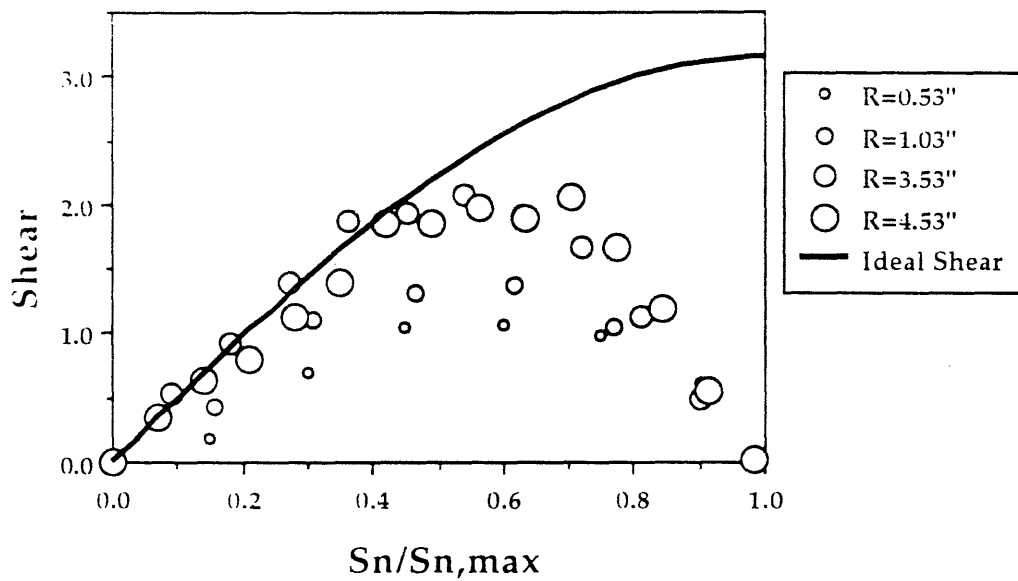


Figure 2.11: Comparison between actual shear and calculated shear for hemisphere and C-channel. [Li]

There is a tendency for the actual shear to depart from the ideal. This is due to the uneven thickness distribution over the part. The difference is due to fiber bunching, fiber spreading, or trellising behavior. It is also interesting to note that the actual shear deviates substantially from the ideal shear near the edges. In fact the ideal fiber placement is almost impossible to achieve for

complex shapes, but there are still many chances for the part to be good from a mechanical point of view. The ideal fiber placement gives an idea of what the fiber mapping should be.

2.3.3 Inter-ply shear

Inter-ply shear is the slippage between two plies of different orientations. Inter-ply shear is accommodated by the resin rich layer present on most prepreg surfaces. (See Figure 2.12) The resin rich layer is caused by the mechanism of percolation of the resin through the fibers [Barnes and Cogswell] and allows the plies to slide past each other.

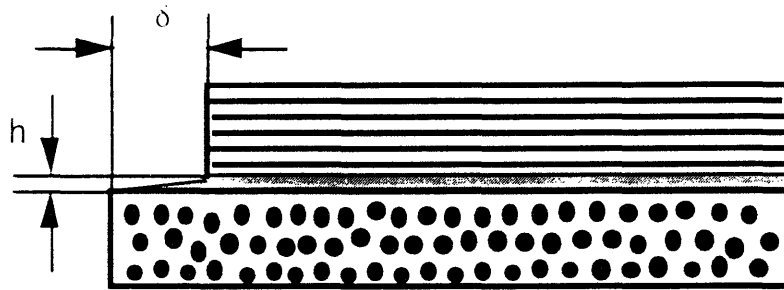


Figure 2.12: Illustration of inter-ply slippage in the rich resin layer

We can define the inter-ply shear as follows:

$$\Gamma_{\text{interply}} = \frac{\delta}{h} \quad (2.5)$$

The inter-ply shear can be orders of magnitude higher than the in-plane shear. The lay-up orientation influences strongly the way the inter-ply shear is achieved. For (0/90) or (+/-45) lay-up the whole laminate behaves similar to a woven material and deforms in a manner similar to trellising. Therefore,

they are easier to form because they don't require too much inter-ply slippage. For (0/90/+45/-45) lay-up, each layer has to move relative to the adjacent one. The induced inter-ply shear can be very large, and thus the part is harder to form than (0/90) or (+/-45) lay-up.

While characterizing the effects of the ply orientation on the flow process [Scherer] has shown, by a finite element analyses, that the inter-ply slip is easier if the plies are oriented transverse to the slip direction and that the resin rich inter-layer accommodates shear more efficiently when the plies have non-parallel orientations.

Usually the inter-ply shear required to form a part is a few orders of magnitude higher than the in-plane shear. For example on a hemisphere the inter-ply shear is on the order of 1,000 whereas the in-plane shear is on the order of π .

2.4 Rheological properties of the material

The above discussion emphasizes the necessity of achieving inter-ply or in-plane shear, but the ability of the plies to shear relative to each other is not only determined by the part geometry, but also by factors influencing the material properties. Temperature and deformation rate are the two main factors influencing the viscosity of the matrix.

An experimental test has been developed by [Neoh] to measure the drape properties of prepregs. Drape is defined as the ability of a material to conform

to a complex shapes. The viscoelastic properties of the thermoset prepreg can be measured with simplicity and repeatability, using a three point bending test, as shown in Figure 2.13.

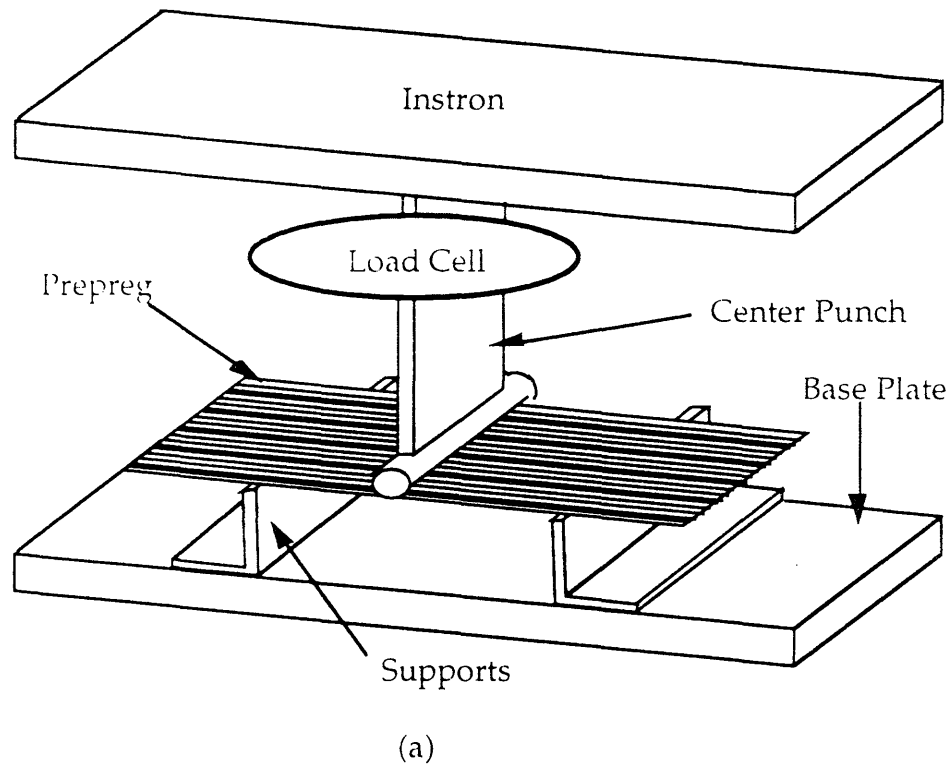


Figure 2.13: Drape test set-up, three point bending apparatus.

Figure 2.14 is an illustration of the rate dependence of load for prepreg material (AS4/3501-6)

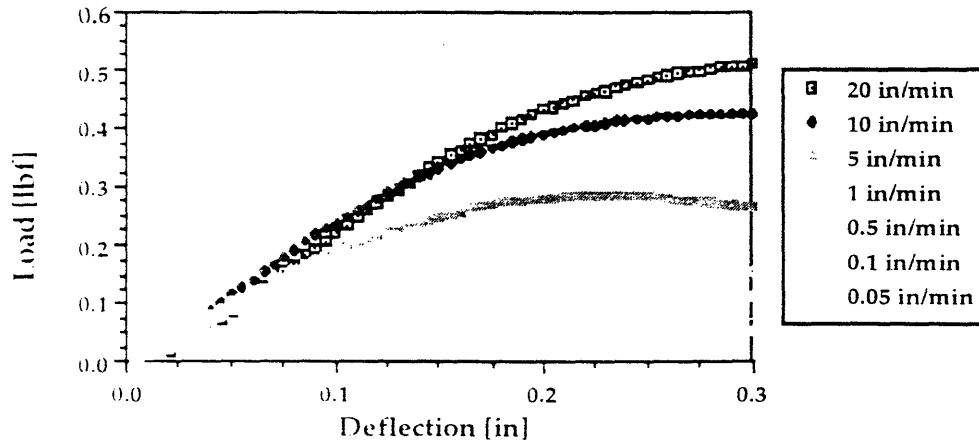


Figure.2.14: Illustration of the sensitivity of the applied load to the cross-head speed [Neoh].

From the above data, it can be inferred that the flow phenomena controlling the deformation is non-Newtonian viscous in nature. The stress strain relation can be modeled by a power-law equation [Neoh]:

$$\tau = m\dot{\Gamma}^n = \eta\dot{\Gamma} \quad (2.6)$$

τ is the shear stress, $\dot{\Gamma}$ is the shear rate, m is the non-Newtonian viscosity function and n is a dimensionless exponent, and η is called the apparent viscosity.

For the experiments carried out in this thesis, two types of materials were used: Hercules AS4/3501-6 and Toray T800H/3900-2 which have significantly different drapability properties. Figure 2.15 illustrates the fact that the viscosity of

Toray material is usually an order of magnitude higher than that of Hercules, Toray material being harder to form as can be seen on Figure 2.15.

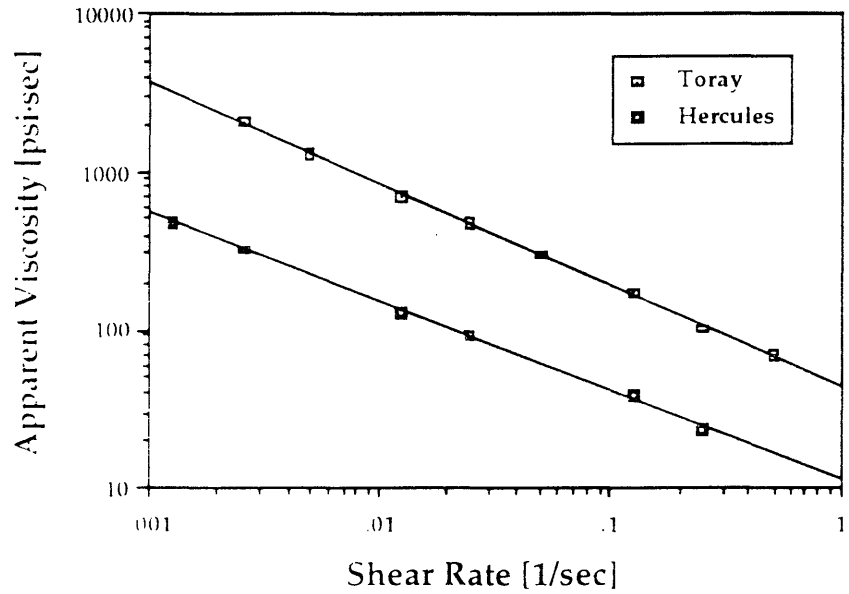


Figure 2.15: Apparent viscosity versus shear rate [Neoh].

The viscosity of these materials is strongly dependent on the temperature as can be seen on Figure 2.16.

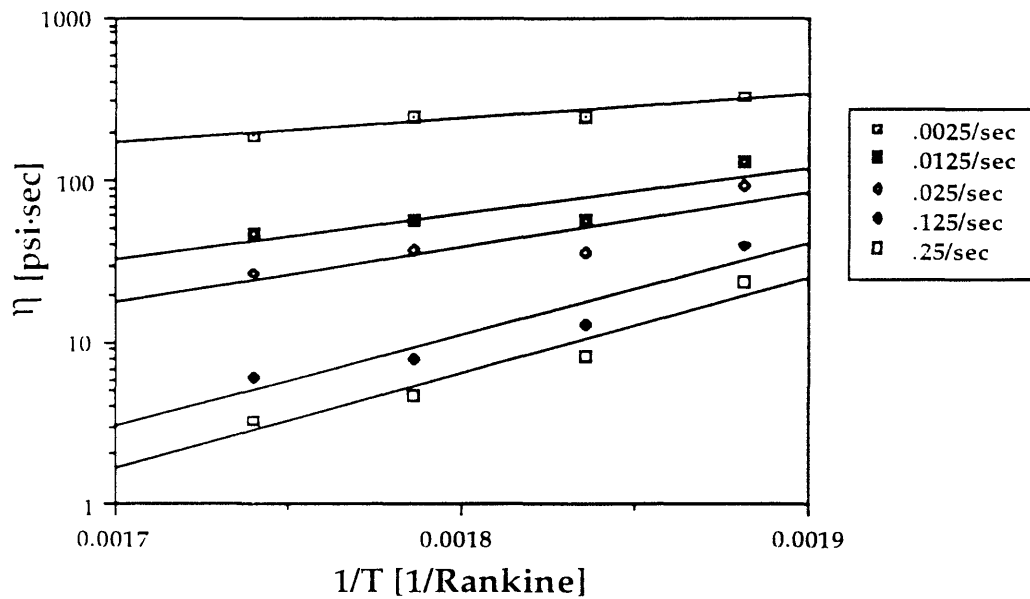


Figure 2.16: Apparent viscosity versus temperature

2.5 Process analysis

In addition to the part geometry, the lay-up, the temperature and the shear rate some other parameters can strongly influence the diaphragm forming process. The parameters we are going to study in this section are the mechanism of supporting the laminate during the forming, the forming sequence, and the means of heat application.

2.5.1 Mechanisms of supporting the laminate

In diaphragm forming the laminate is placed between two elastic diaphragms. While forming thermosets, the processing temperature being relatively low (for thermoset 75-100°C, for thermoplastic 225-370°C), these diaphragms are made of translucent rubber which exhibits a non-linear elastic stress-strain behavior. The two diaphragms are above and below the laminate and then vacuum is pulled between the two diaphragms. The role of vacuum is twofold. First it ensures good contact between the diaphragm and the laminate, and secondly it allows better support of the laminate, thus reducing the risk of laminate wrinkling.

2.5.1.1 Friction transmission

The vacuum between the diaphragms permits a good contact between the laminate and the diaphragms during the forming process. When the diaphragm extends during the forming process, the friction between the diaphragm and the laminate generates tension.

Usually wrinkles appear when a compressive force is built up in the laminate, because the shear stresses are not relaxed. This has been demonstrated by [Hull and al.] who have considered the development of an initially small distortion during the flow of ideal fiber reinforced fluids. They conclude that the important factor for determining the stability of slow viscous flows is the tension of the fibers. This does not conflict with our intuition. So the tensile force induced by the friction between the diaphragms and the laminate tends to oppose compressive forces that could cause wrinkling.

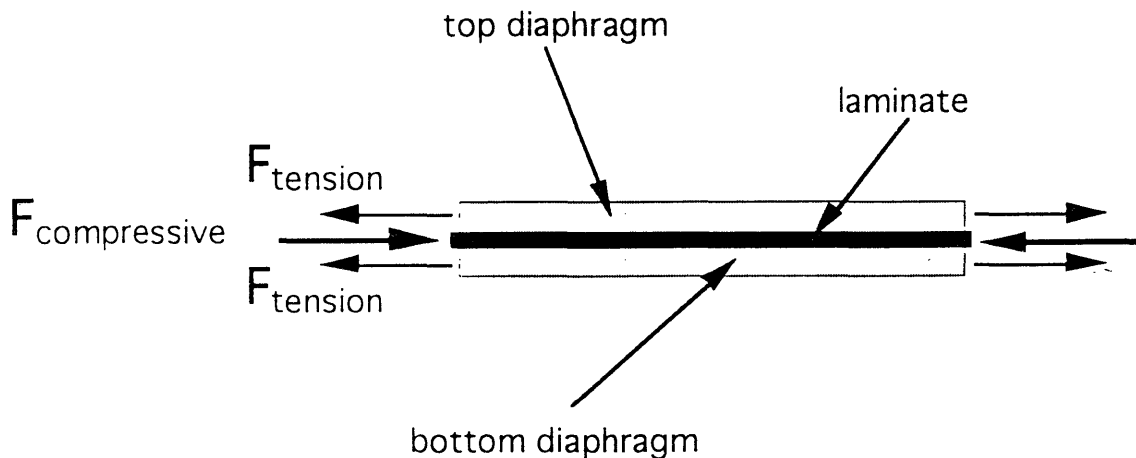


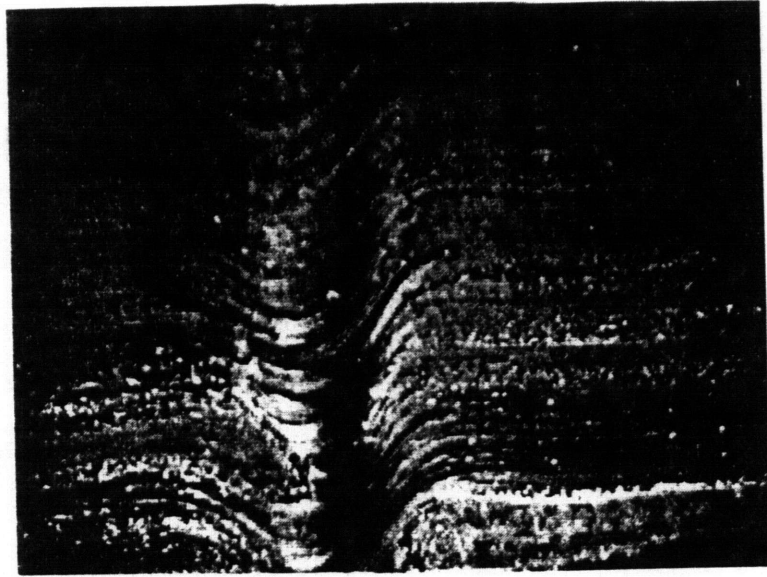
Figure 2.17: Illustration of the laminate being clamped by the diaphragms

2.5.1.2 Support the laminate

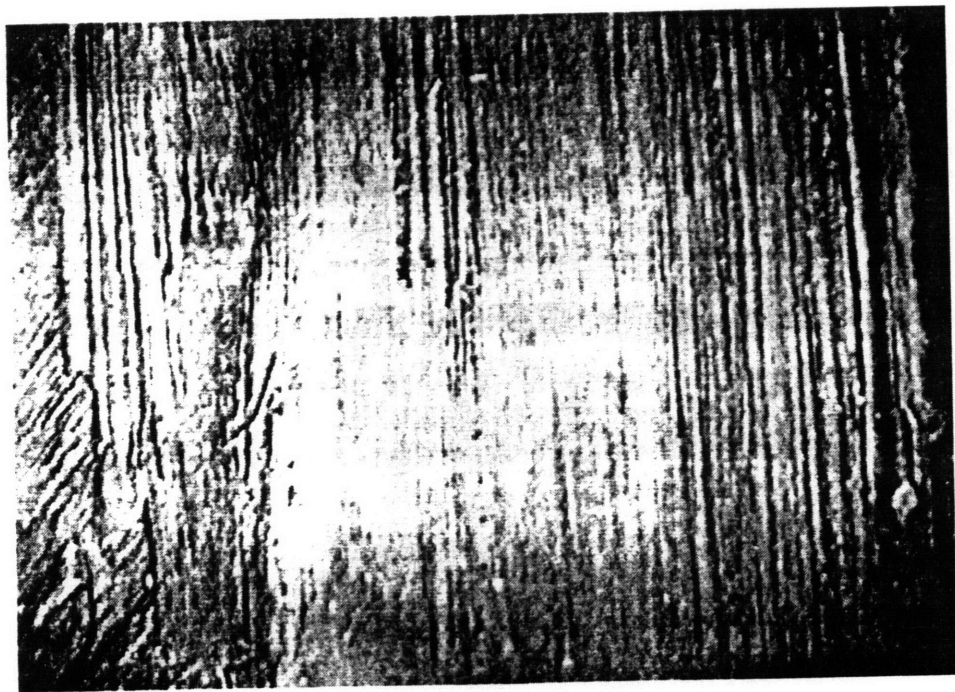
We can also view the laminate as being made up of elastic fiber bundles in a viscous resin sandwiched by two diaphragms with a certain stiffness and subjected to external pressure. In that case the diaphragm stiffness and the external pressure act as a support to the laminate when subjected to the compressive force building up in the composite. Laminate wrinkling can be seen as an instability phenomenon dependent on the buckling of a specific fiber orientation. In the case of a C-channel laminate wrinkling can be seen as buckling of 0 deg fibers. Two pieces of evidence help support this statement.

First, by peeling off each layer and examining them with a laser microscope, the author pointed out a waviness pattern only on the 0 deg ply, and not on the 90 deg, +/-45 deg plies. (See Figure 2.18 for pictures of the fibers in each ply)

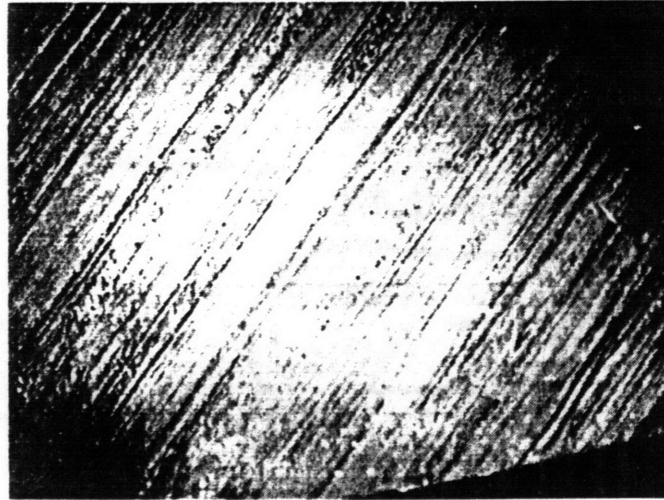
The second piece of evidence comes from the forming of two C-channels with different lay-ups. One was [0/90/+45/-45]_s [case (a)] and the other one was [90/90/+45/-45] [case (b)]. The author observed a big difference in the wrinkle patterns as can be seen in Figure 2.19 and 2.20. In case (a) the difficulty of achieving inter-ply slippage is greatest for the 0 deg plies and, therefore the wrinkle patterns are perpendicular to the 0 deg plies. In case b, there is no such wrinkle pattern, but instead, the 90 deg plies have a tendency to buckle on the inside.



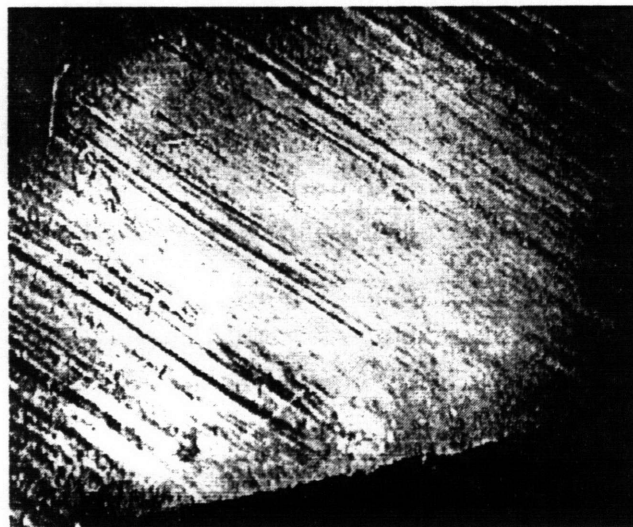
(a)



(b)



(c)



(d)

Figure 2.18: Laser microscope views of the fibers in different ply on the location of a wrinkle. (a) 0 deg ply (b) 90 deg ply (c) +45 deg ply (d) -45 deg ply (magnification X40)

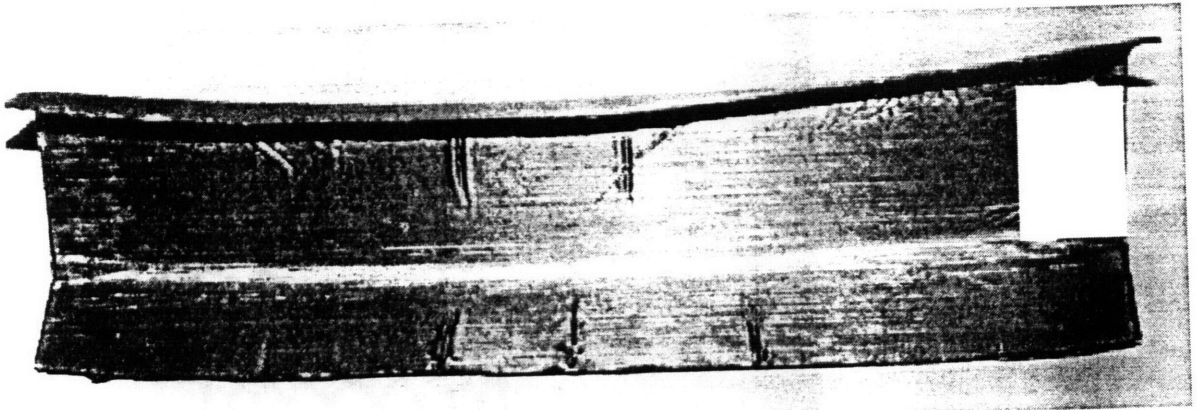


Figure 2.19: Illustration of the wrinkle patterns of a $[0/90/+45/-45]_s$ Toray C-channel

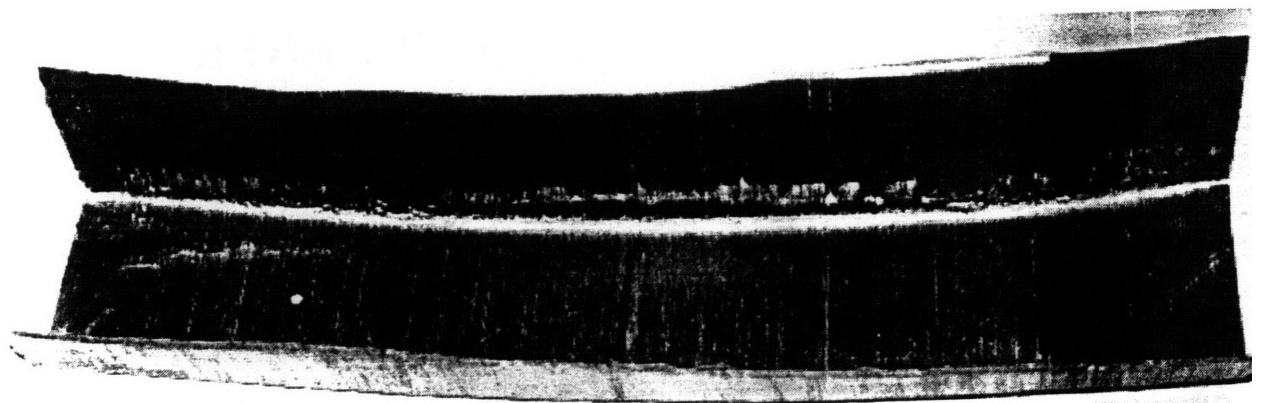


Figure 2.20: Illustration of the wrinkle patterns of a $[90/90/+45/-45]_s$ Toray C-channel

The primary support of the laminates during forming is supplied by the diaphragms. Thus, by increasing the stiffness or the thickness of the diaphragm we effectively increase the support to the laminate. If the contact between the diaphragms and the laminate is tight, the wrinkles have to

deform the diaphragm in order to grow, as can be seen in figure 2.21., therefore, the stiffer the diaphragm, the less likely the wrinkles will occur.

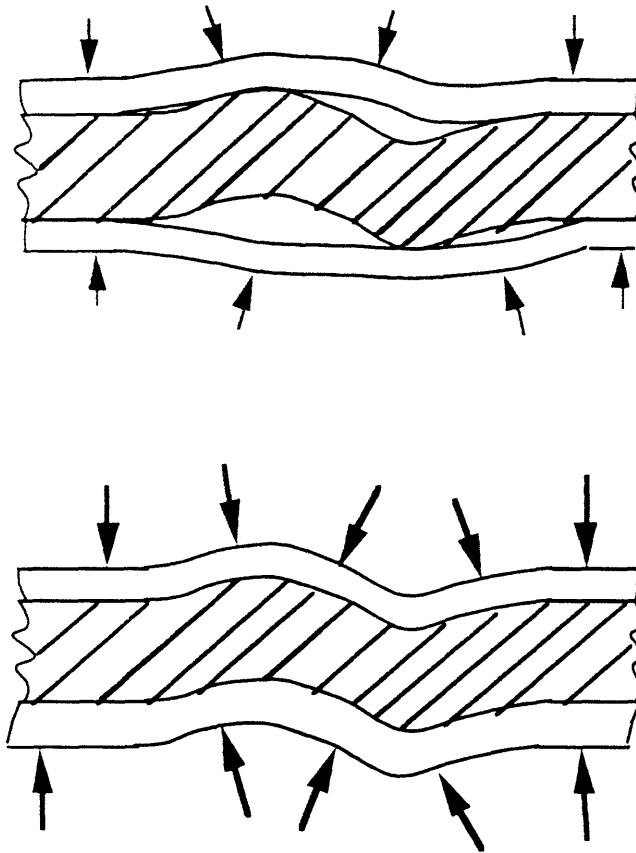


Figure 2.21: Effect of the pressure on the diaphragms.

External pressure may also effect the support by densifying the diaphragm material thus making it stiffer. And also, when the part hits the tool, the outside pressure tends to flatten the wrinkles by squeezing the laminate against the tool. So its seems that the higher the pressure, the better. However, as pointed out by [Bersee and Robroek], increasing the pressure may limit the inter-ply shear. Therefore there may be an optimum external

pressure that increases the support to the laminate without significantly limiting the inter-ply shear.

2.5.2 Forming sequence

Controlling the forming sequence is very important in order to obtain a given shape without wrinkles, as can be seen on Figure 2.22. In case (a) if the material hits the tool first on the edge, the deformation propagates toward the center, generating a wrinkle at the center of the part. In case (b) the deformation originates at the center and develops out toward the free edge.

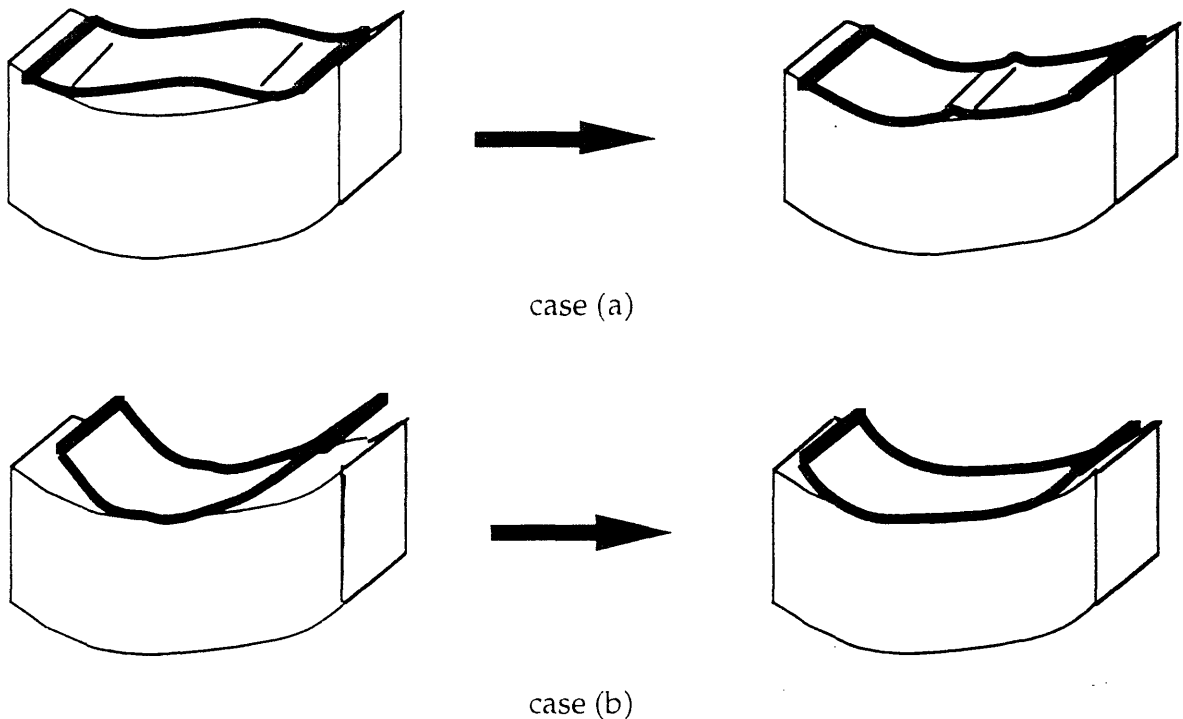


Figure 2.22: Illustration of the forming sequence for the case of the flange of a C-channel

The forming sequence is influenced by the geometry of the machine and the position of the tool in the machine.

2.5.3 Tool heating

This process related parameter is important especially when the tool is heavy and made with a high thermal conductivity material such as aluminum. As shown on Figure 2.23, heating the laminate from the top by convection or radiant heating does not really heat the tool, which may get warmer after a long preheating stage. In the case of an aluminum tool, the latter can be considered as a large cold source, and therefore, during forming when the part starts to form on the tool the inside plies are cooled even though the outside plies are still heated.

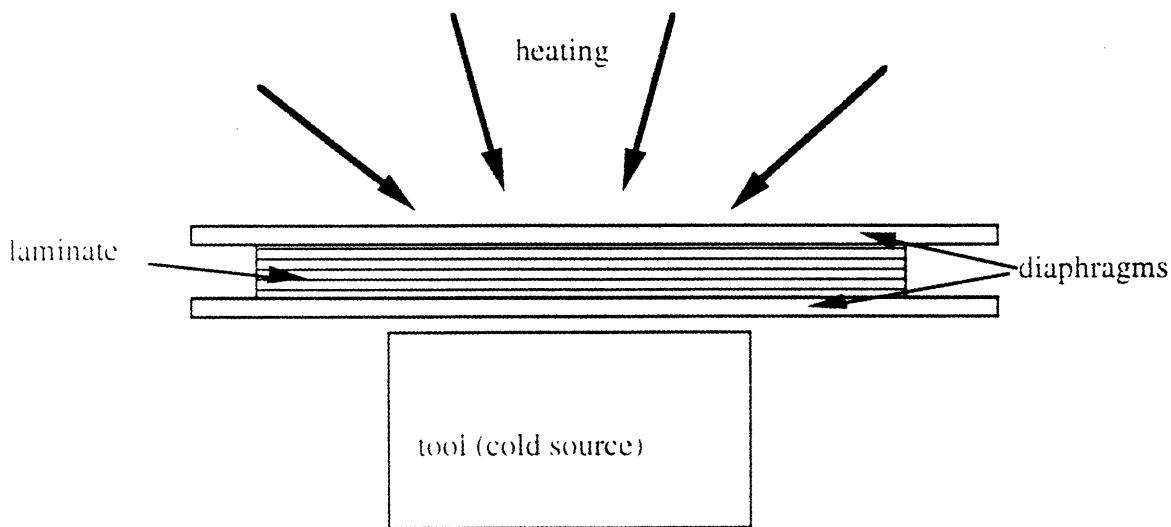


Figure 2.23: Illustration of the heating of the laminate.

By analogy with [Tam and Gutowski]'s work which was a numerical study of the effects of non-isothermal forming on the creation of compressive stress in the laminate. Figure 2.24.a illustrates the temperature distribution

through the thickness of the laminate and 2.24.b illustrates the corresponding approximated stress distribution through the thickness when the laminate hits a cold tool. Therefore the curves 2.24.b shows compressive stresses which can built up in the core of the laminate making it more likely for wrinkles to appear. The effect is also that the temperature distribution is more even over the part, therefore the average temperature is higher with heating the tool and the outside of the part, than the configuration where the part is only heated on the outside.

The effect of heating the tool on the quality of the parts has been confirmed experimentally by the author by forming parts with and without heating the tool. The tendency is that wrinkles are deeper, or more likely to happen when the tool is not heated.

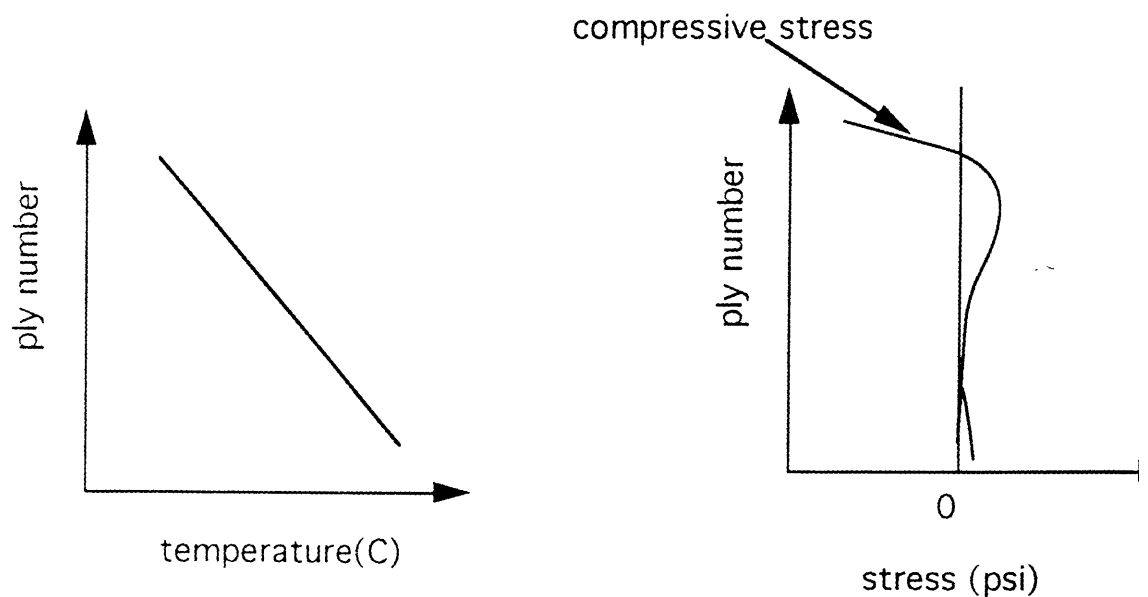


Figure 2.24: Qualitative illustration of the non-isothermal heating on the stress inside the laminate.

2.6 Forming limit diagram

To prevent the loss of many parts because of laminate wrinkling, it is necessary to have a means to determine the forming limits of the diaphragm forming process. The forming limit diagram is aimed at representing graphically the balance between the mechanisms that induce and suppress wrinkling. The primary mechanism that induces wrinkling is the compressive force which builds up in the laminate and the mechanism that suppresses the wrinkling are related to the tension of the diaphragm.

2.6.1 Mechanisms causing Laminate Wrinkling

We have seen in section 2.3.1 that the wrinkles arise in areas where the shear stresses are too large to be relaxed at a given deformation. And as we have seen in section 2.3.1 there will be a compressive force generated in that region. As we have seen in section 2.4 the compressive force is time and rate dependent and as [Li] has shown, the compressive force in an elemental volume can be approximated by:

$$F_{eq} \sim N_p h_{int} \frac{m}{n+1} \frac{\bar{\Gamma}_{3v}^{n+1}}{t^n} \quad (2.7)$$

N_p : Number of plies

h_{int} : Thickness of one ply

$\bar{\Gamma}_{3v}$: Evaluation of the interply shear

t : Forming time

m, n : rheological factor, evaluated experimentally by the drape test.

2.6.2 Mechanism suppressing the wrinkles

[Li] has considered that the main mechanism resisting the laminate wrinkling is the diaphragm tension. The diaphragm tension is given by the diaphragm thickness D and the nominal stress in the diaphragm:

$$T_d \sim D\sigma_{11}^* \quad (2.8)$$

2.6.3 Forming limit diagram

Therefore based on the equation (2.7) and (2.8) we can draw the following forming limit diagram as F_{eq} versus T_d as follows: (Figure 2.25)

The white marks represent the good parts and the black ones, the bad parts.

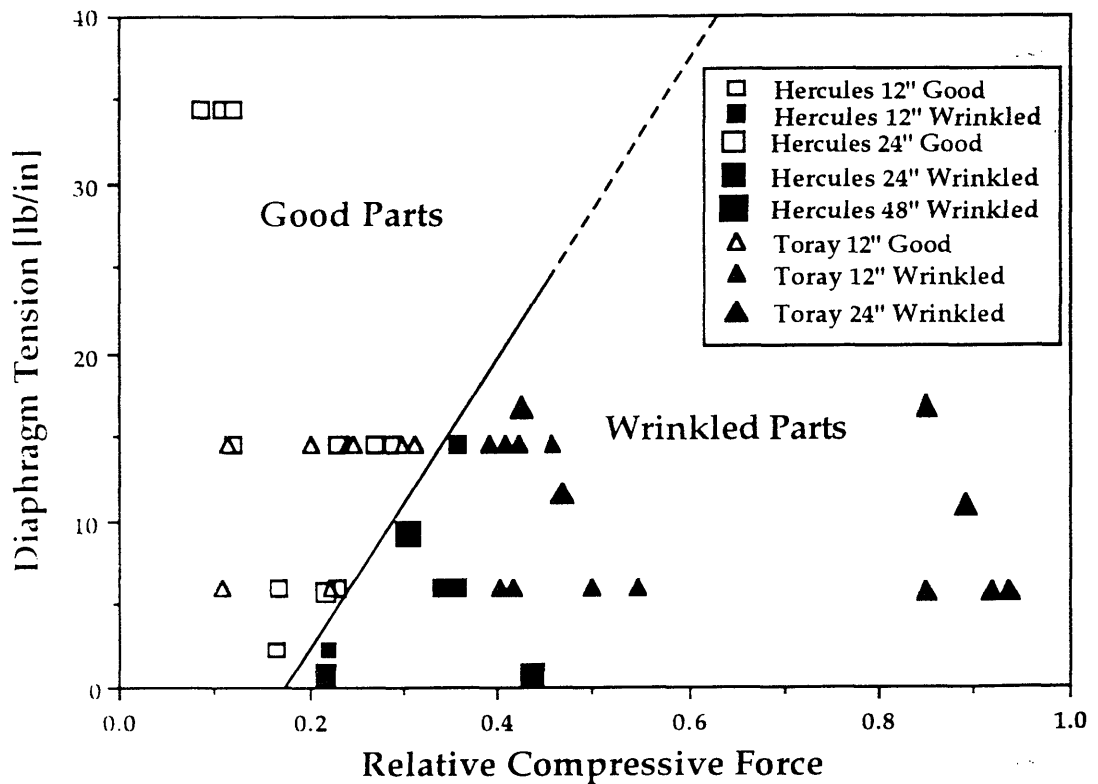


Figure 2.25: Forming limit diagram for C-channels of different sizes

Chapter 3

OCEAN ENGINEERING'S APPLICATIONS

3.1 Introduction

Because diaphragm forming has the potential to manufacture complex shaped parts at a relatively low tooling cost, this processing technique is very attractive for marine applications. Among its many advantages, diaphragm forming must allow better fiber placement control than that of other forming methods like matched metal dies, hydroforming, or rubber pad forming. It also requires lower pressures which may enable this technique to make larger parts [Smiley and Schmitt], and because of its simplicity of handling, the machine can readily accommodate various inexpensive tools and many different materials.

Diaphragm forming or vacuum forming can be used as follows:

- assisting the preforming of the fiber mat for a Resin Transfer Molding (RTM) process.
- forming chopped glass fiber thermoplastic or glass mat reinforced thermoplastic.

- forming big double curved shell-like structures, like boat hulls. This is a challenging task, but diaphragm forming has the potential of forming large parts.
- forming small parts (a few feet long) with carbon fibers.

This chapter will briefly discuss the different potential uses of diaphragm forming with respect to its competing process and will focus on the design of a part of interest to naval architects and that can be made by diaphragm forming. Some work has been done to evaluate how feasible this part would be.

3.2 Different applications related to diaphragm forming

3.2.1 Assisting RTM (Resin Transfer Molding)

Resin Transfer Molding is a close mold process by which dry fibers are laid into a mold and the resin is then injected into this mold.

When a large number of double curved shell-like structures are required, fiber preforms have to be formed in order to apply RTM. K. Van Harten [Shenoi and Wellicome] used a diaphragm forming process where a thermoplastic powder is brushed onto the fiber material, and the material is then formed under vacuum at an elevated temperature and then cooled down so that its shape is stabilized. This technique allows a good fit of the

preform with the mold, avoiding folds or pleats. This is due to the ability of angle variation between the yarn system (weft and warp) as seen on Figure 3.1.

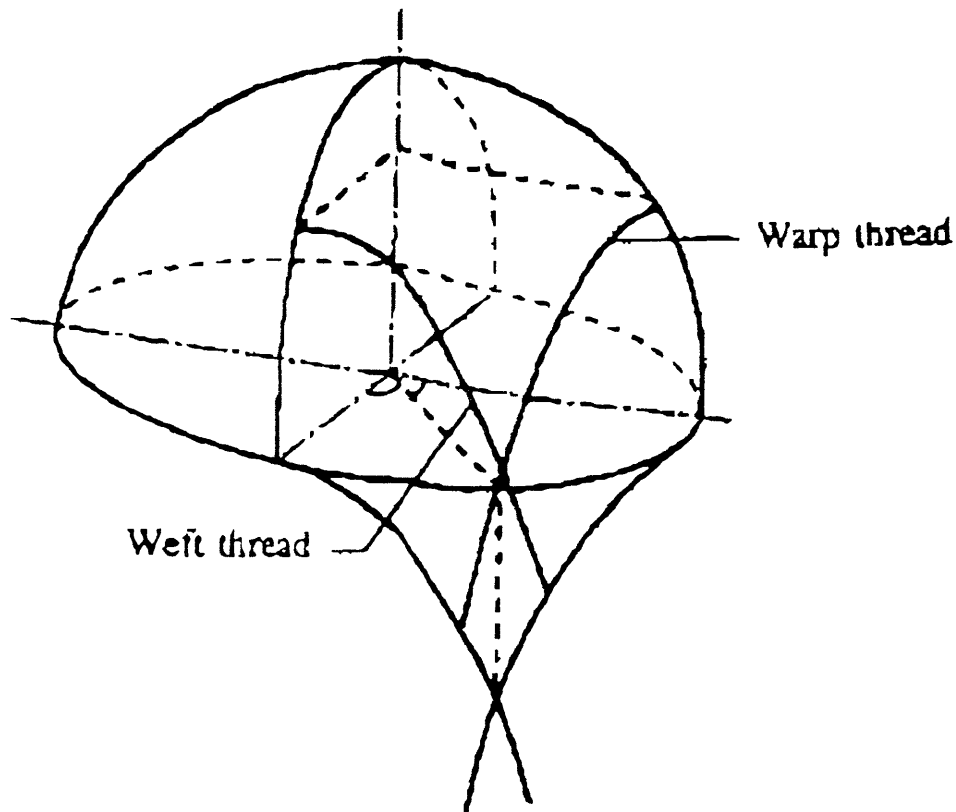


Figure 3.1: Trellising deformation of woven fabric draped over a sphere.

But the problem of this technique is that because of the trellising behavior of the woven fabric, the fibers are no longer evenly spaced and the fiber volume fraction is not constant over the part.

Another variation on this process is the use of the flexible resin transfer molding (FRTM) process. FRTM is an hybrid combination of diaphragm forming and Resin Transfer Molding (RTM) [Foley]. Separate sheets of dry fibers and solid resin are placed between two elastomeric diaphragms and

heated so that the resin liquefies. [Foley] The fiber and resin are then compacted by drawing a vacuum between the diaphragm, and formed to shape by drawing the diaphragm assembly over a hard tool. (See Figure 3.2)

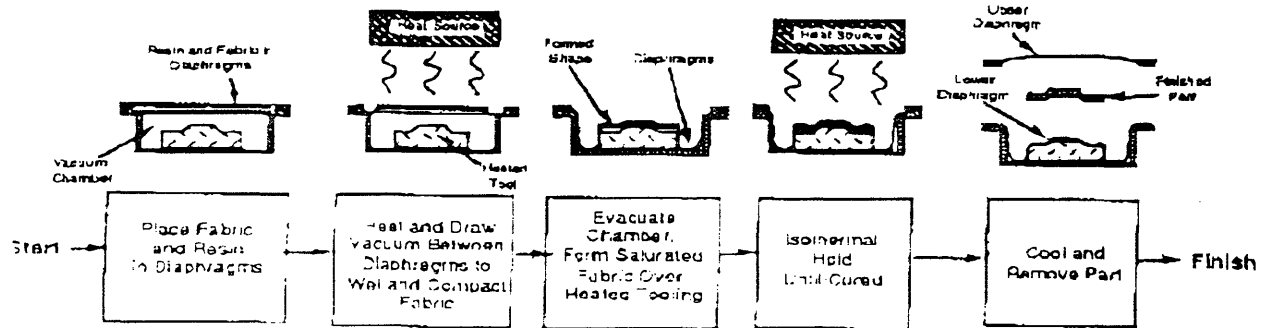


Figure 3.2: Illustration of FRTM process flow diagram.

3.2.2 Glass reinforced thermoplastic forming

The technique of forming chopped glass fiber thermoplastic or glass mat reinforced thermoplastic with the diaphragm forming process capitalizes on the fact that these materials are very easy to form and that the forming pressure used in diaphragm forming is uniformly applied over the diaphragm. Therefore the parts would be smoother and the thickness variation would be less important than with match die forming or stamping. Because the male or female mold tool can be easy and cheap to manufacture, a wide variety of parts could be made by diaphragm forming.

3.2.3 Forming whole hulls

In the author's opinion, this technique has not yet been applied, but the potential is huge for the pleasure craft industry. The main characteristic of ship hulls is that they are usually double-curved shapes with for the most part smooth radius variations, although some areas of the hull like the keel or the bow can have sharper edges. In the pleasure craft industry production runs of 500 units or 6 to 12 foot long vessels can be planned. In this range of size and production run, diaphragm forming seems to fit well as an automated manufacturing process. Among the manufacturing techniques which can be automated for processing ship hulls we can find:

- tape lay-up
- the automated spray-up
- thermoforming of composites

Tape lay-up requires a high tooling investment in order to develop the manufacturing capabilities, therefore high production volumes are required to redeem the investment. But this option is being studied by some shipyards for the case of big hulls (>20 m long) , and some telescopic facilities have been developed[Raymer].

Automated spray-up is actually the main automated manufacturing process for hulls. (See Figure 3.3) This technique has shown good results and is less labor intensive than the hand lay-up, therefore also more economical.

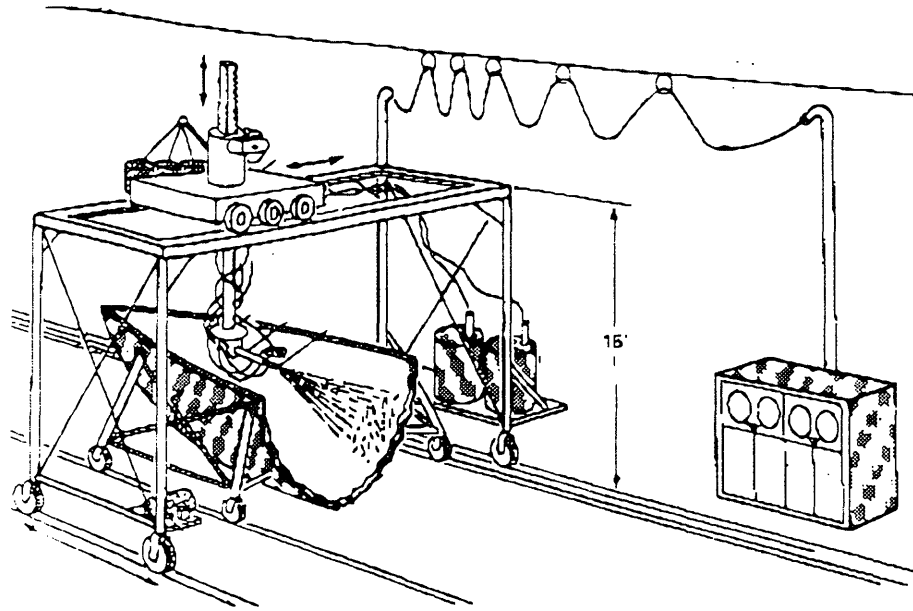


Figure 3.3: Illustration of automatic spray-up

However, the automated spray-up process has some disadvantages, such as:

- Emission of styrene, which can be harmful to the operator, and requires special safety procedures.
- High void content, because air can be entrapped during the spray-up. Therefore this technique, if not applied with care, will result in a laminate with generally a lower quality than that obtain by hand lay-up.
- lack of universality in the use of material. The spray-up techniques require the use of short fibers which have slightly lower mechanical properties than long fibers. Thus requiring, in some case, the use of a manual hand lay-up of prepreg or continuous fibers, if higher structural properties are needed.

In some special cases specific sandwich design requires the lay-up of different materials such as continuous fibers, foam core, or thermoplastic sheets. Therefore a good technique should be flexible enough to accommodate different kinds of materials.

Moreover, in the perspective of increasing governmental regulation of gas emission originating from gel-coat fiber reinforced polyester manufacturing processes, new closed molding techniques are being investigated by boat manufacturers. The work of [Young] focuses on the thermoforming of thermoplastic composite hulls and decks for the market of 7 meters long boats with production runs exceeding 250 units a year. And [Young] points out that the thermoforming technique (such as matched die molding) has the potential of dividing by five the manhours to produce the hull and deck for these boats, from 25 - 40 hours for conventional FRP manufacturing technique to 5 - 7 hours with a thermoforming process.

From these perspectives, diaphragm forming has some advantages over automated spray-up because the technique is more flexible and can handle different types of materials. Moreover, it is a less hazardous technique which allows a better control of toxic fumes. Diaphragm forming has the potential to yield better results than matched die molding at a significantly lower tooling cost.

However, before this technique can be applied, the size scaling effects must be understood and fully prospected [Li]. This can be overcome by "Reinforced Diaphragm Forming" as developed in the chapter 4.

Another problem related to the use of double diaphragm forming is the presence of an inner diaphragm which does not allow a good control of the

inner dimension of the part. This is due to the fact that while stretching, the thickness of the diaphragm can vary a lot. This variation may not be crucial for a hull, but the inner diaphragm can be eliminated by using a thin disposable diaphragm, or by using the "Inflated Tool Forming" developed by the M.I.T composite forming group. (see Figure 3.4 for a brief description of Inflated Tool Forming").

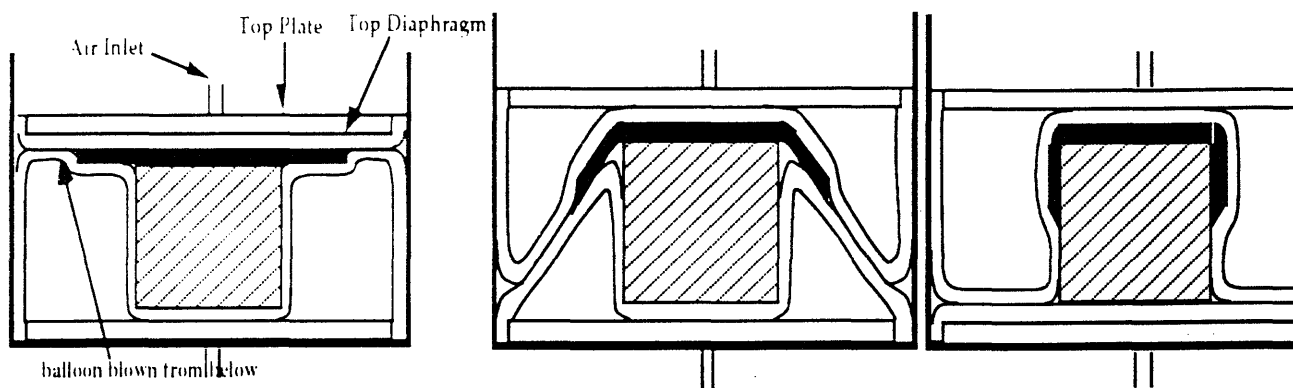


Figure 3.4: Inflated Tool Forming

3.2.4 Forming advanced composite for marine applications

Many Ocean Engineering applications require the use of high strength and high stiffness composites which are not subject to static fatigue. For applications like submarines, high speed boats where weight is an important issue, the use of carbon fibers is increasing. Many small size parts made out of carbon fibers are then required, the study will now focus on the feasibility of manufacturing a part which would realize the intersection of two orthogonal stiffeners.

3.3 Design and proof of concept

3.3.1 Design of the part

When building a stiffened single skin vessel, the intersection of two orthogonal sets of stiffeners (Longitudinal and Transversal) is a critical aspect in the design of a ship hull. Stiffener intersections are difficult to fabricate, heavy, and produce stress concentrations. For marine applications, the design of composite stiffeners is referred to as "top hat" shape, as shown in figure 3.5.

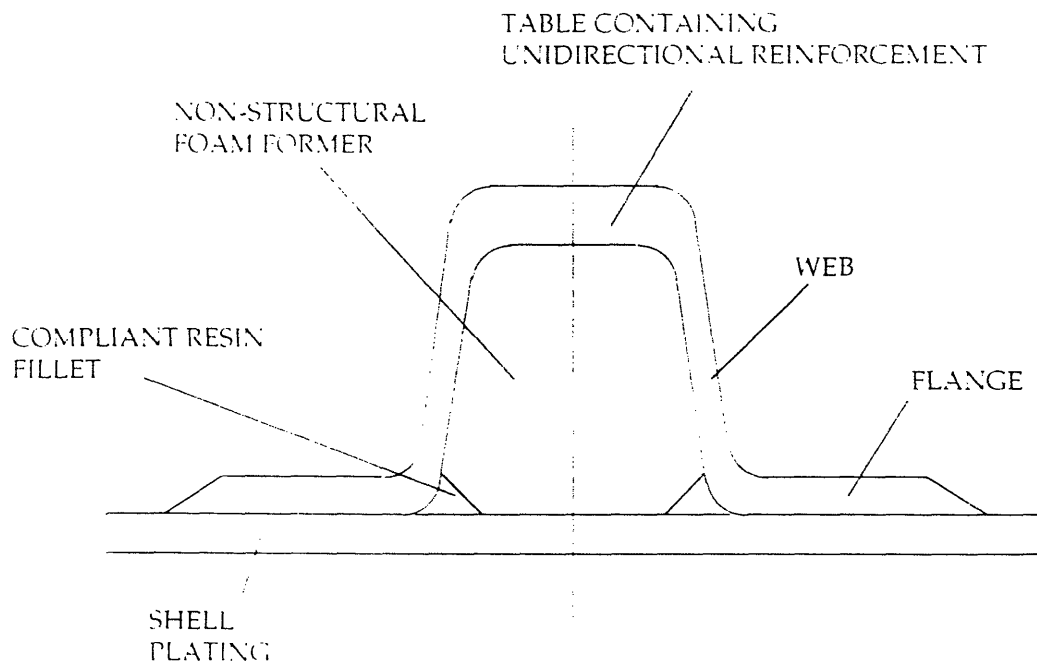


Figure 3.5: Single skin hull typical stiffener top hat shape

Figure 3.6 shows a cross section of the structural arrangement of a transversely framed single skin hull

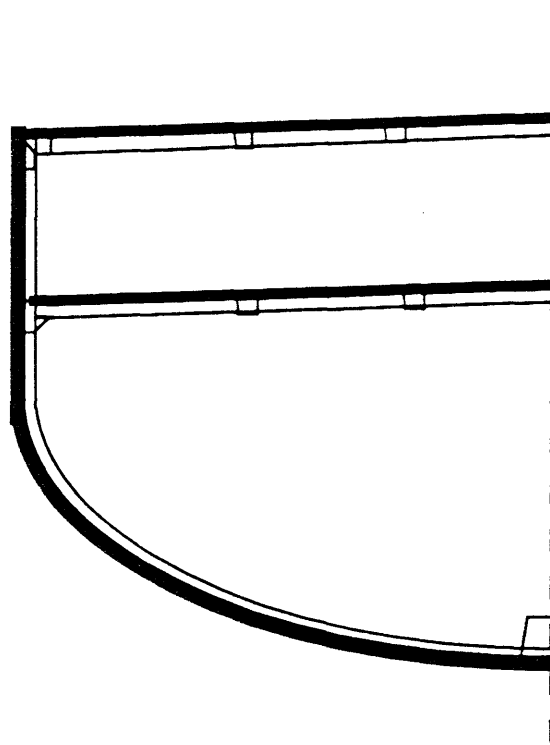


Figure 3.6: Transversely framed single skin hull

Figure 3.7 shows a typical stiffened plate with transverse and longitudinal stiffeners intersecting each other in many places.

Figure 3.8 shows the structural arrangement of the Sandown Class minehunter with a longitudinally stiffened bottom to avoid, as much as possible, stiffener intersections, although, as we can see on fig 3.7, it is not always possible.

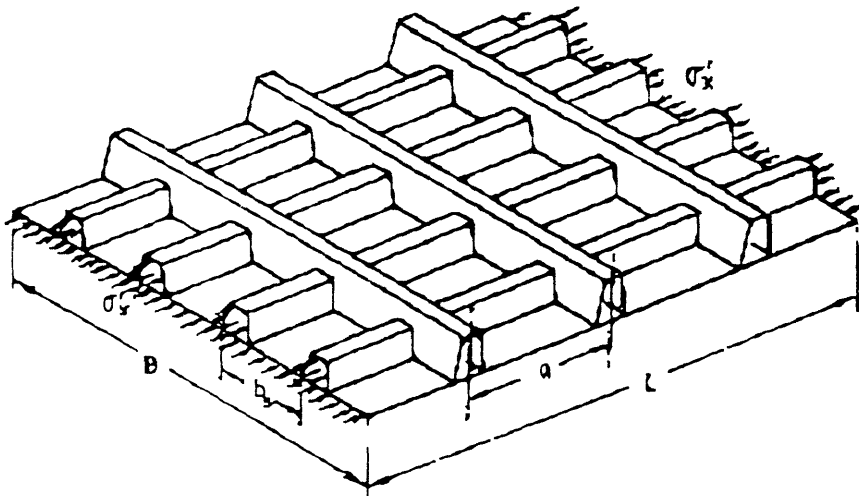


Figure 3.7: Stiffened plate with transverse and longitudinal stiffeners.

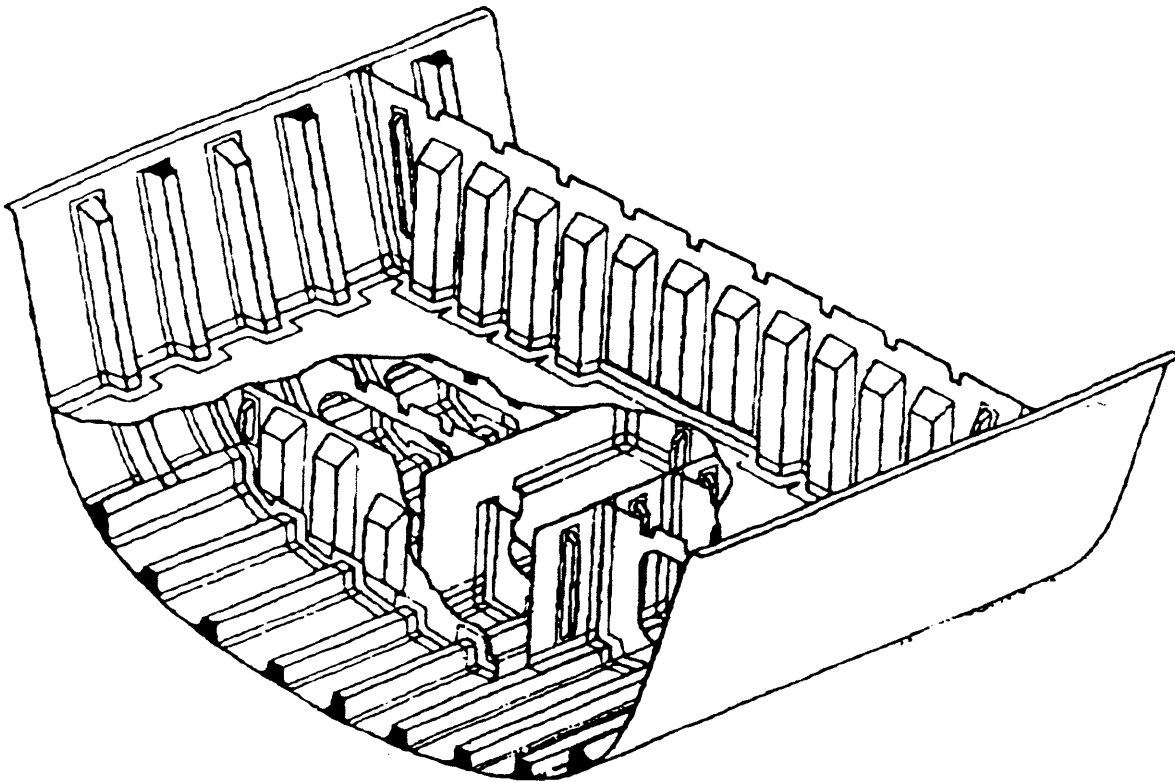


Figure 3.8: Longitudinally stiffened single skin hull

The idea underlying this work is to design a unique cross-shaped part which would more easily accommodate the intersection of stiffeners. The part has the shape shown in Figure 3.9. In Figure 3.9, the two intersecting stiffeners have the same dimensions, but this is not a requirement.

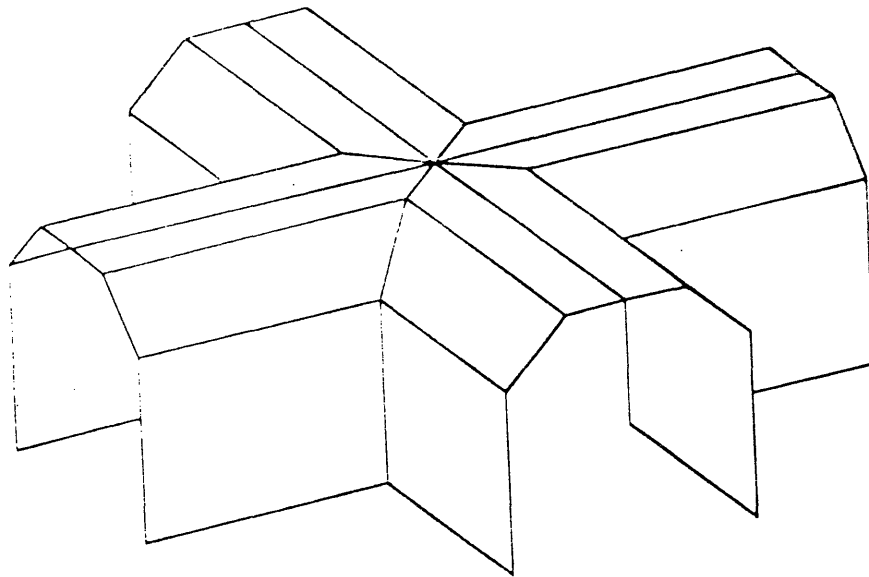


Figure 3.9: Illustration of a Top-hat shape intersection cross with sharp corners

This part is not easy to hand lay up because of its many different curvatures. This part presents interesting problems for diaphragm forming because it has a reverse curvature which has not been investigated before. In order to improve the cost effectiveness of this process this part should be standardized, so that one tool can process many intersections. In order to do

so, the number of different stiffeners sections require to reinforced a hull should be minimized. If this is not possible, a composite part which would make a transition between a stiffener and an intersection with different dimensions can be designed as in Figure 3.10. Trying to standardize the part difficult to manufacture is an important task in order to track down the cost. If this type of part could be standardize, its cost could be sharply cut down by using the diaphragm forming process.

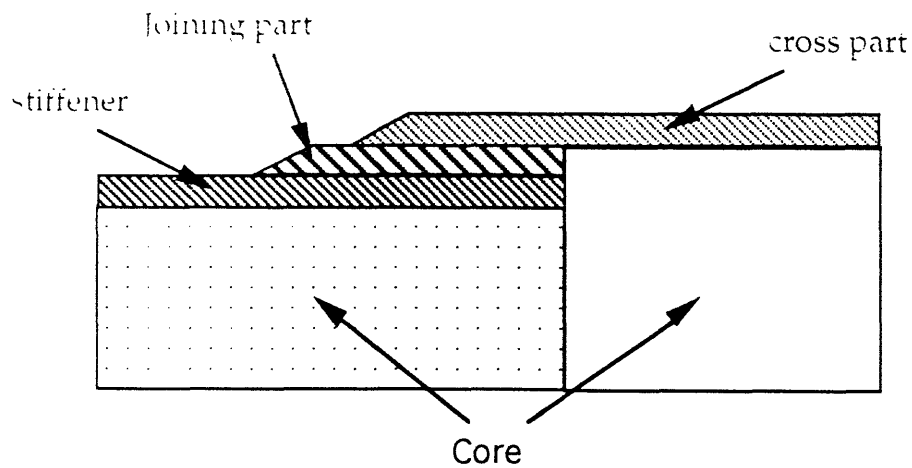


Figure 3.10: Joining part for different stiffeners sizes.

3.3.2 Experimental approach

The process of manufacturing this part starts by the realization of a tool, in our case, the easiest and cheapest way was to build a male wooden tool with some fillers for the fillet. The dimensions of the tool are shown in figure 3.11.

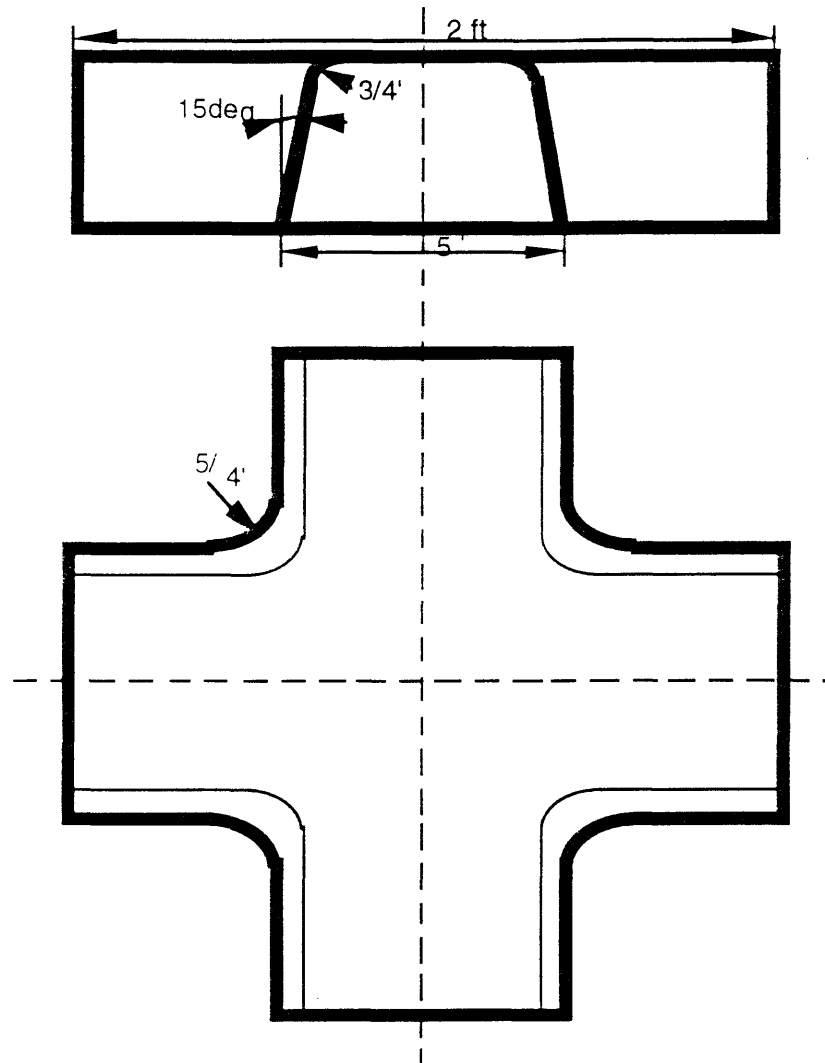


Figure 3.11: Top view and front view of the top-hat shape intersection part.

The forming machine was set up as described in Figure 3.12

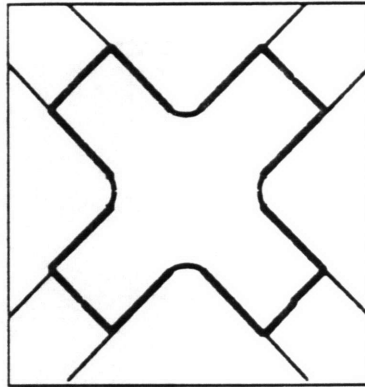
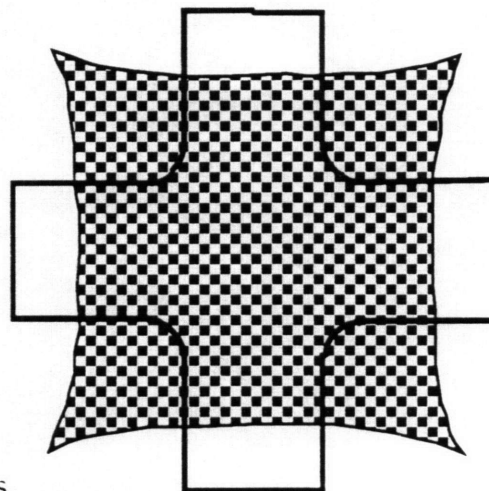
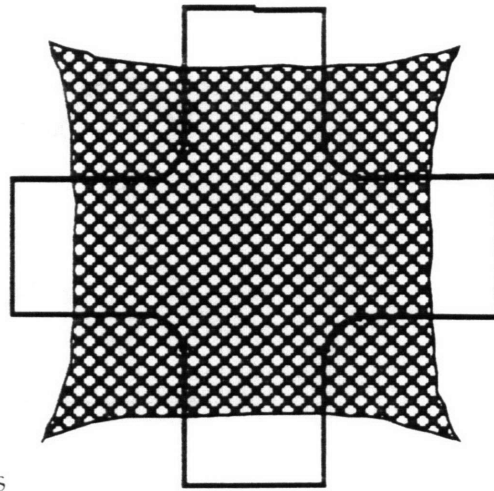


Figure 3.12: Illustration of the set up of the forming machine.

The first set of experiments was aimed at understanding where the wrinkles were the most likely to occur. In order to do so, two sets of four plies of AS4/ 3501-6 Hercules woven material with different ply orientations have been tested at room temperature and with a high forming rate on the order of two minutes. As seen in chapter 2 these conditions are drastic because at room temperature the inter-ply shear stresses are very high and with a high forming rate the shear stress have only little time to be relaxed.



Experiment 1.a: (0/90)s



Experiment 1.b: $(+/-45)_s$

It is very interesting to note that the forming ability of these two laminates depends strongly on the ply orientation.

Figure 3.13.a and 3.13.b illustrates the forming of $(0/90)_s$. Although the forming conditions were drastic, as described above, the part appear quite acceptable, apart for some difficulty in forcing the laminate to conform exactly to the fillet.



a) side view

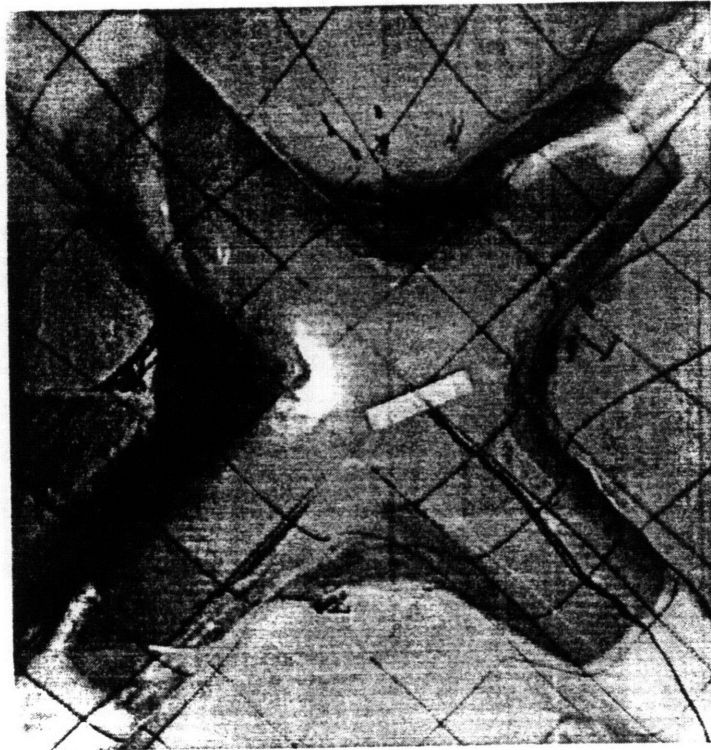


Figure 3.13: Illustration of the forming of $(0/90)_s$

Whereas Figure 3.14 shows the result of experiment 1.b, with a ply orientation of $(+/-45)_s$. The wrinkles are due to the fact that because the diaphragms effectively pin the fibers on the top surface of the tool, the fibers can no longer shear to accommodate to the fillet shape.

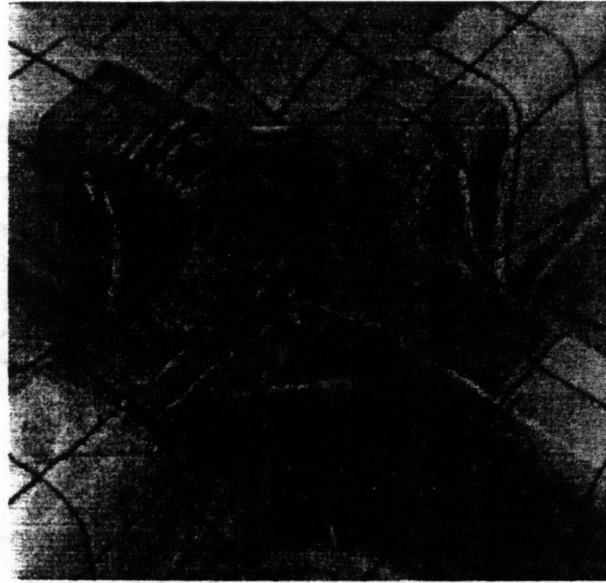


Figure 3.14: Illustration of the wrinkling phenomena for (+/-45) plies

The problems of wrinkling and lack of conformance to the fillet radius can be overcome somewhat by increasing the temperature and by tailoring some plies in order to improve the ability of the plies to shear relatively to each other. As seen in Section 2.4 increasing the temperature will reduce the inter-ply shears building up in the laminate. The aim of tailoring the fibers is to help reducing the inter-ply slippage, and to reduce somehow the propagation length of the shear along the fibers, because as seen in section 2.2.2, the local deformation must propagate out to the edge of the ply, the cut out can be compared to a kind of edge created in the core of the structure to relax the shear stresses. Of course, the tailoring should be done with great care, because it tends to weaken the structure. Therefore the cut-outs should not be on top of each other, but as far as possible from each other, and if possible in areas where they will not damage too much the structural integrity of the part.

Figure 3.15 and 3.16 illustrates the different cut outs that can be done in order to improve the formability of the parts.

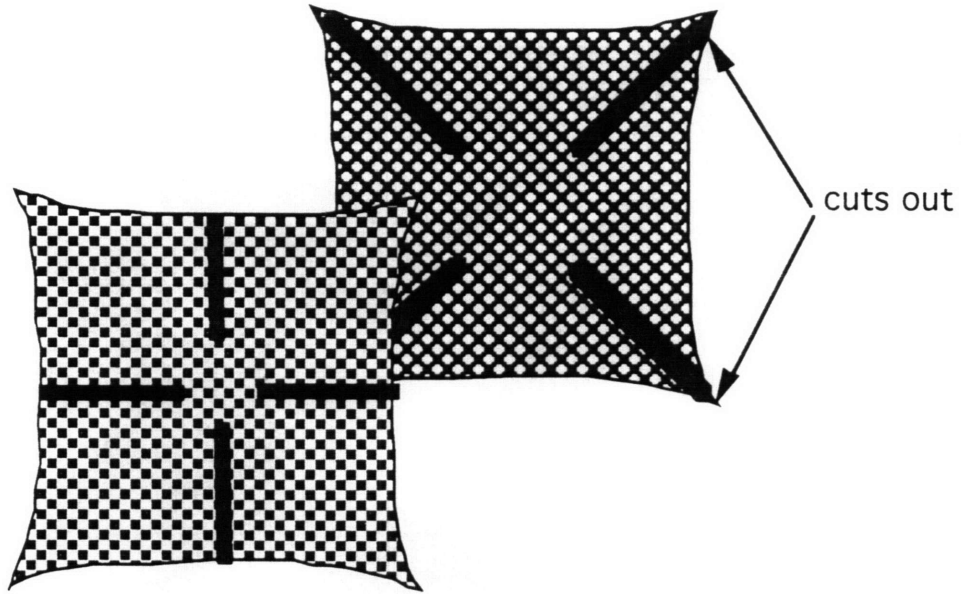


Figure 3.15: Illustration of the cut out of second set of experiments.

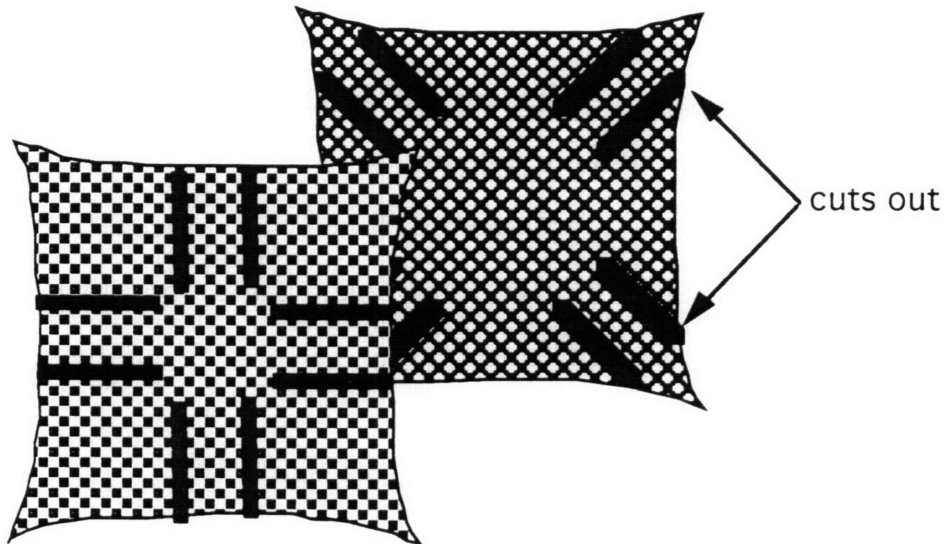


Figure 3.16: Another design of cuts out

The second set of experiments was aimed at verifying that the temperature and the presence of cuts helps the forming of the cross shape part. Figure 3.17 illustrates the effect of the cut-outs on the (+/-45) lay up, formed at room temperature, it is interesting to compare this picture with that from Figure 3.14 which was made in the same conditions.

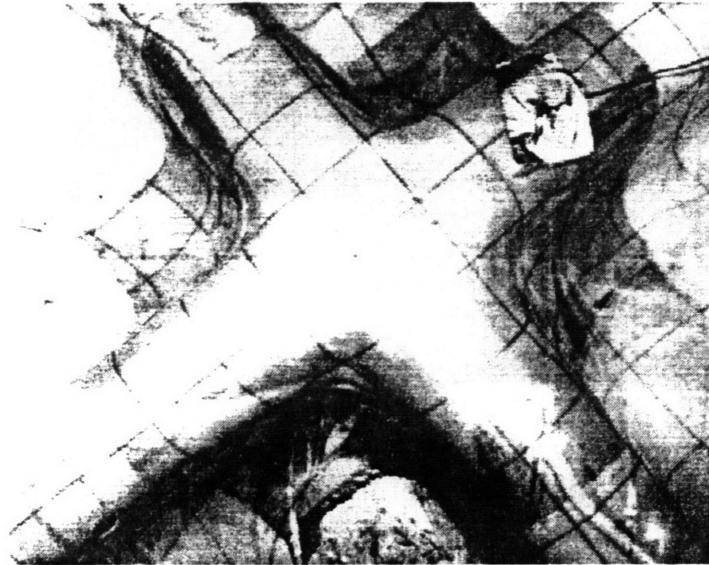


Figure 3.17: Effect of the cut-outs on (+/-45) lay-up

Figure 3.18 show a 16 plies $[0/90/+45/-45]_2s$ part which has been formed at 180°C with cut-outs as shown in Figure 3.15. A substantial reduction in the ply wrinkling of the (+/-45) orientation was noticeable and a better conformance to the fillet radius was obvious. But many other different cut-outs combinations can be designed (Figure 3.16 gives another combination, but the examples are many) and more work should be carried out in order to get a better understanding of the best place to cut.

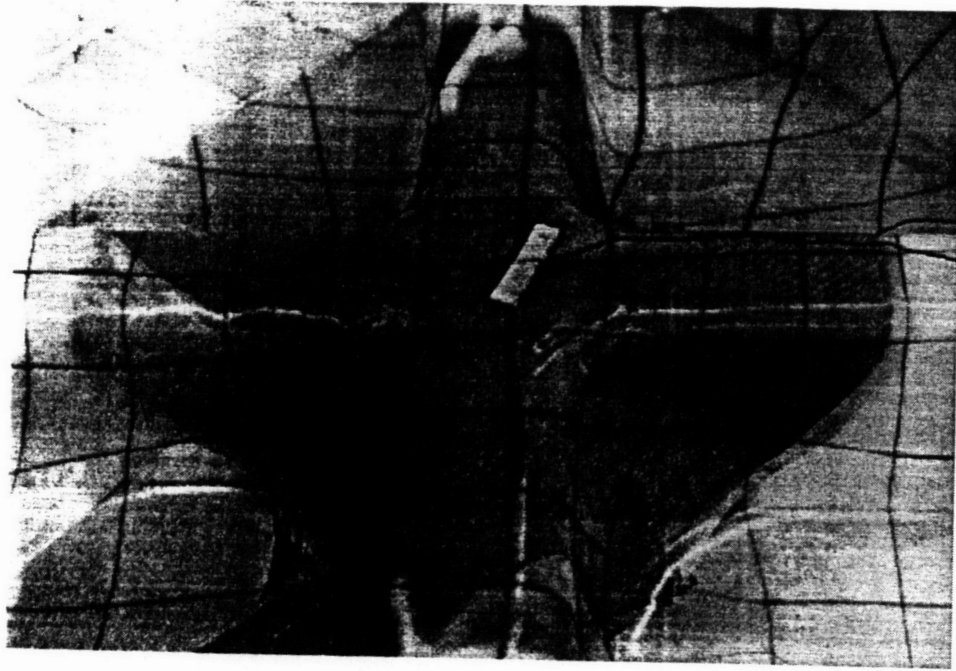
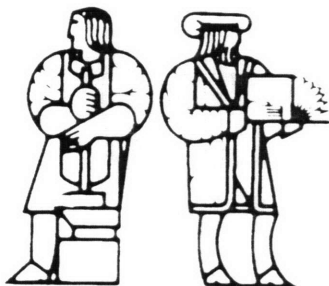


Figure 3.18: 16 plies part formed at 180°C with cut-outs



Chapter 4

INNOVATION: REINFORCED DIAPHRAGM FORMING

4.1 Introduction

This chapter is aimed at studying an interesting innovation in the diaphragm forming process. In order to reduce undesirable deformation modes such as laminate wrinkling, the “reinforced diaphragm forming process” increases support supplied to the composite by effectively increasing the stiffness of the diaphragms..

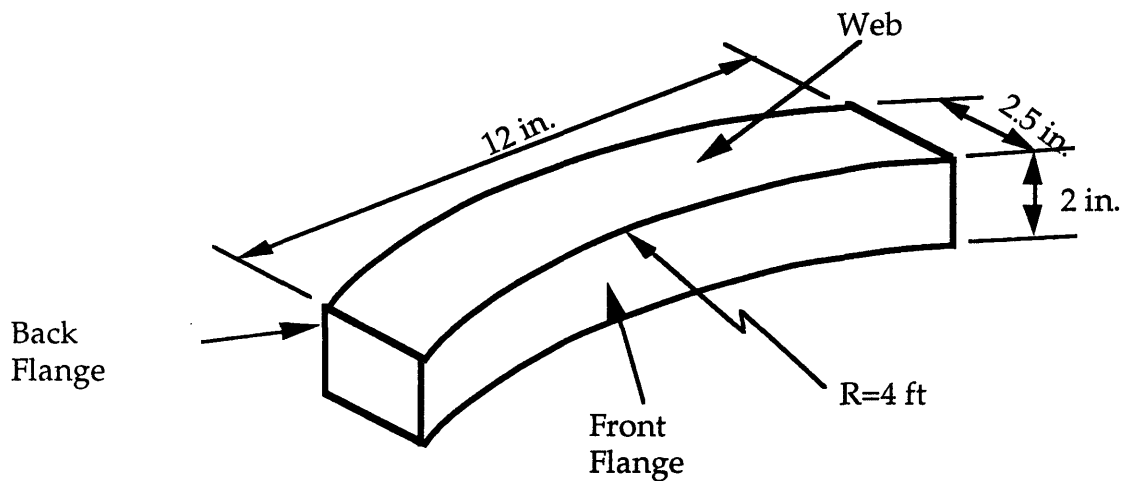
Based on the observations in section 2.5 the stiffness of the diaphragm is an important factor in the ability to form a laminate into a desired shape. This suggests the potential benefit of reinforcing the diaphragm. However, because of the relatively low forming temperature of thermosets (75 °c) and the use of no external pressure except atmospheric, we cannot use stiffer diaphragms like the aluminum based diaphragms used by [Monaghan, et al.] for forming thermoplastics (forming temperature: 225 °c). The aluminum diaphragm would have provided the necessary stiffness but would be more difficult to

deform at 75 °c. The idea behind the reinforced diaphragm forming technique is to tailor the stiffness of the diaphragm by increasing it locally. The technique chosen to do so is to weave together metal rods

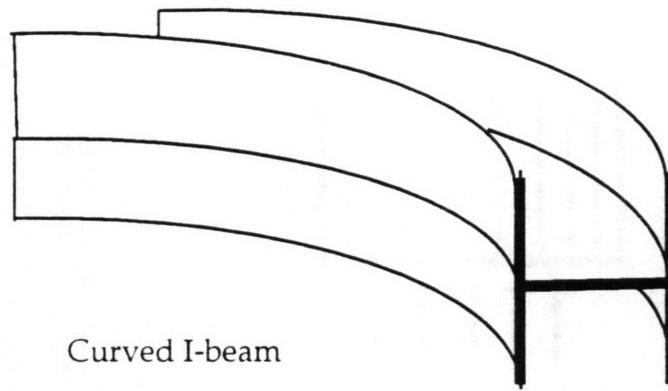
The technique for reinforcing the diaphragm using woven wires has been developed by the author. First we will explain how to weave reinforcement from different engineering materials such as nylon and steel. Then we will focus on the indentation problem, where the reinforcements become embedded in the deforming composites, causing surface irregularities, and determine the relationships between the reinforcement orientation, the optimum spacing of the wires and the materials. We will determine the net effect of the reinforcement on the formability of C-channels and finally we will see how this technique can be applied to different shapes.

4.2 Problem definition

The part which is the focus of our attention is a curved C-channel. Figure 4.1.a and 4.1.b illustrate the C-channel and its structural applications.



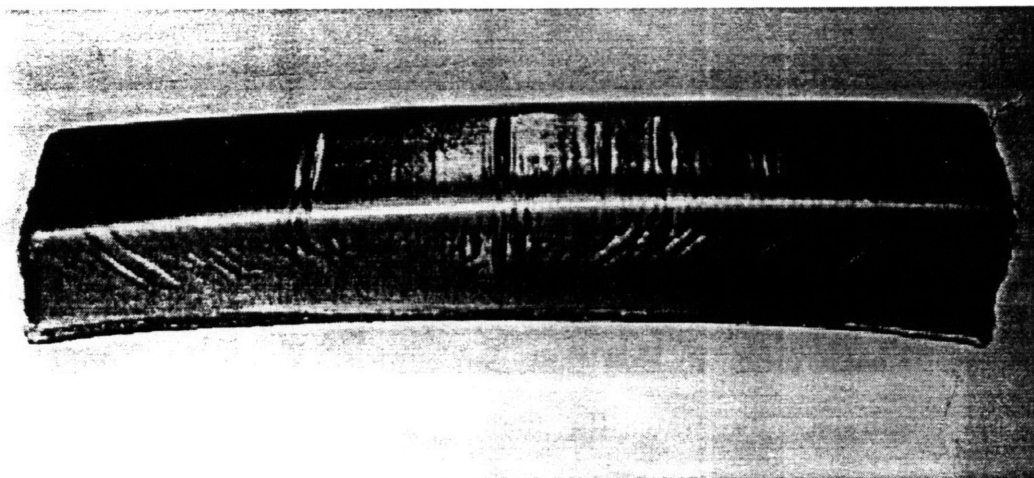
(a)



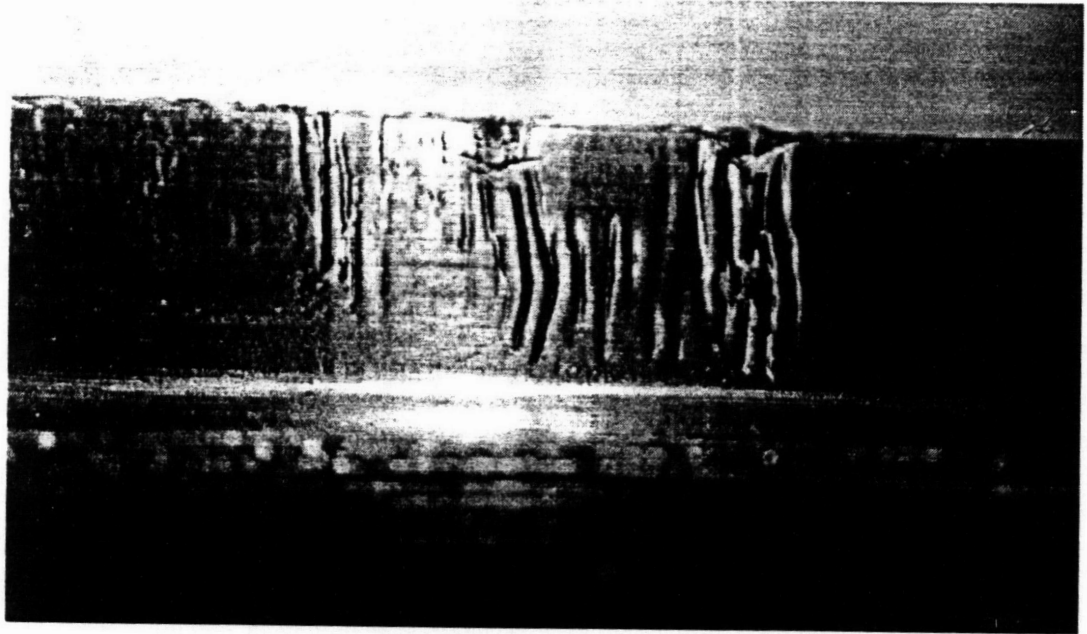
(b)

Figure 4.1: Illustration of a C-channel and its structural application as an element of an curved I-Beam

A typical wrinkling pattern for this type of part is shown in Figure 4.2.a and 4.2.b. Most of the wrinkles can be considered as buckling of the 0 deg plies, therefore it is more appropriate to support the laminate by stiff rods along this direction.



(a)



(b)

Figure 4.2: Illustration of the wrinkles patterns (a) on the Web (b) on the back flange

4.3 The Woven Reinforcement

The idea for making the reinforcement is to use unidirectional stiff rods linked together by another material to allow some slippage of the rods relative to each other so that they can conform easily to a double curved shapes. Figure 4.3 illustrates the shaping assembly. The technique we have adopted is to weave stiff rods in the fill direction with thread on the warp direction (see Figure 4.4). The woven fabric was made on the loom shown in Figure 4.5.

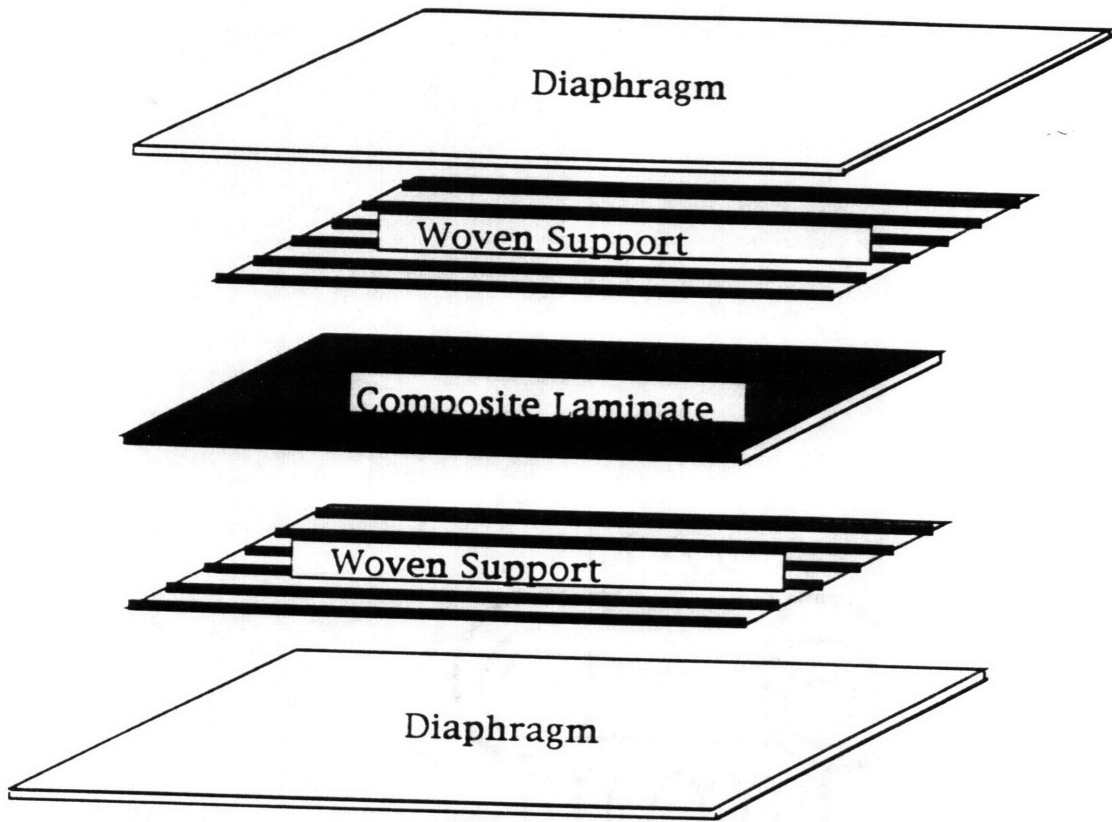


Figure 4.3: Shaping assembly

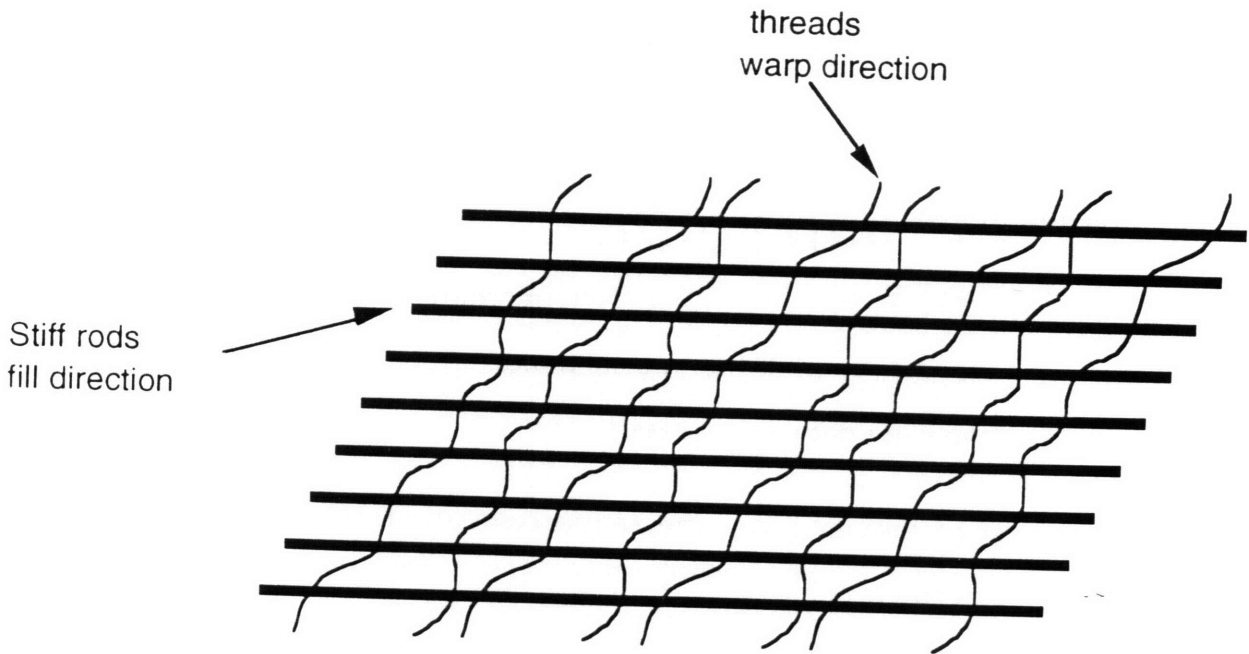


Figure 4.4: Reinforcement

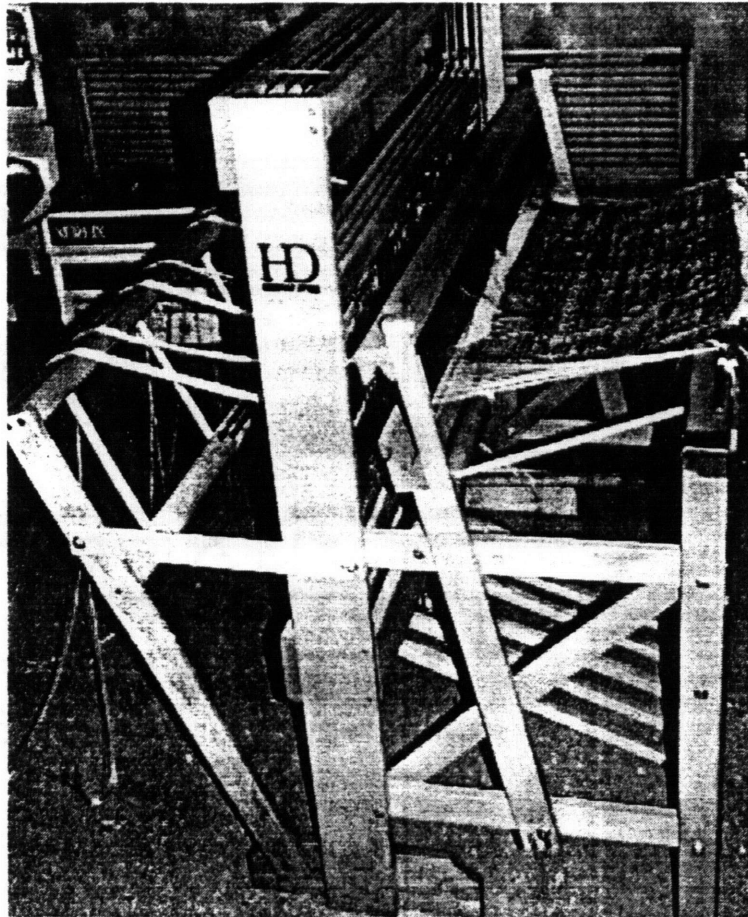


Figure 4.5: Loom

It is very important to join the stiff rods by another material in the warp direction, for the following reasons:

- (a) The fabric is easier to set up than individual wires not linked together, and the fabric makes it easier to maintain an even spacing between the rods.
- (b) In woven form, the reinforcement can easily be pulled off the formed part.
- (c) The reinforcement can be reused.

4.4 The indentation problem

The indentations caused by the reinforcement becoming embedded in the forming laminate, was of concern, as can be shown on Figure 4.6.

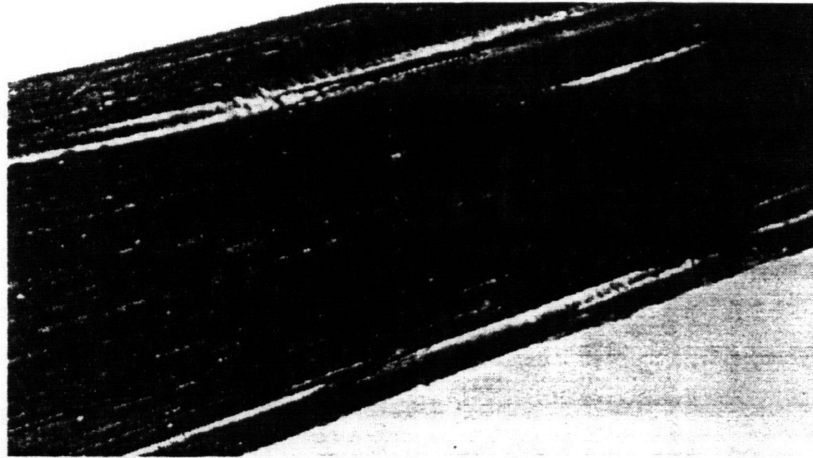


Figure 4.6: Illustration of the indentation problem for a two foot long C-channel

The indentation problem is even more dramatic if the rods are directly in contact with the laminate and become deeply embedded in the first plies, Thus while removing the fabric some carbon fibers can come with the rods as can be observed on Figure 4.6 where small strips of fibers are missing. But this problem can be easily solved by using a release element such as teflon fabrics or spray between the rods and the laminate. Thus the rods become easier to remove and separate from the composite. However, there still remains some marks on the surface of the laminate. It has been noted that this problem of indentation was not so severe, because after the removal of the reinforcement, the part is bagged to be cured in the autoclave or simply put back onto the tool and by pulling vacuum again between the two diaphragms, heated back up for a *partial cure*. (*partial cure* means that the part has been

put to the cure temperature , about 170 °C for about two hours, but without extra external pressure other than atmospheric. The shape is then stabilized, but the part is not fully consolidated because of the presence of voids or defects which have not been expelled by applying an outside pressure of a 7 or 8 times the atmospheric pressure). In both cases, because of the outside pressure and low viscosity of the matrix , the indentation marks are completely removed. Figure 4.7 shows the quality of a part which has been made by reinforced diaphragm forming and autoclave cure.

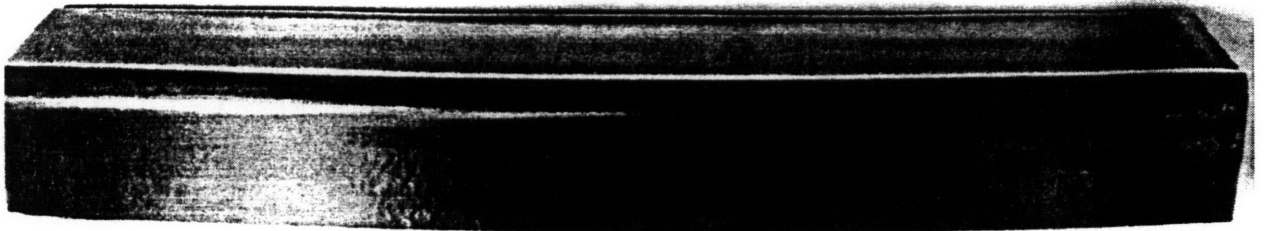
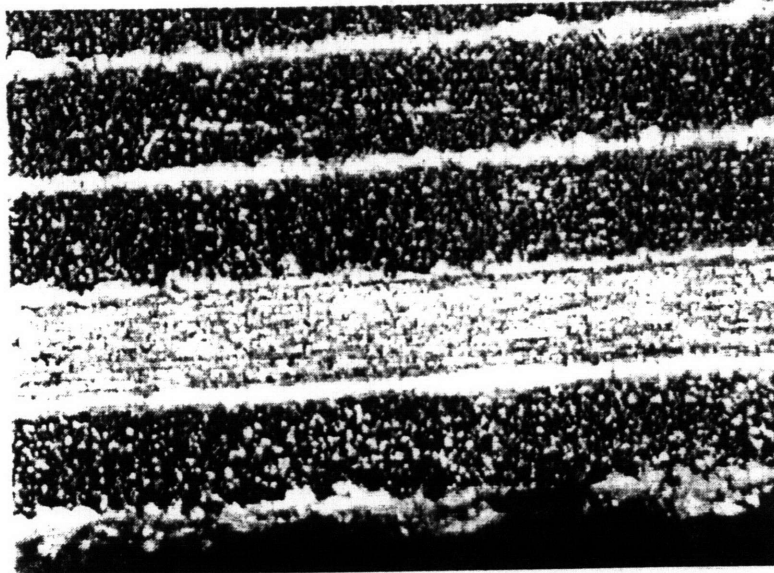
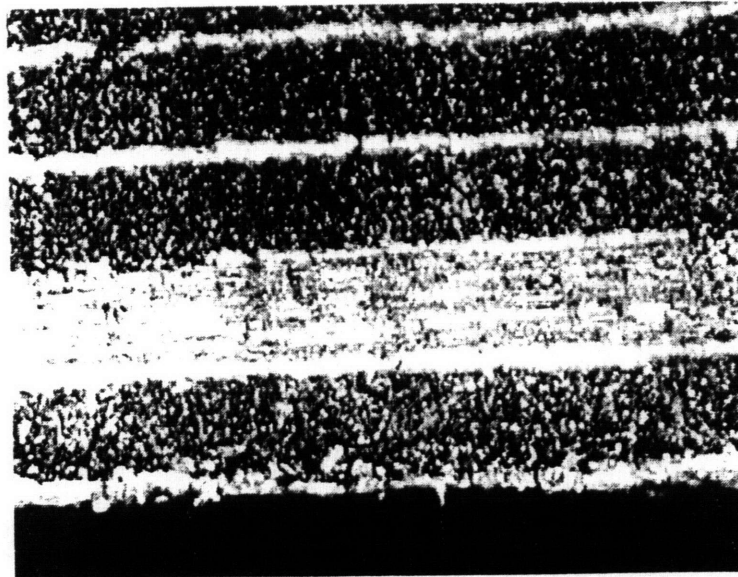


Figure 4.7: Part formed with reinforced diaphragm forming and cured in the autoclave.

The residual effect of the reinforcement on the plies after forming and cure is minimal as can be seen by the shape of the resin rich layer in the two laser microscope views of Figure 4.8 a and b. The lighter line represent the rich resin layer, between the plies and on top of the first ply. Figure 4.8.a is a view across the thickness of a part made without reinforcement. Figure 4.8.b is the same view, but for a part with reinforcement.



(a)



(b)

Figure 4.8: Laser microscope views of the cross section of part made (a) without reinforcement (b) with reinforcement.(magnification X40)

For thick laminates, it has been noted that sometimes, a part that does not show wrinkles after the forming with the reinforced diaphragm, may develop them after the curing process. It is believed that these wrinkles are due to internal stresses which are relieved during cure.

4.5 Experimental set-up

To assess the reinforced diaphragm forming process three sets of experiments have been carried out.

(a) On the small machine, Figure 4.9, one foot long C-channels have been formed in order to evaluate the effect of reinforced diaphragm forming and optimize features of the reinforced architecture such as the rod spacing, the rod material, the rod diameter, the thread material, the size of the fabric.

(b) On the small machine, one foot long parts were made in order to define the limits of reinforced diaphragm forming for a family of parts.

(c) On the 6 foot long forming machine, Figure 4.10, two foot long C-channels have been made to see if there is a length scaling effect for the reinforcement.

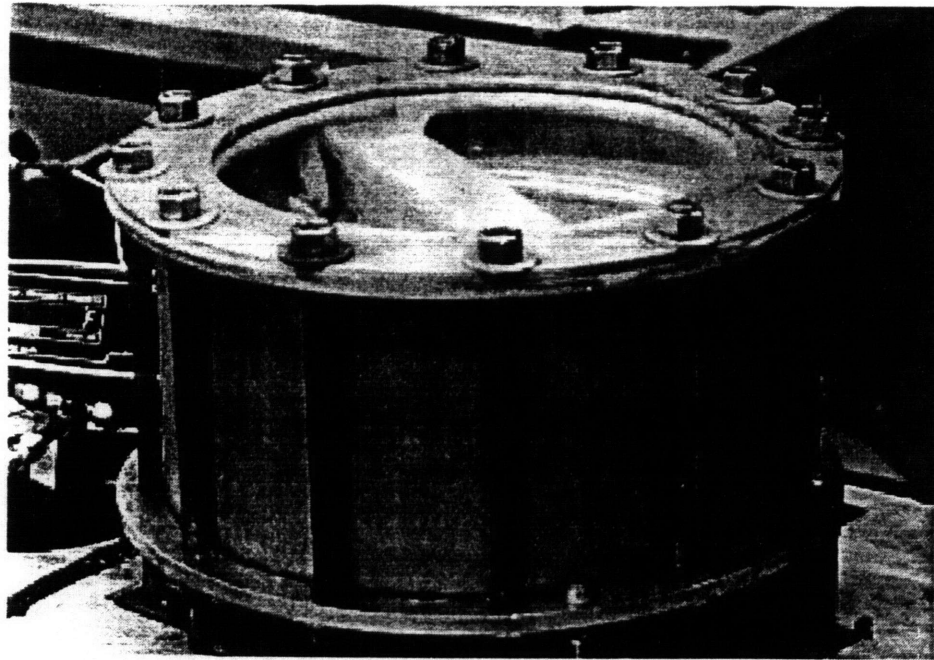


Figure 4.9: Small forming machine

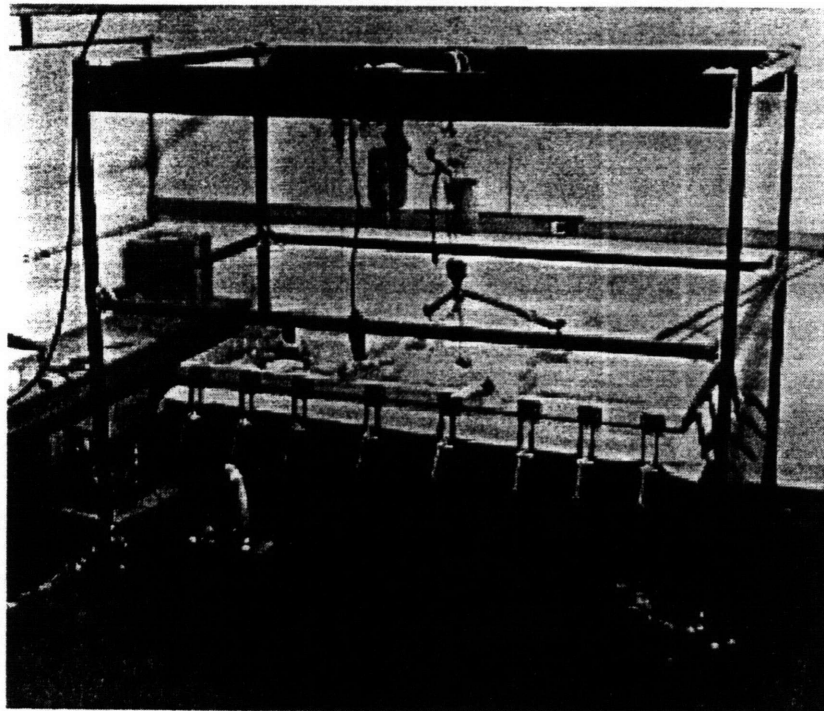


Figure 4.10: 6 foot long forming machine used for forming 2 foot long and 4 foot long parts.

As mentioned previously, because of the indentation problem, examining the parts just after forming was not a reliable method for assessing if a part was good or not. Therefore the following experimental procedure was developed;

- 1) Form the part with reinforcement. (See figure 4.11)

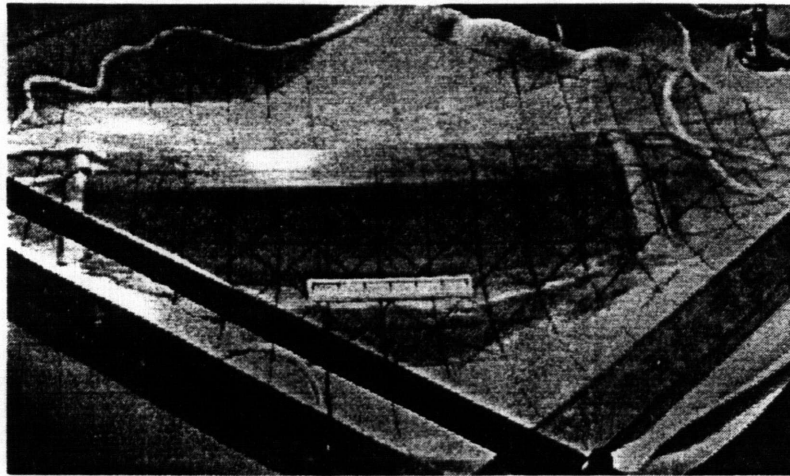


Figure 4.11: Forming a part with reinforcement

- 2) Remove the reinforcement from the part by allowing air between the two diaphragms and removing the top diaphragm. (see Figure 4.12)

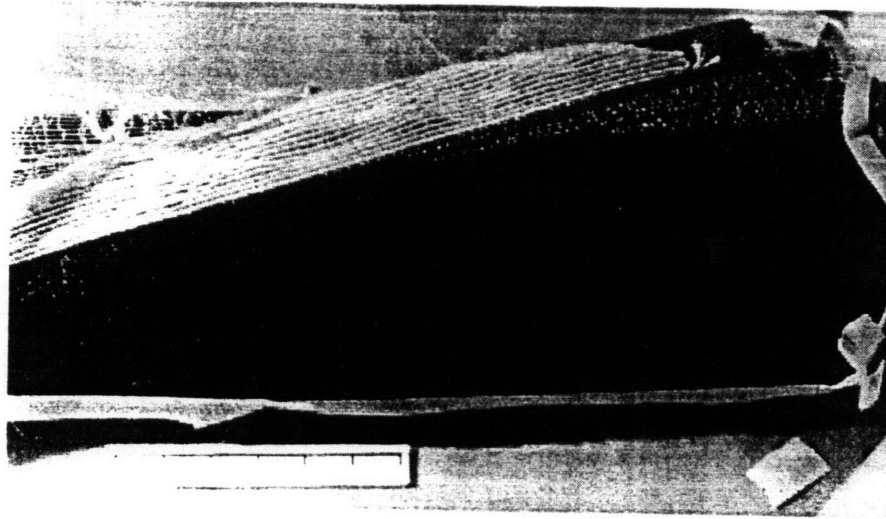


Figure 4.12: Removal of the reinforcement

3) partially cure the laminate by pulling vacuum between the two diaphragms and heating the laminate so that its shape stabilizes. It is important to note that assessing the quality of the part (from a forming point of view) after a half cure is more stringent than after a complete autoclave cure, because the external pressure in the autoclave may eliminate some wrinkles developed during.

Two types of materials have been used for the experiments, Hercules AS4/3501-6 and Toray T800H/3900-2.

4.6 Optimization of the fabrics

On the small forming machine a set of experiments has been carried out in order to evaluate which is the best rod material, what is the optimum rod spacing and rod diameter and what is the best material for the threads.

For evaluating the influence of these different parameters, the experiments have been carried out with the same forming conditions (i.e. material, forming temperature, forming rate, diaphragm tension.) and the effects on the wrinkles on the web or on the back flange have been compared. The experimental standard was the forming of a Toray part at room temperature with a forming rate on the order of two minutes. These experimental conditions are interesting, because they lead to a good part when the reinforcement is used with some potential wrinkling on the back flange, and a bad part when the reinforcement is not used.

Figure 4.13 illustrates a typical fabric made of mild steel and nylon threads. The white strips at both ends of the fabric are aimed at preventing disintegration of the reinforcement.

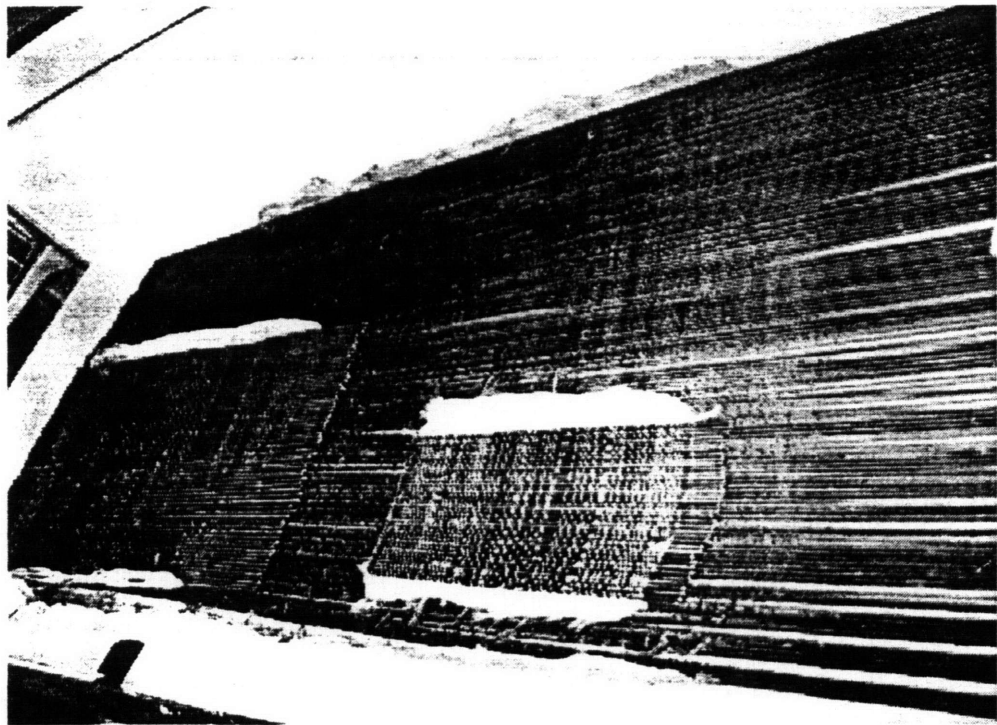


Figure 4.13: illustration of a typical mild steel fabric

4.6.1 Rods

Different types of materials have been tested such as polyethylene strips (see Figure 4.14), aluminum screens, mild steel rods (see Figure 4.13) or cold drawn steel rods.

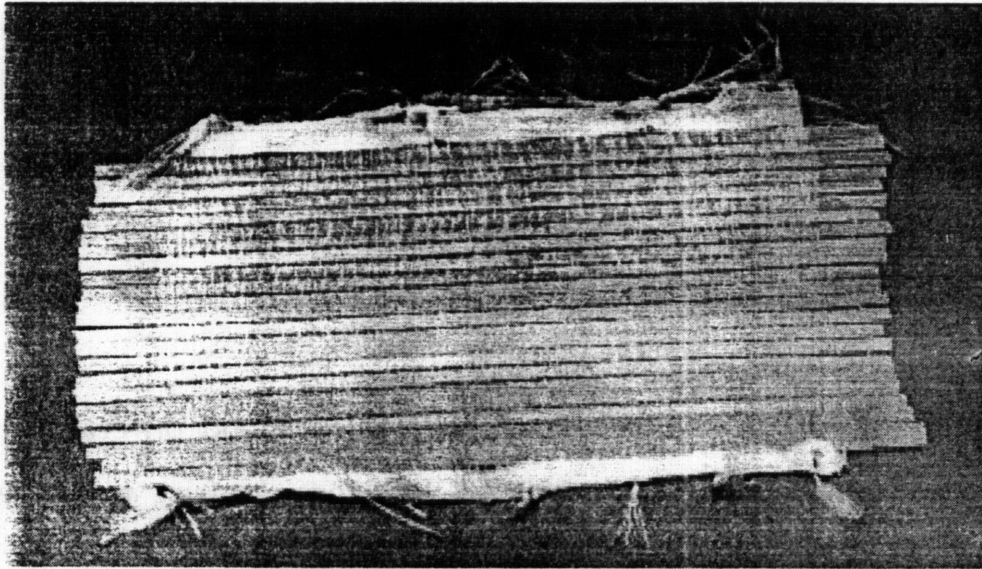


Figure 4.14: illustration of a polyethylene fabric

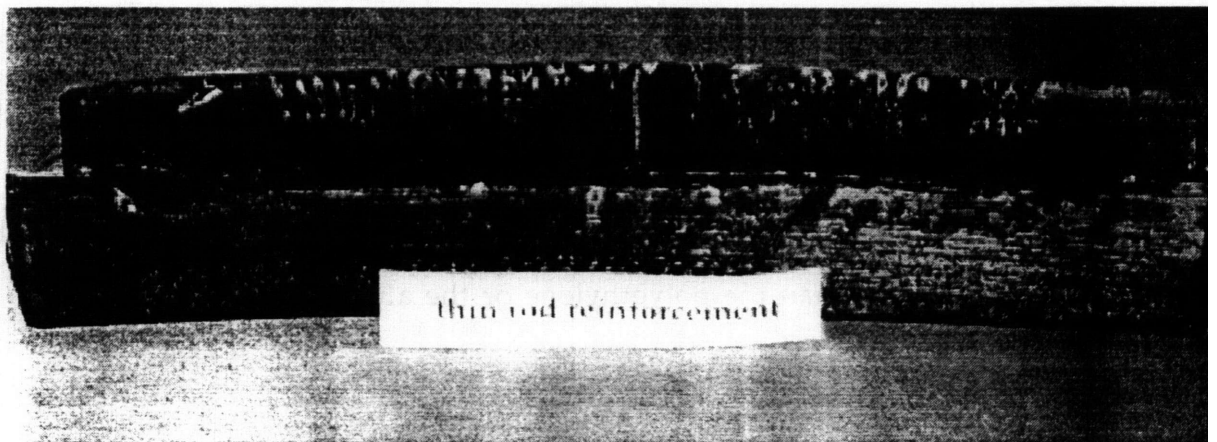
It was found that better results were obtained with mild steel or cold drawn steel rods. Although the polyethylene and the aluminum screen have a good effect on suppressing the wrinkles, the web wrinkles are best suppressed with steel rods. This comes from the fact that these two fabrics were far stiffer than the polyethylene or the aluminum screen fabrics.

Another set of experiments has been carried out in order to check the effect of the rod diameter. Table 4.1 shows the different fabrics which have been tested.

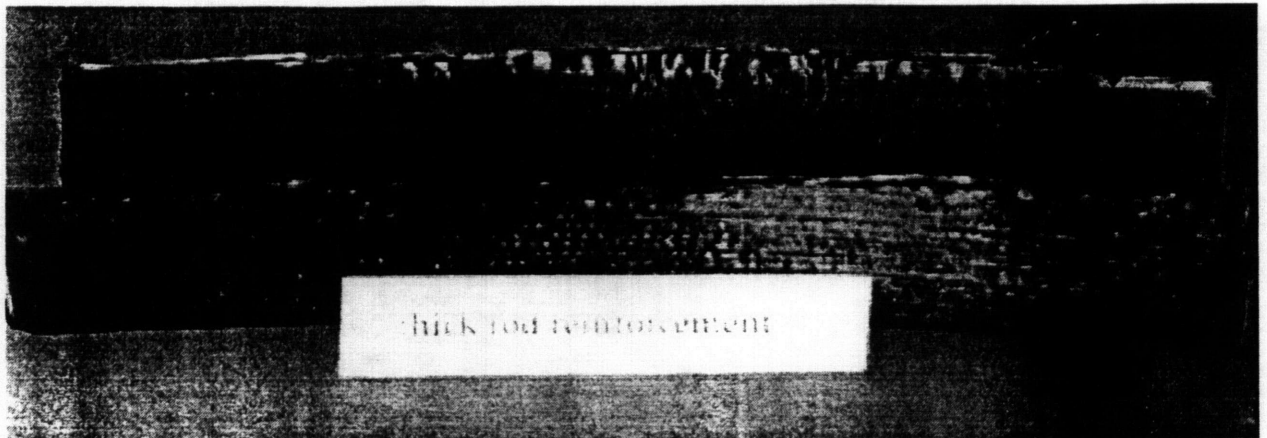
#nb ref	rod number	rod diameter(in)	rod spacing(in)
1	56	0.06	0.04
2	74	0.03	0.04
3	38	0.125	0.02

Table 4.1: Different fabrics

For each fabric the result has been rather good on erasing the web wrinkles, but the effect is different on the flange wrinkles as can be seen on Figure 4.15.a and Figure 4.15.b. Figure 4.15.a shows the back flange of a part made with thin rod reinforcement, and we can see large wrinkle patterns whereas with thick rod reinforcement the back flange wrinkling does not occur.



(a)



(b)

Figure 4.15: Illustration of the effect of reinforcement on the back flange of Toray C-channels. (a) case of thin rod reinforcement (b) case of thick rods reinforcement

For the optimum spacing, the experiments carried out with fabrics with different spacing shows the same trends that the closer the rods are, the stiffer the fabric is, therefore the better the part. the rods should almost touch to each others, but the fabric should not be too tight, otherwise, the forming can be perturbed, the rods cannot deform properly.

4.6.2 Effect of the reinforcement size

An experiment has been carried out using a small fabric, shown in Figure 4.16, which was only covering the area where for the forming conditions without reinforcement wrinkles were expected. This technique is efficient to get rid of the wrinkles, but the drawback as can be seen on Figure 4.17 is that some marks appeared on the part along the edge of the reinforcement, defining a border between the area on the laminate which had the reinforcement and the area on the laminate which had no reinforcement.

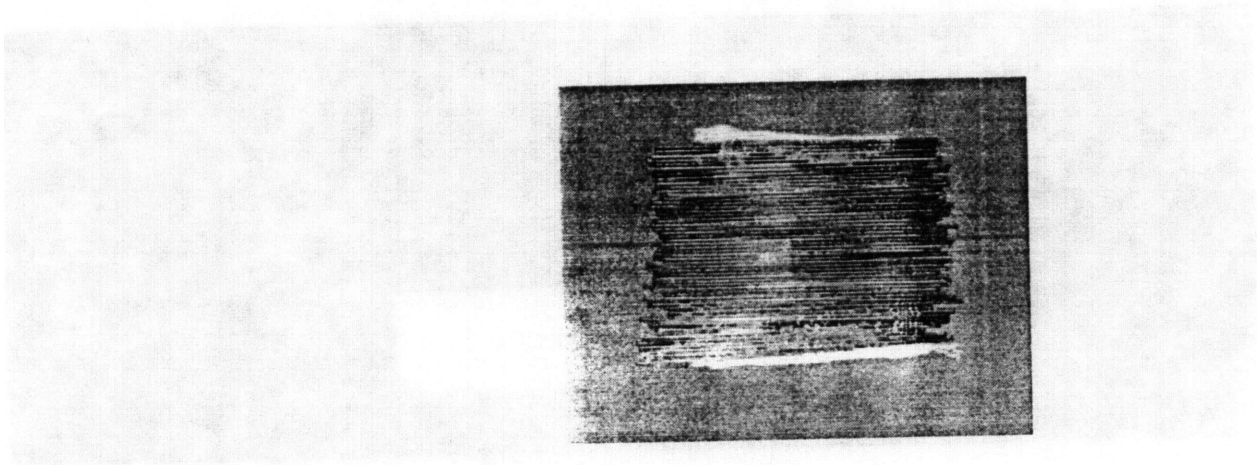


Figure 4.16: Small reinforcement

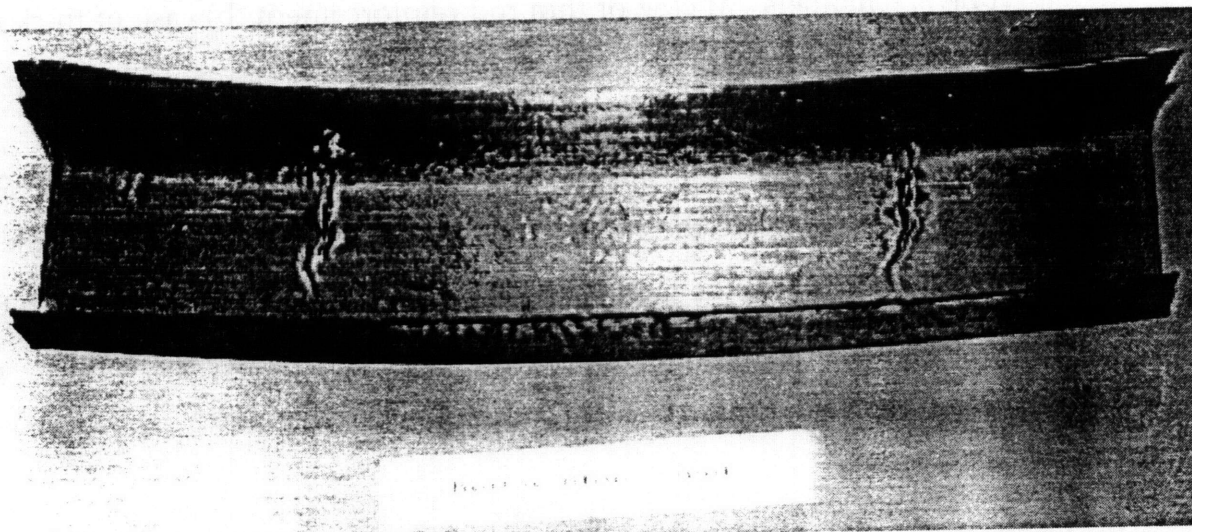


Figure 4.17: Illustration of the marks left by the small reinforcement

4.6.3 Threads

For the ease of fabrication and because during forming the fabric can be tensioned, it was decided to use strong threads like nylon or Kevlar line. And

for reducing the transverse indentation due to the threads passing over the rods it was decided to use thin threads.

4.7 Effect of reinforced diaphragm forming

In this section, we will discuss the overall results of reinforced diaphragm forming in terms of improving the range of the parts that can be made. As stated previously, this section considers only the case of C-channel parts. The experiments were carried out on Hercules and Toray materials which have, as stated in section 2.4, substantially different drape properties, Toray material being more difficult to form. The parts made were either the 1 foot long part made on the small machine or the 2 foot long part made on the big machine. The data for these parts are plotted on forming limit diagrams to show how the reinforcement shifts the boundary between the good parts and the bad ones. The plotted data are joined in the Appendix for further details. All the parts made had a [0/90/+-45] lay-up orientation. The importance of this ply orientation lies in the fact, that it is a frequently used lay-up, it shows quasi-isotropic properties from a structural point of view, and it is one of the most difficult lay-ups to form. (i.e. 2 foot long C-channel [0/90]4s or [+/-45]4s are much easier to form as discussed in section 2.3)

In order to present the different results obtained, the experimental data have been plotted into a forming limit diagram as plotted in section 2.6. The compressive force and the diaphragm tension following the rules exposed in section 2.6. The experimental data values are in Appendix. For the clarity, the

forming limit diagram has been splitted in sub-diagrams, each of which displays a different material or part size.

Figure 4.18 is the Forming Limit Diagram for Hercules one foot long part. The shifting of the boundary between the good and the bad parts is very obvious, the parts represented with a circle are those made without reinforcement and those represented by a diamond are those made with reinforcement.

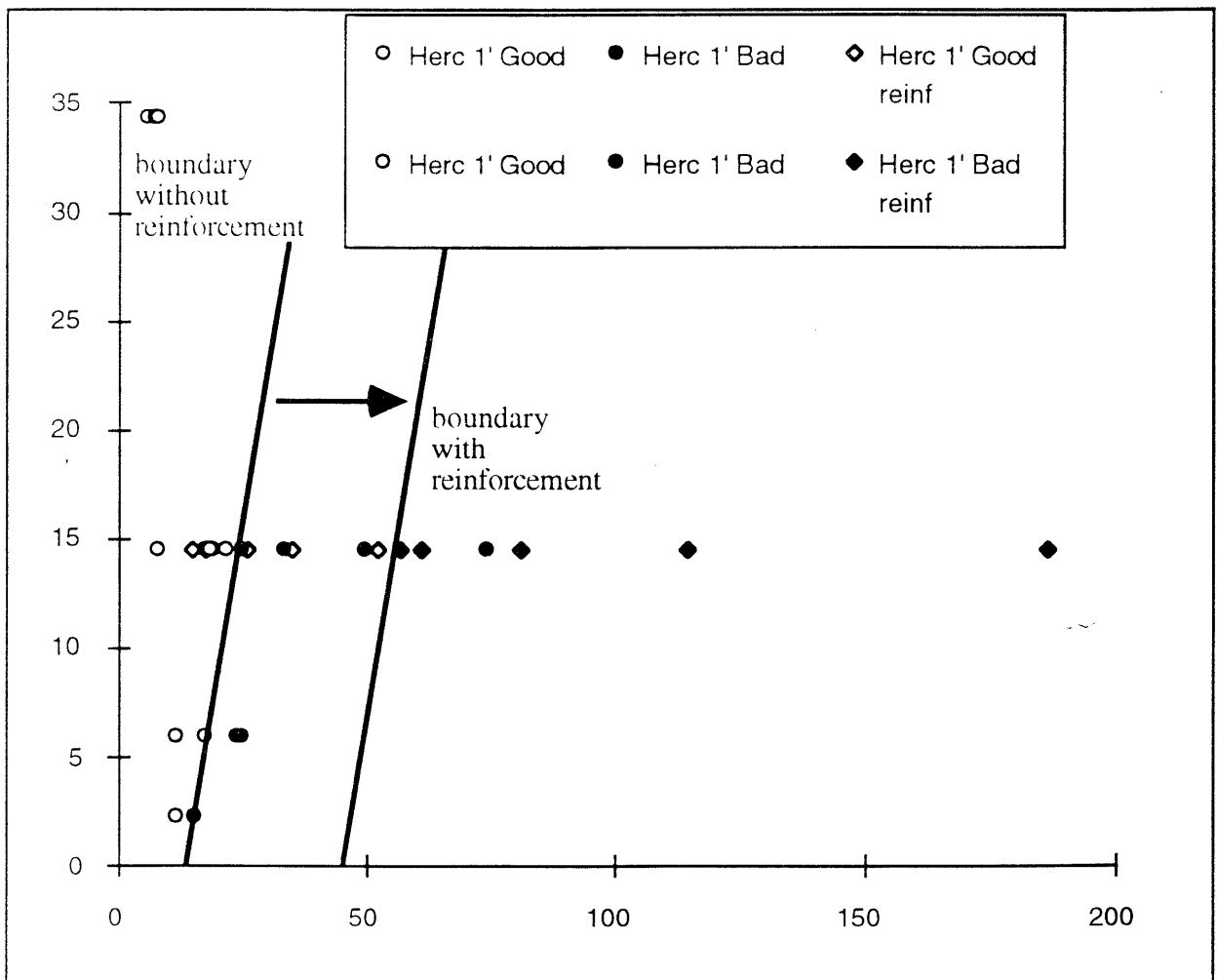


Figure 4.18: Forming limit diagram for 1 foot long Hercules C-channel with a [0/90/+45] lay-up.

Figure 4.19 illustrates the case of small Toray C-channels, the shift in the boundary is also very clear.

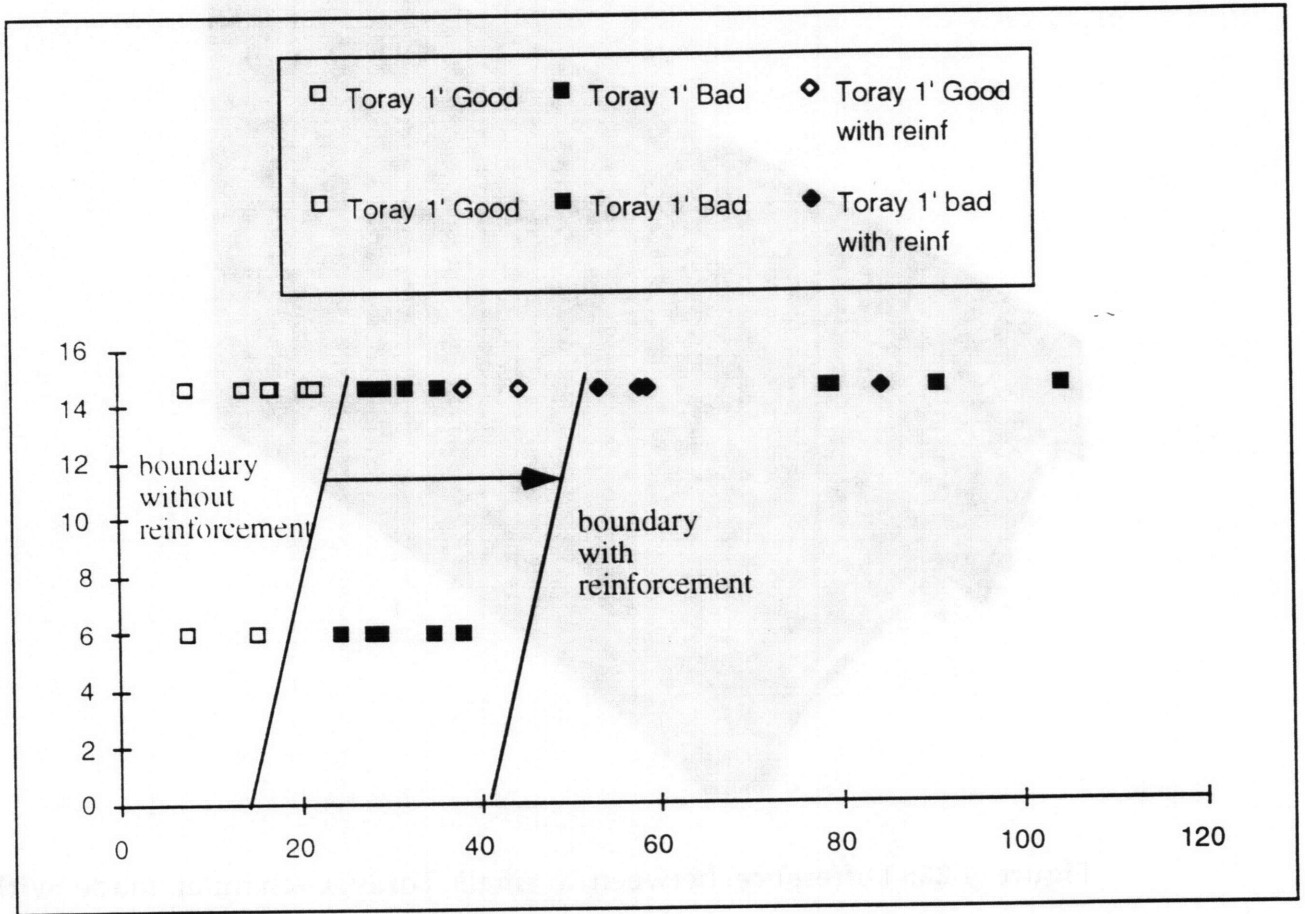


Figure 4.19: Forming limit diagram for 1 foot long Toray C-channels with a [0/90/+-45] lay-up.

Figure 4.20 illustrates the difference between a small Toray C-channel made with reinforcement and without reinforcement.

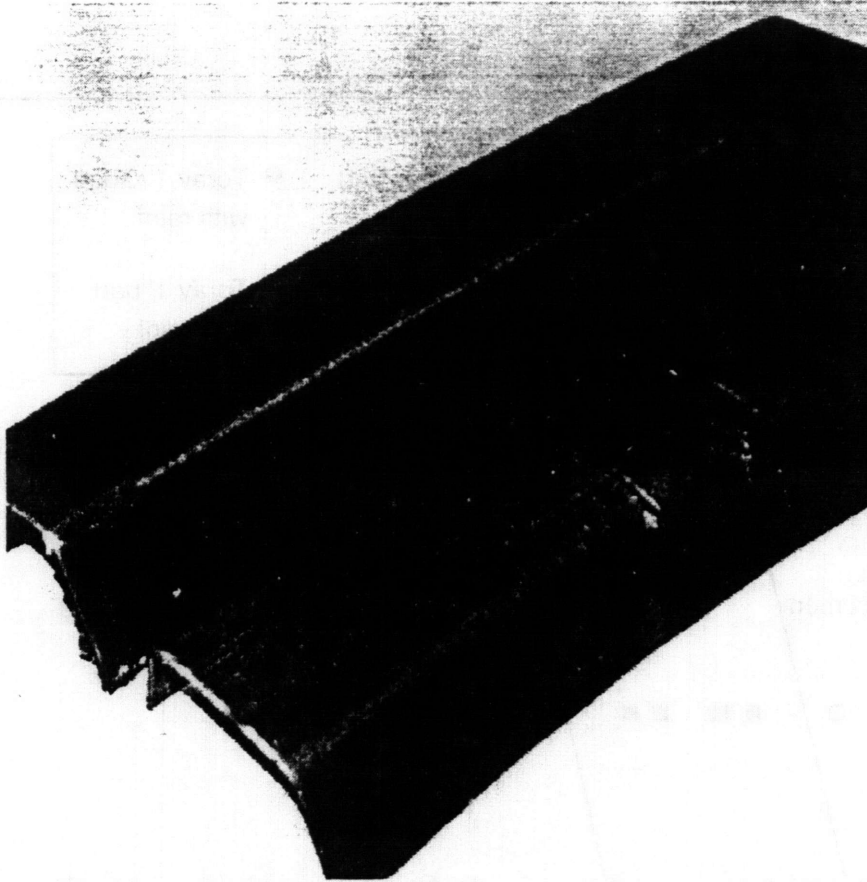


Figure 4.20: Difference between a small Toray C-channel made with reinforcement and without reinforcement

Figure 4.21 illustrates the case of 2 foot long C-channels, and the improvement brought about by using the reinforcement is even more impressive, because, without the rod reinforcement no 2 foot long C-channel [0/90/+-45] could be made, and as can be seen in Appendix D, with reinforcement we were able to make a 32 ply [0/90/+-45]_{4s} C-channel.

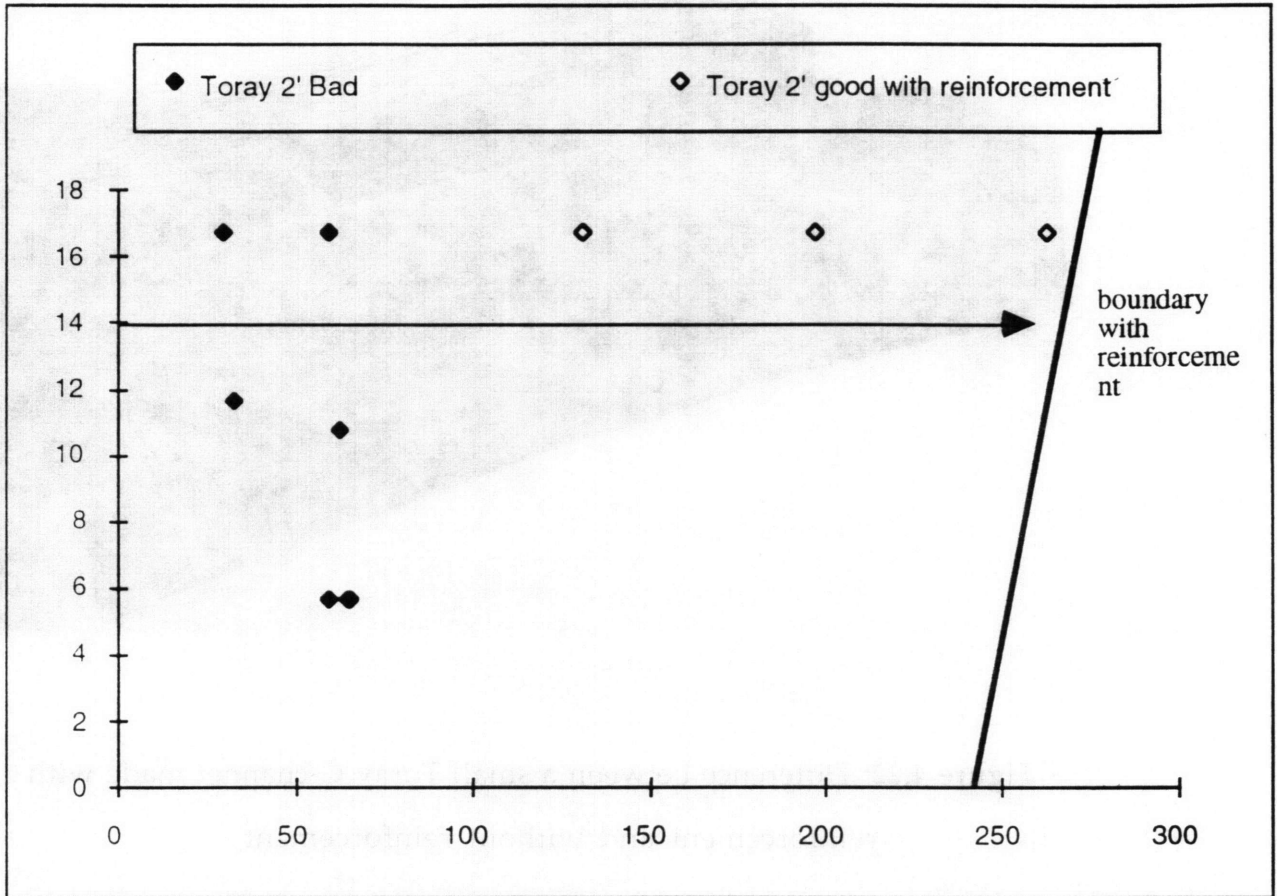


Figure 4.21: Forming limit diagram for 2 foot long Toray C-channels.

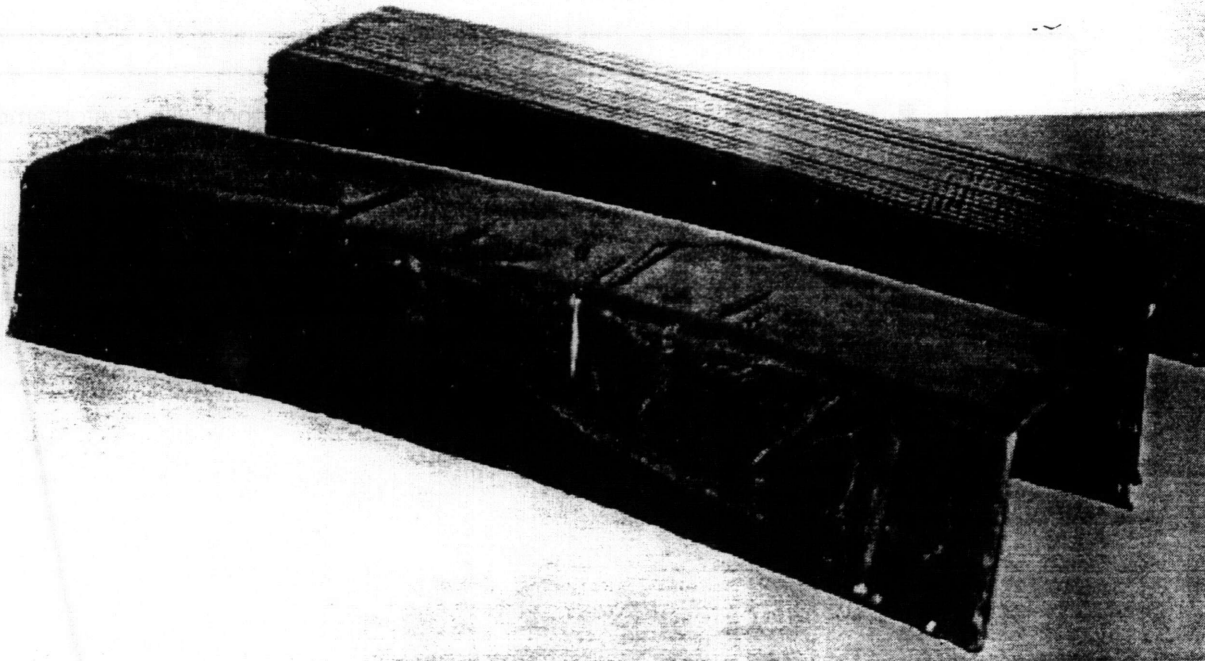


Figure 4.22: Difference between a small Toray C-channel made with reinforcement and without reinforcement

Therefore, with reinforcement we can manufacture bigger parts. The net result of the reinforcement is to extend the number of part that can be made and make the process more economical. For instance can be seen in Appendix B an 8 ply Toray part can be made in 2 min. at 120 degrees without reinforcement, or in 2 min. at 90 with reinforcement.

4.8 Design reinforcement for different shapes

It has been seen in the previous section that reinforced diaphragm forming has the potential to increase the range of C-channels that can be made, therefore, it may be useful to use reinforcement for different shapes. For instance, for an hemisphere, using woven straight rods seems inappropriate. Therefore, new designs for the reinforcement should be developed. It may be advantageous to use woven screens, as shown in section 4.5.1, though material stiffer than aluminum should be used. Another possibility could be to knit steel wires in order to get a tailored screen for maximum efficiency.(see illustration in figure 4.23)

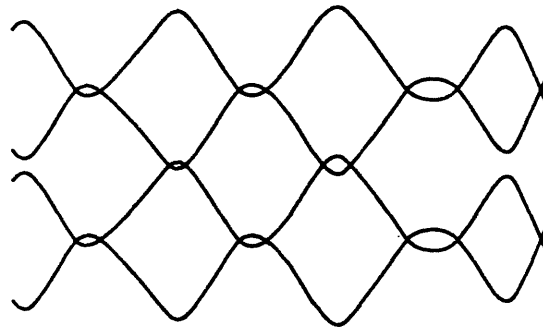


Figure 4.23: Illustration of knit

A technique which seems promising, but has not yet been tested would be to embed rods, or chopped rods (see Figure 4.24) or curved rods (see Figure 4.25) or stiff spherical particles (see Figure 4.26) into a rubber matrix. The rubber would have the ability to link together the reinforcing elements, and would also have the ability to deform and allow some slippage or shear movement of the reinforcing elements.

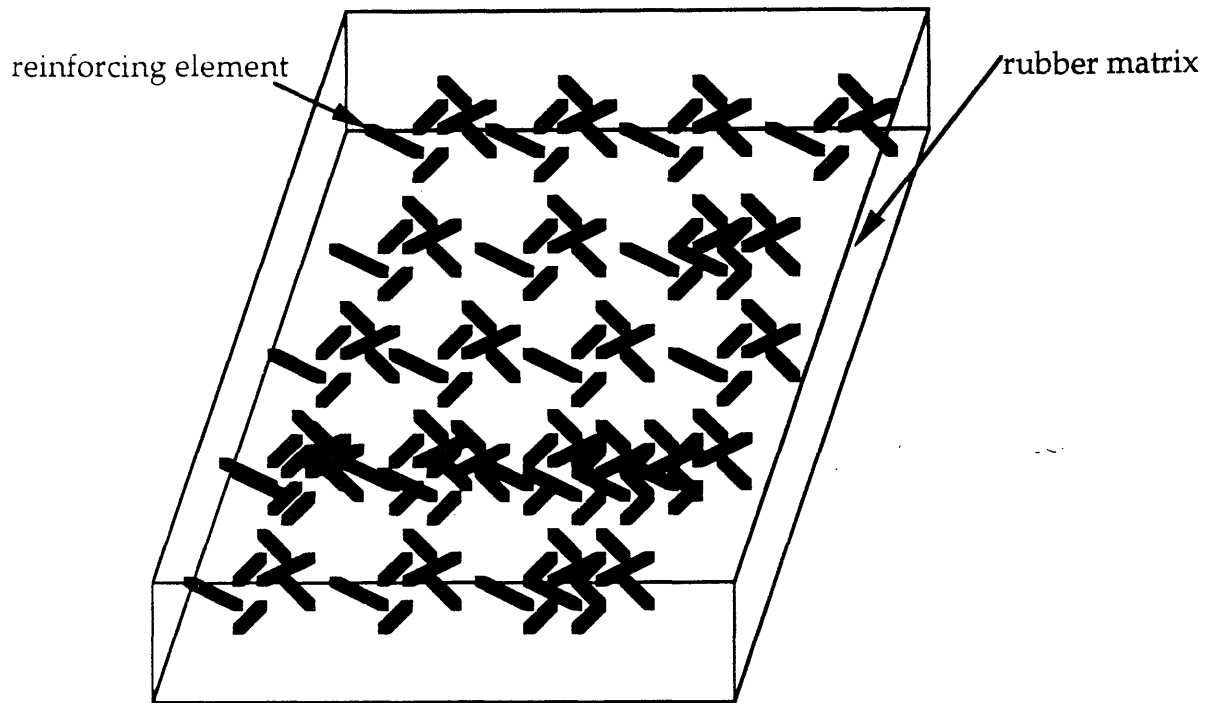
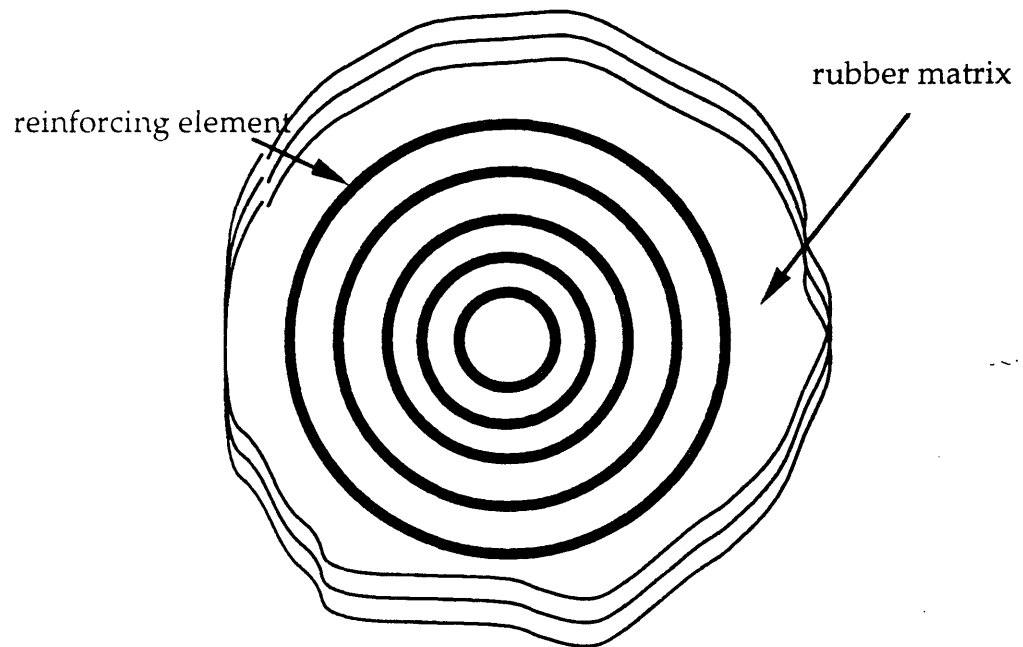


Figure 4.24: Illustration of chopped rods embedded into a rubber matrix



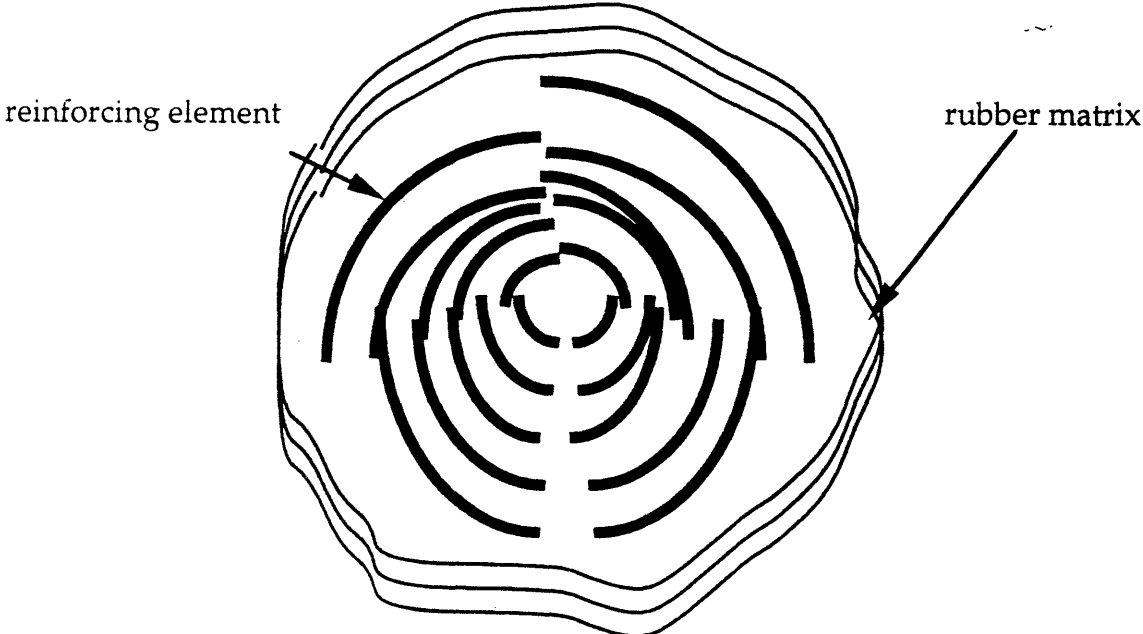


Figure 4.25: Illustration of curved rods embedded into a rubber matrix

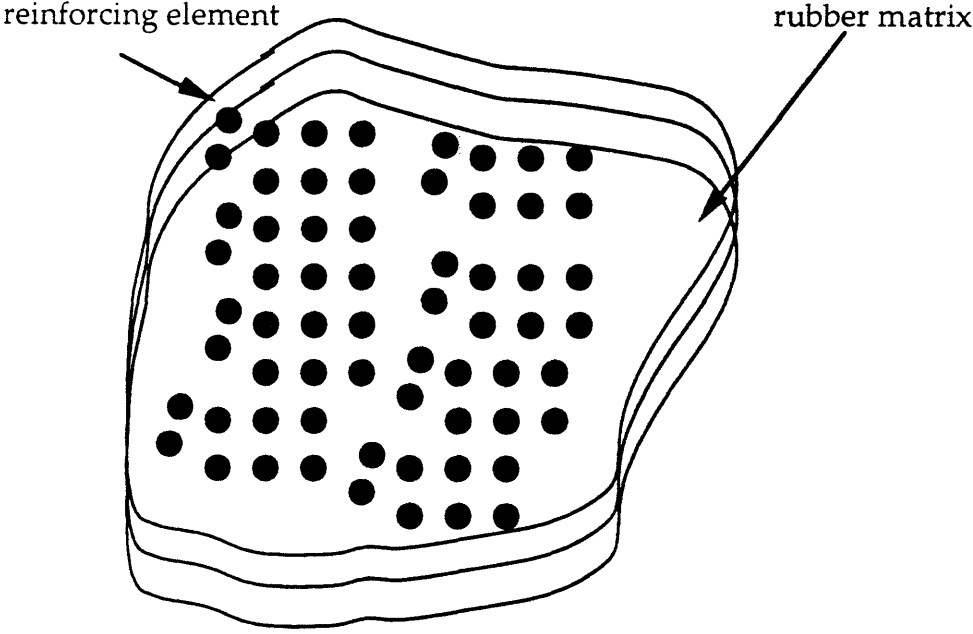
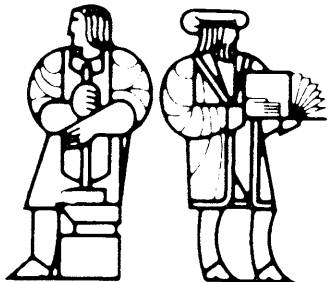


Figure 4.26: Illustration of stiff particles embedded into a rubber matrix



Chapter 5

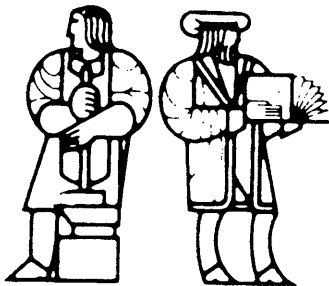
Conclusion

Two main conclusions result from this work.

First, the reinforced diaphragm forming is an innovative technique which has the potential to expand the size and the range of parts that can be made by diaphragm forming. This technique has been investigated and shows some effective improvements in the process. The different forming limit diagrams show clearly that the boundary between good and bad part is shifted by using the reinforcement. And even better, the reinforcement has proven to be efficient to manufacture 2 foot long parts which were impossible to make without reinforcement. But this exploratory research on reinforced diaphragm forming should be continued, first to expand even more the size of parts that can be made with reinforcement, and to develop various designs of reinforcement aimed at improving the forming of specific shapes. A few ideas have been suggested in section 4.7.

The second major conclusion is related to the potential application of diaphragm forming for different Ocean Engineering applications ranging from forming whole fiber glass hulls to different kinds of advanced composite parts for more specific applications. Diaphragm forming should

capitalize on the potential for automation with low tooling cost. This has been illustrated by showing the possibility of manufacturing a top hat intersection part with woven carbon fiber embedded in an epoxy resin. This part also expands the geometry of the parts that can be made with diaphragm forming. It could be also interesting to study in more depth the tailoring of plies in order to achieve complicated shapes,



Bibliography

- [Bersee and Robroek] Bersee H.E.N. and Robroek L.M.J., "The role of thermoplastic matrix in forming processes of composite materials", *Composites manufacturing* Vol 2 No3, 1991, p 217-222.
- [Barnes and Cogswell] Barnes J.A. and Cogswell F.N., " Transverse flow process in continuous fibre-reinforced thermoplastic composites", *Composites*, Vol 20, No.1,1989, p38-42.
- [Chey] Chey, S., "Laminate Wrinkling During the Forming of Composites", S.M. Thesis, Department of Mechanical Engineering , M.I.T., Cambridge, MA, May 1993.
- [Foley] Foley M. F., "The flexible Resin Transfer Molding (FRTM) Process", *SAMPE Journal*, Vol.28, N0.6, Nov/dec 1992.
- [Gonzalez-Zugasti] Gonzalez-Zugasti, J., "Computer Modelling of Advanced Composites Forming", S.M. Thesis, Department of Mechanical Engineering, M.I.T., Cambridge, MA, September 1991.
- [Gutowski and Sentovich] Gutowski T. G. and Sentovich M. F., " Manufacturing Issues for Composite Materials in Marine Structures", *Automation in the Design and Manufacture of Large Marine Systems*, Chryssostomos Chryssostomidis, 1990.
- [Hull and al.] Hull B. D., Rogers T. G. and Spencer A. J. M., "Theory of fibre buckling and wrinkling in shear flows of fiber-reinforced composites", *Composites manufacturing* Vol 2 No3, 1991, p185-189.
- [Li] Li, H., "Preliminary Forming Limit Analysis for Advanced Composites", S.M. Thesis, Department of Mechanical Engineering , M.I.T., Cambridge, MA, May 1994.

- [Masubuchi] K. Masubuchi, Private communication and class notes.
- [Monaghan and al.]
Monaghan M.R. O'Bradaigh C. M., Mallon P. J. and Pipes R. B., "The effect of diaphragm stiffness on the quality of Diaphragm formed thermoplastic composite components", 35th International SAMPE Symposium, 1990.
- [Neoh] Neoh, E.T., "Drape Properties of Thermosetting Prepregs", S.M. Thesis, Department of Mechanical Engineering, M.I.T., Cambridge, MA, May 1992.
- [Raymer] Raymer J.F., "Large-Scale Processing Machinery for Fabrication of Composite Hulls and Superstructure", *J. of Ship Production*, Vol. 7, No.4, Nov, 1991, pp220-226.
- [Shenoi and Wellicome]
edited by Shenoi R.A. and Wellicome J.F., "Composite materials in maritime structures", Cambridge University Press, Vol 1 & 2, 1993.
- [Scherer, Friedrich] Scherer R., Friedrich K., "Modelling of Flow Processes during Thermoforming of Continuous CF/PP Laminates", ICCM/8, Honolulu, Hawaii, July 15-19, 1991.
- [Smiley and Schmitt] Smiley A.J. and Schmitt T.E., " Assessment of aligned fiber reinforced thermoplastic composite sheet forming processes", 23rd International SAMPE Technical conference, October 21-24, 1991.
- [Tam] Tam, A.S., "A Deformation Model for the Forming of Aligned Fiber Composites", Ph.D. Thesis, Department of Mechanical Engineering, M.I.T., Cambridge, MA, June 1990.
- [Tam and Gutowski] Tam, A.S., and T.G. Gutowski, "Ply-Slip during the forming of Thermoplastic Composite Parts", *J. of Composites Materials*, Vol. 23, June 1989.

Appendix

Experimental DATA for the forming limit diagram

As discussed in the section 2.6, the two axis of the forming limit diagrams are:

$$\text{Equivalent compressive force: } F_{\text{eq}} = N_p h_{\text{int}} \frac{m}{n+1} \frac{\bar{\Gamma}_{2v}^{n+1}}{t^n}$$

N_p : Number of plies

h_{int} : Thickness of one ply

$\bar{\Gamma}_{2v}$: Evaluation of the interply shear

t : Forming time

m, n : rheological factor, evaluated experimentally by the drape test.

$$\text{Diaphragm tension: } T_{11} = D \dot{\sigma}_{11}$$

D : Diaphragm thickness

$\dot{\sigma}_{11}$: Nominal in the diaphragm, given by the extension ratio of the diaphragm in direction 1 and 2, and by the stiffness of the diaphragm.

.....

• L

~

~

Table1: Hercules C-channel(0/90/+/-45) good parts

(The data with an experimental number are those done by the author)

without reinforcement

Expt #	Np	Radius(in)	Geometry	Diaph. t(in.)	Time(min)	Temp(F)	1/T(1/K)	m	n	Td	Feq	remarks
	16	48	(0/90 +45) 2S	0.125	120	70	0.0034	10.4717	0.4489	34.3840	5.9897	
	24	48	(0/90 +45) 3S	0.125	180	70	0.0034	10.4717	0.4489	34.3840	7.4894	
	16	48	(0/90 +45) 2S	0.125	60	70	0.0034	10.4717	0.4489	34.3840	8.1760	
	16	48	(0/90 +45) 2S	0.0625	5	110	0.0032	1.7368	0.2121	14.5600	16.1447	
	20	48	(0/90 +45) 2.5S	0.0625	5	110	0.0032	1.7368	0.2121	14.5600	20.1809	
	20	48	(0/90 +45) 2.5S	0.0625	5	100	0.0032	1.7368	0.2121	14.5600	20.1809	
	16	48	(0/90 +45) 2S	0.03125	5	100	0.0032	1.7368	0.2121	5.9640	16.1447	
	16	48	(0/90 +45) 2S	0.03125	25	85	0.0033	4.1604	0.3272	5.9640	11.7343	
	16	48	(0/90 +45) 2S	0.0625	60	70	0.0034	10.4717	0.4489	14.5600	8.1760	
	8	48	(0/90 +45) S	0.01563	3.1666	85	0.0033	4.1604	0.3272	2.3250	11.5364	
	16	48	(0/90 +45) 2S	0.0625	7.5	78	0.0033	6.3596	0.3832	14.5600	18.8679	
16	16	48	(0/90 +45) 2S	0.0625	1.5	100	0.0032	1.5375	0.2121	14.5600	18.4497	heating the tool
	8	96	(0/90 +45) S	0.0625	30	130	0.0032	1.7368	0.2121	5.6713	15.2115	

with reinforcement on top

Expt #	Np	Radius(in)	Geometry	Diaph. t(in.)	Time(min)	Temp(F)	1/T(1/K)	m	n	Td	Feq	remarks
10	8	48	(0/90/ +45)S	0.0625	25	76	0.0034	17.8059	0.3994	14.5600	14.7839	heating the tool
15	16	48	(0/90 +45) 2S	0.0625	2	100	0.0032	1.5375	0.2121	14.5600	17.3577	heating the tool
17	24	48	(0/90 +45) 3S	0.0625	2	100	0.0032	1.5375	0.2121	14.5600	26.0365	heating the tool
19	32	48	(0/90 +45) 4S	0.0625	2	100	0.0032	1.5375	0.2121	14.5600	34.7154	heating the tool
23	48	48	(0/90 +45) 6S	0.0625	2	100	0.0032	1.5375	0.2121	14.5600	52.0730	heating the tool
##	32	96	(0/90 +45) 4S	0.0625	30	180	0.0032	1.5375	0.2121	16.7375	45.2869	heating the tool

Table2: Hercules C-channel(0/90/+/-45) wrinkled part
 (The data with an experimental number are those done by the author)

without reinforcement

Expt #	Np	Radius	Geometry	Diaph. t(in.)	Time(min)	Temp(F)	1/T(1/K)	m	n	Td	Feq	remarks
	16	48	(0/90 +45) 2S	0.0625	5	70	0.0034	10.4717	0.449	14.56	24.946	
	16	48	(0/90 +45) 2S	0.03125	5	70	0.0034	10.4717	0.449	5.964	24.946	
	8	48	(0/90 +45) S	0.03125	0.91666	74	0.0034	8.14539	0.416	5.964	23.7189	
	8	48	(0/90 +45) S	0.01563	3.1666	70	0.0034	10.4717	0.449	2.32505	15.3118	
12	16	48	(0/90 +45) 2S	0.0625	2.5	76	0.0034	17.8059	0.399	14.56	74.1724	
18	24	48	(0/90 +45) 3S	0.0625	2.5	100	0.0032	1.53749	0.212	14.56	24.8331	heating the tool
20	32	48	(0/90 +45) 4S	0.0625	2.5	100	0.0032	1.53749	0.212	14.56	33.1108	heating the tool
24	48	48	(0/90 +45) 6S	0.0625	2.5	100	0.0032	1.53749	0.212	14.56	49.6662	heating the tool
27	32	48	(0/90 +45) 4S	0.0625	2.5	100	0.0032	1.53749	0.212	14.56	33.1108	
	8	96	(0/90 +45) S	0.0625	30	130	0.0032	1.73678	0.212	0.8125	15.2115	
	16	96	(0/90 +45) 2S	0.0625	30	130	0.0032	1.73678	0.212	0.8125	30.423	
	8	96	(0/90 +45) S	0.0625	30	130	0.0032	1.73678	0.212	0.8125	15.2115	
	4	192	(0/90 +45)	0.0625	30	170	0.0032	1.73678	0.212	9.18125	21.2401	

with reinforcement on top

Expt #	Np	Radius	Geometry	Diaph. t(in.)	Time(min)	Temp(F)	1/T(1/K)	m	n	Td	Feq	remarks
6	8	48	(0/90 +45) S	0.0625	2	71	0.0034	30.4993	0.441	14.56	57.0344	heating the tool
8b	16	48	(0/90 +45) 2S	0.0625	2	71	0.0034	30.4993	0.441	14.56	114.069	heating the tool
11b	8	48	(0/90 +45) S	0.0625	2	70	0.0034	34.0066	0.449	14.56	61.1167	heating the tool
13	16	48	(0/90 +45) 2S	0.0625	2	76	0.0034	17.8059	0.399	14.56	81.0869	heating the tool
14	16	48	(0/90/+ -45)2s	0.0625	2	64	0.0034	65.9177	0.5	14.56	186.225	heating the tool

Table3: Toray C-channel(0/90/+/-45) good part

without reinforcement

Expt #	Np	Radius(in)	Geometry	Diaph. t(in.)	Time(min)	Temp(F)	1/T(1/K)	m	n	Td	Feq	remarks
	4	48	(0/90/ +45)	0.0625	28	120	0.0031	4.2245	0.1740	14.5600	7.7856	
	4	48	(0/90/ +45)	0.03125	35	120	0.0031	4.2245	0.1740	5.9640	7.5683	
	8	48	(0/90/ +45)s	0.0625	64	120	0.0031	4.2245	0.1740	14.5600	14.0419	
	8	48	(0/90/ +45)s	0.0625	15	150	0.0031	4.2245	0.1740	14.5600	16.8807	
	8	48	(0/90/ +45)s	0.03125	29	120	0.0031	4.2245	0.1740	5.9640	15.5018	
	8	48	(0/90/ +45)s	0.0625	3	150	0.0031	4.2245	0.1740	14.5600	20.9929	
	8	48	(0/90/ +45)s	0.0625	13	120	0.0031	4.2245	0.1740	14.5600	17.2015	
	8	48	(0/90/ +45)s	0.0625	2.25	120	0.0031	4.2245	0.1740	14.5600	21.8571	
32	8	48	(0/90/ +45)s	0.0625	15	120	0.0031	4.2245	0.1740	14.5600	16.8807	
	2	96	0/90	0.0625	30	150	0.0031	4.2245	0.1740	11.6188	16.3932	

with reinforcement on top

Expt #	Np	Radius(in)	Geometry	Diaph. t(in.)	Time(min)	Temp(F)	1/T(1/K)	m	n	Td	Feq	remarks
34	8	48	(0/90/ +45)s	0.0625	12	90	0.0033	15.3297	0.2721	14.5600	38.3142	heating the tool
37	16	48	(0/90/ +45)2S	0.0625	12	110	0.0032	6.3945	0.2055	14.5600	44.3791	heating the tool
26	8	48	(0/90/ +45)s	0.0625	2	90	0.0033	15.3297	0.2721	14.5600	53.3672	heating the tool
	32	96	(0/90/ +45)4s	0.0625	30	150	0.0031	4.2245	0.1740	16.7375	262.2913	
	16	96	(0/90/ +45)2s	0.0625	30	150	0.0031	4.2245	0.1740	16.7375	131.1456	
	24	96	(0/90/ +45)3s	0.0625	30	150	0.0031	4.2245	0.1740	16.7375	196.7185	

Table4: Toray C-channel(0/90/+/-45) wrinkled part

without reinforcement

Expt #	Np	Radius(in)	Geometry	Diaph. t(in)	Time(min)	Temp(F)	1/T(1/K)	m	n	Id	Feq	remarks
	4	48	(0/90/+45)	0.03125	9	70	0.0034	39.259	0.34361129	5.964	38.2724601	
	4	48	(0/90/+45)	0.03125	50	70	0.0034	39.259	0.34361129	5.964	29.1536537	
	4	48	(0/90/+45)	0.03125	65	70	0.0034	39.259	0.34361129	5.964	28.1741914	
	4	48	(0/90/+45)	0.03125	210	70	0.0034	39.259	0.34361129	5.964	24.7307952	
	4	48	(0/90/+45)	0.0625	80	70	0.0034	39.259	0.34361129	14.56	27.4592527	
	4	48	(0/90/+45)	0.03125	15	70	0.0034	39.259	0.34361129	5.964	34.9754215	
	16	48	(0/90/+45)2S	0.0625	43	120	0.00311	4.2245	0.1739881	14.56	29.5004194	
	16	48	(0/90/+45)2S	0.0625	22	150	0.00311	4.2245	0.1739881	14.56	32.1208193	
	16	48	(0/90/+45)2S	0.0625	55	150	0.00311	4.2245	0.1739881	14.56	28.6121814	
25	8	48	(0/90/+45)s	0.0625	2	70	0.0034	39.259	0.34361129	14.56	104.262626	
28	8	48	(0/90/+45)s	0.0625	2	74	0.00337	32.345	0.32887184	14.56	90.6183537	
31	16	48	(0/90/+45)2S	0.0625	2	100	0.00322	9.8238	0.23820064	14.56	78.4739791	heating the tool
35	16	48	(0/90/+45)2S	0.0625	10	90	0.00327	15.33	0.27205912	14.56	79.0656028	heating the tool
36	16	48	(0/90/+45)2S	0.0625	10	120	0.00311	4.2245	0.1739881	14.56	35.6216515	heating the tool
	8	96		0.0625	65	180	0.00311	4.2245	0.1739881	5.67125	59.5414485	
	8	96		0.0625	35	180	0.00311	4.2245	0.1739881	5.67125	64.3047339	
	8	96		0.0625	45	180	0.00311	4.2245	0.1739881	10.80625	62.3089037	
	8	96		0.0625	65	180	0.00311	4.2245	0.1739881	16.7375	59.5414485	
	4	96		0.0625	65	180	0.00311	4.2245	0.1739881	16.7375	29.7707242	
	4	96		0.0625	30	180	0.00311	4.2245	0.1739881	11.61875	32.7864103	

2808-24

Expt #	Np	Radius(in)	Geometry	Diaph. t(in)	Time(min)	Temp(F)	1/T(1/K)	m	n	Id	Feq	remarks
21	8	48	(0/90/+45)s	0.0625	2	76	0.00336	29.391	0.32158466	14.56	84.5856789	heating the tool
22	8	48	(0/90/+45)s	0.0625	2	90	0.00327	15.33	0.27205912	14.56	1.20836684	heating the tool
30	16	48	(0/90/+45)2S	0.0625	2	110	0.00316	6.3945	0.20553081	14.56	53.3671679	heating the tool
33	16	48	(0/90/+45)2S	0.0625	12	100	0.00322	9.8238	0.23820064	14.56	57.365	heating the tool